Characterisation and Applications of Marine Derived Calcium Phosphates and Carbonates

A thesis
submitted in partial fulfilment
of the requirements for the degree
of
Master of Science (Research) in Chemistry
at
The University of Waikato
by
LIAM Jack MACKINTOSH

THE UNIVERSITY OF
WAIKATO
Te Whare Wānanga o Waikato

2018

Abstract

The purpose of this study was to characterise extensively, and process fishbone derived and shellfish mineral powders, followed by the investigation of potential applications for these materials. A variety of spectroscopic, microscopic and analytical techniques were used in this study, including FT-IR, SS-NMR, pXRD, SEM, ICP-MS, and laser diffraction particle sizing. These techniques enabled tracking of changes in the chemical and physical nature of the materials as a function of processing techniques. The potential applications covered in this study were the investigation of the immobilisation of the enzyme malL to bone materials with the aid of a coupling reagent, as well as investigations into the removal of various ionic species from aqueous water samples.

Differences in the mineral components of the materials between species were insignificant. Slight variations were found in the organic component of the bone materials, however these were most likely due to varying levels of oils remaining in the materials after processing by Plant and Food, Nelson, as the organic matter was found to be primarily composed of collagen in all species.

Thermally treating the bone samples to 800 ^{o}C was found to be the most effective and reliable method for removing the organic content from the bone materials. Synthetic HAp powders were successfully produced through the digestion and reprecipitation of bone-derived materials and an optimum method to produce these powders was devised.

Promising yet unexpected results were found in the enzyme immobilisation studies, results suggest that there is the potential for some enzymes to be bound to the bone materials, however more thorough investigations are required to understand the complex system. Promising results were also found from the adsorption experiments involving ionic species. The species trialled were Ni^{2+}, Cd^{2+}, Sr^{2+}, AsO_4^{3-} and F^{-}. Bone materials heated to 500 ^{o}C were consistently the most effective material for adsorption of the divalent metal cation species trialled. Adsorptions between this material and the divalent nickel and cadmium ions were found to follow pseudo second order kinetics, with Langmuir type isotherm behaviour. Fluoride adsorptions were also found to have a Langmuir type isotherm however the adsorption kinetics of this system were not investigated.

Overall the results from this study outline a few potential applications, which if investigated and developed further could add significant value to materials which

are currently produced in high volumes as waste by-products from the fishing industry in New Zealand.

Acknowledgements

Firstly, and most importantly I would like to offer my sincere gratitude towards Associate Professor Michael Mucalo, for his extremely helpful guidance as the chief supervisor on this project. Without his help, I would never have been able to achieve the results in this work. Secondly to Professor Bill Henderson, for his contributions and guidance towards to the enzyme immobilisation studies as my co-supervisor, an important piece of this project.

I would also like to thank Dr Matthew Cummings, Dr Kathleen Hofman and the rest of the team at Plant and Food, Nelson, for the provision of the raw materials, their assistance in the project, the financial support they provided, and for sitting through my lengthy presentation. The project would never have been possible without their contributions.

Thank-you to the many staff at the University of Waikato, in no particular order, who assisted with various aspects in this project:

- Professor Chris Battershill and Mr David Culliford from the Tauranga branch, for provision of the shell materials.
- Dr Erica Prentice for her assistance in the immobilisation of enzymes and kind donation of enzymes to be used in the project.
- Annie Barker for her amazing support in the running of the AAS, and IC analytical instruments.
- Steve Cameron for the running of all ICP-MS samples in this project.
- Helen Turner for guidance and training in the use of the SEM instrument.
- Dr Mark Lay for his guidance and training in the use of the XRD instrument.
- Renat Radosinsky and Annette Rodgers for training and allowing for the use of the ring mill equipment.

Thank you to the University of Waikato for providing the facilities, and means to complete this thesis, and for the financial assistance through the MSc (research) scholarship.

A special mention of thanks goes to my fellow postgraduate chemistry students, who assisted with numerous stressed days and allowed for excellent debriefing sessions over a cup of coffee

Finally, I would also like to acknowledge the people in my life who have supported me throughout the completion of this degree, especially – Alana, Nigel, Anthea and Rory, I would not have been able to complete this achievement without your continued support.

Table of contents

List of Figures

List of Tables

List of Abbreviations

°C	degrees Celsius
AAS	atomic absorption spectroscopy
CP	Cross Polarisation
EPA	Environmental Protection Agency
FT-	Fourier Transform
g	gram
HAp	hydroxyapatite
IC	ion chromatography
ICP-	inductively coupled plasma
IR	infrared
MAS	magic angle spinning
mg	miligram
Min	minutes
mL	mililitre
$molL^{-1}$	moles per litre
MS	mass spectrometry
NMR	nuclear magnetic resonance
ppm	parts per million
SEM	scanning electron microscopy
SS	solid state
TCP	tricalcium phosphate
TGA	thermogravimetric analysis
WHO	World Health Organisation
XRD	X-ray diffraction

Chapter One: Introduction and Literature survey

1.1 Bone as a by-product from the fishing industry

In New Zealand over 1 million tonnes of fish are caught every year and it is estimated that from this catch, approximately 75 % of the weight is used directly for human consumption, with the remaining 25 % either being discarded, or used in the production of fish oil, fish meal, fertiliser and pet foods, all of which are of relatively low economic value[1-2]. It would therefore be significantly beneficial, both environmentally and economically, if these materials could be utilised in a higher value application, especially if this were to obviate the need to dispose of large volumes of waste by-products in landfills.

A main portion of this waste is the bone skeleton in the fish (~ 10 – 15 % of the total body weight[3]), with the principal component of this bone being hydroxyapatite (HAp)[4], which in natural bone is manifest as a calcium-deficient carbonated hydroxyapatite.

1.2 Calcium Phosphates

1.2.1 Hydroxyapatite (HAp)

Hydroxyapatite is one of the many calcium phosphates, with the chemical formula $Ca_{10}(PO_4)_6(OH)_2$. HAp is one example of an apatite, the general term for crystalline minerals with the general formula of $M_{10}(ZO_4)_6X_2$. Several chemicals can take the place of M, Z and X. Some of these possibilities are summarised in Table 1-1 below.

Table 1-1: Examples of chemicals which can make up apatites[5]

Component	Possible elements
M	Ca, Sr, Cd, Mg, Pb, K, Na
Z	P, CO3, V, Cr, B, As
X	OH, CO3, O, F, Br, Cl

HAp has a molecular weight of 1004.8 g/mol, the crystal structure exists in a hexagonal lattice system, with the space group $P6_3/m$.[6] A schematic of the HAp crystal structure is given below in Figure 1-1.

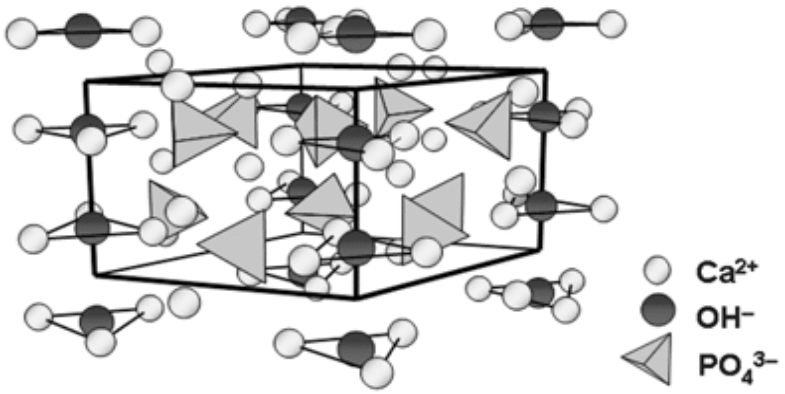

Figure 1-1: Crystal structure schematic of hydroxyapatite[7]

The substitution of other atoms or groups for Ca, PO_4 or OH in the lattice influences changes to the morphology and lattice parameters. Some of these effects are summarised later in Table 1-2.

1.3 Composition of Natural Bone Materials

1.3.1 Principal components of animal bone

Natural bone materials are made up of approximately 60 % mineral phase by weight, 10 % water, and the remaining 30 % is composed of organic materials such as oils, fats, and collagenous matter[4].

1.3.1.1 Inorganic mineral phase

The inorganic mineral component of bone is primarily composed of carbonated hydroxyapatite, which means that carbonate is substituted into the HAp lattice. This can occur via two modes of substitution, type-A and type-B, where the carbonate ion replaces either the hydroxide, or phosphate ions in the HAp crystal lattice respectively[8]. These two types influence the crystal lattice differently, in type-A, the substitution for the smaller OH ion leads to an expansion in the a-axis and contraction in the c-axis, giving an overall expansion in the lattice. In type-B however, the phosphate ion is larger than the carbonate ion, and so the effect is opposite, leading to an overall contraction in the lattice. Several other substitutions, both anionic and cationic may take place with these being heavily influenced by the physiology of the surrounding solution, as well as the climate the organism exists in[9], the diet, sex and age of the individual. Some anionic substitutions include F^-, Cl^-, and SiO_4^{4-}, and some cationic substitutions include Na^+, Mg^{2+}, K^+, and Al^{3+}. Additionally, trace levels of heavy metals are also able to be incorporated into the lattice, such as Sr^{2+}, Pb^{2+} and Cd^{2+}, all of which can have negative impacts on the structure of bones. The effects of these substitutions on the lattice parameters and crystallinity are summarised in Table 1-2 below.

Table 1-2: Effects of some substituents for Ca^{2+}, OH^- and PO_4^{3-} in HAp ($Ca_{10}(PO_4)_6(OH)_2$) on lattice parameters and crystallinity[10].

Substituent	Ionic radii (Å)	a-axis (Å)	c-axis (Å)	Crystallinity
Calcium (Ca^{2+})	0.99	9.438	6.882	
		for Calcium, Ca^{2+}		
Strontium (Sr^{2+})	1.12	+	+	nc (no change)
Lead (Pb^{2+})	1.20	+	+	-
Sodium (Na^{+})	0.97	nc	nc	nc
Cadmium (Cd^{2+})	0.97	-	-	-
Magnesium (Mg^{2+})	0.66	-	-	-
Aluminium (Al^{3+})	0.51	+	+	-
		for OH^-		
Fluoride (F^-)	1.36	-	nc	+
Chloride (Cl^-)	1.81	+	-	nc
		for PO_4^{3-}		
Carbonate (CO_3^{2-})		+	nc	nc

Due to this lability in the HAp lattice, the environment in which an organism resides is likely to influence the elemental composition. Hence, bones originating from different species are likely to have different levels of trace metals i.e. bones from a bovine origin are likely to have different compositions to bones from a marine environment. Bones from marine species are likely to have elemental compositions mimicking the relative level of elements in the oceans, while bones from a bovine origin are more likely to be influenced by the grass/feed diet of this herbivorous animal[11].

1.3.1.2 Organic materials

The organic matter in bone materials is primarily composed of collagen. There are several different types of collagen[9], however the most commonly found collagen in bone is type I collagen[12-14] (~ 90 % of organic weight). The remaining 10 % is made up of ~5 % noncollagenous proteins, ~2 % lipids, and water[14].

Mineralisation of collagen fibres in the structure of bone, and its intimate integration with the inorganic mineral of bone, are both vital to the strength of the overall material[15]. In bone, collagen has a multi-hierarchal suprastructure[16]. The smallest unit, the peptide chain contains approximately 1000 amino acids, which contain a repeating glycine-x-y motif where x and y are often proline and hydroxyproline respectively. This characteristic motif enables the formation of a left-handed helix. Three peptide chains twist into a right-handed coil forming a triple helical[9, 17] structure to form a collagen molecule, which are aligned in a

staggered array with other collagen molecules to form collagen fibril. The structures of the components which make up the collagen fibrils are given in Figure 1-2 below.

Figure 1-2: Structures of components which make up collagen fibrils[17].

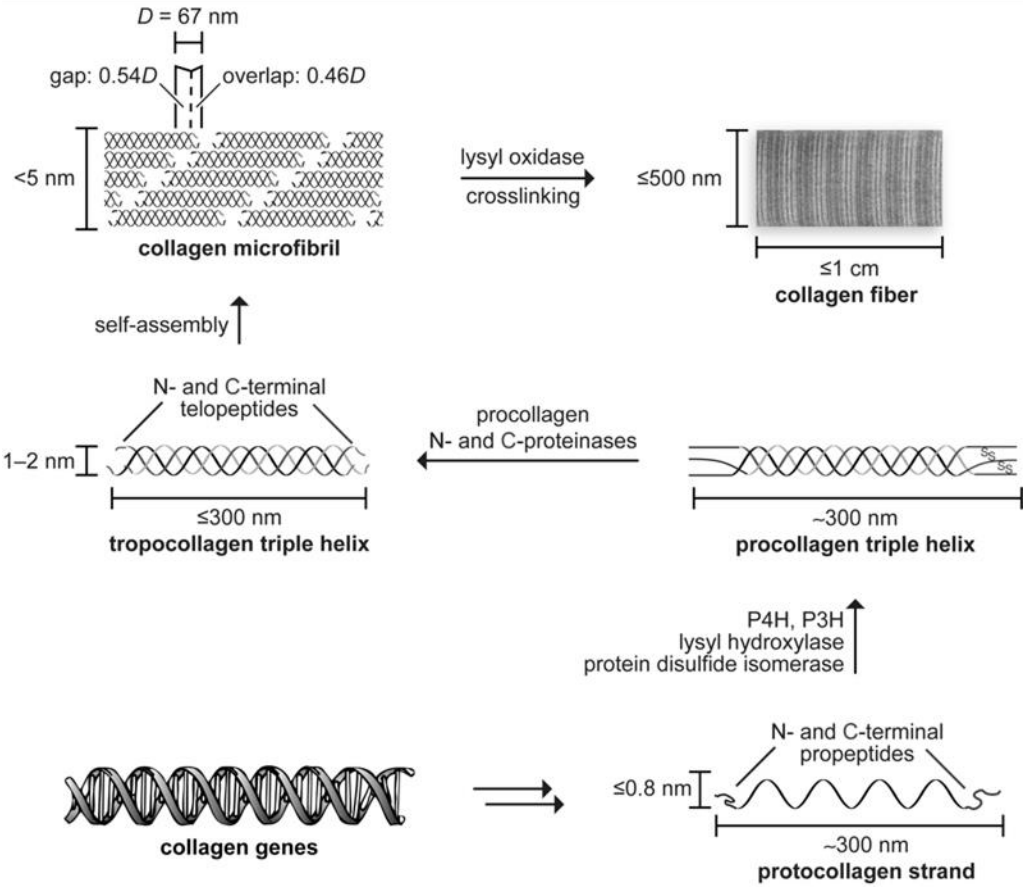

The non-collagenous proteins consist of ~30 proteins with varying functions[13], such as extra cellular matrix proteins, and growth factors The relative amounts of these proteins in bone varies with a range of factors, such as age, position in body, gender and health status[14]. Lipids found in the bone matrix are mainly composed of triesters of fatty acids and glycerol (termed triacylglycerol).

1.3.2 Principal components of marine animal shells

The composition of marine shells is less complex than the bone matrices in animals. The majority of marine derived shells is composed of > 90 % calcium carbonate[18] by weight, as aragonite, calcite, or a mixture of the two polymorphs[19]. The remainder of the material is composed of organic matter, such as protein molecules throughout the mineral, and an outer layer of chitin on the shells[20].

1.4 Background and Literature Survey for the Study

1.4.1 Characterisation techniques for bone and shell materials

A wide range of techniques is available to characterise these materials, including Fourier transform-infrared spectroscopy (FT-IR), solid state nuclear magnetic resonance spectroscopy (SS-NMR), X-ray diffractometry (XRD), scanning electron microscopy (SEM) and inductively coupled plasma mass spectrometry (ICP-MS). These techniques are often used in conjunction with each other to provide detailed characterisations.

1.4.1.1 FT-IR characterisation

FT-IR spectroscopy is a widely used analytical technique which is based on the vibrations of bonds between atoms in a molecule. Infrared radiation is passed through a sample, the bonds between atoms in the sample will absorb specific energies, and the unabsorbed radiation will pass through the sample to the detector. The resulting interferogram over a range of infra-red wavelengths is converted through a mathematical function (known as a Fourier transform) to an infrared spectrum (intensity vs frequency). As bonds between atoms absorb specific frequencies, the observed spectra give valuable information on the specific types of bonds present in a given sample.

FT-IR can be used to give details on mineral phases present in a given material. For example, small differences are found in the IR spectra of the two polymorphs aragonite and calcite, the use of FT-IR can therefore aid differentiation between which polymorph is present in a shell material[21]. The technique also gives valuable information on the nature of the hydroxyapatite present in a bone sample. The presence of phosphate, carbonate, and collagen can be easily identified by their characteristic peaks in the IR spectrum. It can also be used to distinguish different calcium phosphate phases through characteristic spectral patterns.

1.4.1.2 Solid State Nuclear Magnetic Resonance Spectroscopy

Nuclear magnetic resonance (NMR) spectroscopy utilises the magnetic properties of atomic nuclei and gives detailed information on the structure of compounds. Nuclei which do not have an even number of both neutrons and protons, such as ^{1}H and ^{13}C, are said to have a property called spin, which enables them to be NMR active. The NMR spectrometer utilises a strong magnetic field with a radio-

frequency generator, which interact with nuclei containing spin. When this interaction occurs, the NMR active nuclei can be excited to a higher energy level, these are allowed to relax and during this relaxation the nuclei emit an amount of energy characteristic to the nucleus targeted, as well as the chemical environment surrounding it. The chemical environment influences a property termed chemical shift, and so values of the chemical shift for a given nuclei give detailed information on the surrounding structures. Another feature of NMR spectra is the splitting of peaks due to spin-coupling, termed multiplicity. This occurs when one or more NMR active nuclei are bonded to neighbouring atoms. The distance between splitting of a peak allows for calculations of coupling constants and adds to the valuable structural information obtained through peak multiplicities. The number of atoms contributing to a line can also be determined through the size of the given peak, as these are proportional to each other.

Generally, NMR spectra are recorded in the liquid state, and require the sample to be dissolved in an appropriate solvent. However due to the insoluble nature of the materials used in this study, solid state NMR (SS-NMR) was instead utilised. SS-NMR is not as simple as conventional NMR to carry out due to the loss of free motion in the samples. The molecules in solid samples are relatively static (compared to liquid phase molecules) and so the interactions described above are strongly dependent on the orientation of the solid in the magnetic field. In a given solid the molecules will be fixed in a range of orientations, and so the resulting peaks in the NMR spectrum will be much broader compared to a typical liquids NMR spectrum. This issue can be mitigated however through the employment of a magic angle spinning (MAS) unit. The samples are spun at high speeds (5 kHz in this study) at a specific orientation called the 'magic angle' (at 54°44' relative to the direction of the magnetic field). This significantly reduces the broadness observed in the peaks of the NMR spectra and therefore allows the structural characterisation of solid state samples.

1.4.1.3 Powder X-Ray Diffraction

The wavelengths of X-rays are of similar magnitude to the distances between atoms in crystalline materials. This similarity allows crystal materials to scatter x-rays, giving constructive interference patterns at specific angles (**Figure 1-3** below), which are characteristic of the atomic structure of a material.

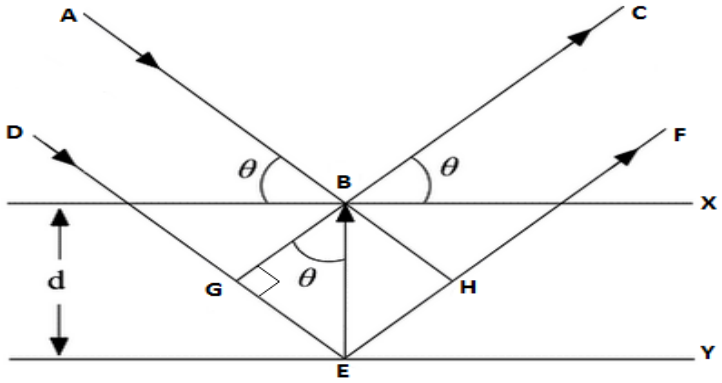

Figure 1-3: Diffraction of X-rays by the planes in a crystal

Diffractions occur according to Bragg's Law:

$$n\lambda = 2dsin\theta$$

Where n is an integer, λ represents the wavelength of the incident wave, d is the interlattice spacing in the crystal, and θ is the scattering angle. To obtain detailed crystal structures, large single crystals are required. However, a diffraction pattern containing useful information can still be obtained from analysing a fine powder. This is possible through the assumption that the sample is randomly arranged, hence a statistically significant number of each plane of the crystal will be in the correct orientation to satisfy the Bragg equation and diffract the x-rays. Scans are performed at a range of incident angles, which generate a diffraction pattern unique to the sample being analysed. The observed diffraction pattern can then be compared to databases containing a vast number of known materials for identification.

Both hydroxyapatite and calcium carbonate can be turned into powders for analysis using XRD. It is possible to analyse pure known samples of these materials using XRD, to be compared and matched to unknown samples for ease of identification.

1.4.1.4 Scanning electron microscopy (SEM)

A scanning electron microscope is a type of electron microscope which generates images of a sample by exposing the surface of the material (which has been coated in a conductive metal material) to a focussed electron beam. The electrons are back-scattered to a secondary electron detector, which provides information on the surface topography of a material. This information is then converted to a grey-scale image.

1.4.1.5 Inductively coupled plasma mass spectrometry (ICP-MS)

Inductively coupled plasma mass spectrometry (ICP-MS) is a form of mass spectrometry which is capable of performing multi-elemental analyses at extremely low concentrations (parts per billion and parts per trillion). Samples are introduced to the instrument as liquids, so solid samples need to first be digested in a suitable acid, generally HNO_3. The liquid sample is converted into a fine aerosol spray in the spray chamber by a nebuliser, the aerosol then enters an argon plasma flame which rapidly breaks down the sample to its constituent atoms and ions, creating a beam of singly charged positive ions. These ions then pass through a series of cones into a high vacuum mass analyser. Mass to charge ratios are used to determine the isotopes of elements present. Computer software connected to the instruments allows the calculation of elemental concentrations using the intensity of the peaks observed.

Elemental analyses on digested bone-derived materials gives valuable information on the type of environment the bone samples may have come from. Bones derived from saltwater fish species are likely to have metal concentrations mimicking the natural level of these metals in the oceans. If bone-derived materials are to be used in biomedical applications it is important to know the levels of different elements, especially those which are regarded as toxic, such as Cd, Hg and Pb. Elemental analyses also enable the calculation of the calcium: phosphorus ratio for a bone material. This gives information on the nature of the calcium phosphate phase present in the material. Stoichiometric HAp has a Ca:P ratio of 1.67, however as mentioned above animal bones generally have an altered apatite called carbonated hydroxyapatite. These usually have Ca:P ratios exceeding 1.67.[22] Therefore ICP-MS can be used to determine the extent of carbonate substitution. One of the disadvantages of ICP-MS is that the technique is destructive, and requires solid samples to be digested which adds time to analysis. It is however still a powerful tool for the characterisation of these materials.

1.4.1.6 Atomic absorption spectroscopy (AAS)

Atomic absorption spectroscopy is a form of spectroscopy which detects and analyses the optical radiation emitted by free atoms in a gaseous state and relates these back to a concentration of these elements in the sample. Samples must be atomised prior to analysis, the most common type of atomiser is the flame atomiser, which is also the apparatus used in this study. Liquid samples are introduced into

the instrument through a capillary tube, and are transformed into an aerosol, which is exposed to and mixed in with the flame gases. The atoms in the flame mix are exposed to optical radiation from lamps in the instrument usually specific to the element of interest. This radiation passes through a monochromator to isolate the specific wavelength of interest for a given element, which is then measured by the detector. AAS is generally considered an inferior technique to ICP-MS as the latter is capable of analysing a wide variety of elements simultaneously. AAS however can only measure one element at a time and is hence time consuming. However, in instances where the concentration of only one or two elements is desired, AAS can be the superior technique as the costs are significantly lower than ICP-MS. AAS was used in the metal ion adsorption experiments in this study because of this low-cost advantage, and quick turn-around time of results.

1.4.1.7 Ion chromatography (IC)

Ion chromatography is an analytical chromatographic technique which enables the separation and determination of ionic species in liquid samples. Samples are introduced to the top of the column, and are then passed through the column using an eluent. Different ionic species will pass through the column at different rates and hence will be detected at different times, which produces a chromatogram. Computer software can then be used, along with a standard calibration curve, to calculate concentrations of elements based on the peak sizes in the chromatogram. A wide range of different mechanisms for interaction between ionic species and the column are understood to exist and influence the rate at which a species will elute from the column. In this study, ion chromatography was utilised to analyse the concentration of the fluoride anion in water samples following adsorption experiments.

1.4.2 Processing techniques for bone-derived materials

To qualify for use in biomedical applications, natural bone samples must be free from all organic species to reduce the risk of infection/spread of diseases. For this reason, several processing techniques have been developed for bone materials.

Thermally treating bone materials is a common method of processing to remove organic matter from the materials[23-25]. It is understood that at temperatures above 600 ^{o}C, all detectable organic material is lost due to being burnt off from the

materials[26]. This method is simple to carry out, however includes some key disadvantages. One of these consequences is that these high temperatures cause the materials to become brittle and lose a significant amount of mechanical strength. Another risk is that phase changes may occur within the material as the treatment temperature is increased. It is understood that calcium carbonate decomposes at temperatures exceeding 700 ^{o}C to form CaO and CO_2. The small amounts of $CaCO_3$ which exist in the bone materials also are susceptible to this conversion, which can result in the deposition of CaO on the surface of the HAp material. CaO induces alkalinity when placed in an aqueous medium, such as in the body, and it is well known that alkalinity is cytotoxic, which can lead to complications around the area of an implant in the body. This can be avoided, through thorough washing of the HAp material to remove any residual CaO.

Chemical treatments can instead be used to treat the materials. Several chemical methods have been employed to either remove organic material from natural bone, or synthetically produce HAp using natural bone as a starting material.

As there are two major components to the organic material in bone, collagen (proteins) and lipids (fats) there is often the need for two steps, deproteination and defatting. Deproteination can be achieved using several chemicals, commonly used examples are bleach (either NaOCl or H_2O_2) and alkaline materials (KOH and NaOH). The use of bleach has been found to be the superior method for deproteination of bone materials as it can achieve higher removals, and has the smallest influence on the structural integrity of the bone[27].

Johnson, 1998[9] trialled a number of solvents for the defatting of bone materials. His work found that the most efficient solvent for defatting bone materials was methyl acetate. Solutions of NaOH however have been shown to be efficient in both deproteination and defatting of bone materials. And so, it is possible that both of these steps can be achieved in just one step instead. Achieving complete removal of organic material is difficult using chemical methods, however thermally treating the bones at a high enough temperature is essentially guaranteed to achieve complete removal of organics, and so this will be the main technique used in this study.

It is also possible to use bone-derived materials as starting materials for synthetic hydroxyapatite, such as through the digestion and subsequent reprecipitation of the material[28]. This involves the use of a strong mineral acid to digest the bone structure, followed by the addition of strong base to the digest solution. It has been shown

that this process can be scaled up to produce synthetic hydroxyapatite in large volumes. Depending on the source of the bone, some pre-treatments are necessary before this method can be carried out. For example, if bovine bones are used, these first need to be cut and ground down to an appropriate size. The study aimed to utilise much smaller fish bones, which could be reduced to the appropriate size (to fit inside reaction vessels) with ease.

1.4.3 Potential applications of bone materials

A range of potential applications for bone materials has been investigated in the literature.

1.4.3.1 Biomedical applications

Both synthetic and naturally derived HAp can have a variety of biomedical applications. The most common of these is the use of HAp in implants/bone replacements. This was first referred to by an Austrian ophthalmologist, who used spheres of cancellous bone which had been heated in a furnace[29]. These materials however were found to be very fragile after exposure to the high temperatures, which would cause degradation and removal of the collagen. Due to the risk of infections and spreading of diseases, these materials must have their organic components removed prior to incorporation into living bodies. This can be done through a range of methods, however the most simple is to treat the materials with such high temperatures (> 1000 ^{o}C) that the organic content is burnt off[30]. Chemical treatments can also be used to remove the organic matter, such as supercritical fluid, bleach, H_2O_2[31], and lactic acid bacteria[32], all of which are able to simultaneously remove the protein and lipid content of the bone material. A common issue with these bone materials after processing is that they become brittle and unsuitable for load bearing applications[29].

Because of this, a more common biomedical use for these bone materials is to use HAp (derived from natural bone sources), as a coating on metallic based implants. This coating can be done throul several methods, such as sol-gel dip coating[33], pulsed laser deposition, and thermal spraying (plasma spray). Plasma spray is widely used in the literature and is generally regarded as the superior method for coating implants with HAp[34]. The use of plasma spray generates high temperature HAp particles, which have a fast cooling rate and produce amorphous calcium phosphate on the surface of the material once it cools down. This is advantageous

for implants as it produces a coating which dissolves faster than a crystalline HAp phase. Plasma spray does however have its drawbacks as it is unable to coat porous implants, and is also unable to incorporate biologically active materials[35] (as a result of the high temperatures). Regardless of this, it is still an effective technique using HAp material obtained from natural sources.

1.4.3.2 Environmental applications

The calcium ion in the HAp lattice is labile and can be substituted out with a range of other metal ions, including some heavy metal ions such as nickel[36], cadmium[37], and strontium[38]. The presence of these metals in nature and through introduction to water bodies through industrial processes is an issue due to their toxicity, and non-biodegradable, cumulative nature, hence developing methods to remove these from contaminated waters is of particular interest. The use of natural bone samples as adsorbents for these materials has not been the focus of many studies, but these would offer an extremely cheap method of water treatment and metal removal if these could be utilised in a similar manner to synthesised HAp.

1.4.3.2.1 Nickel and cadmium

Most nickel and cadmium waste comes from manufacturing processes, such as the production of Ni-Cd batteries[28]. Nickel is hazardous to human health, the adverse effects of exposure to nickel depending on the type of exposure (i.e. dermal, ingestion, inhalation) but generally, for acute exposures the symptoms are contact dermatitis dizziness, headaches. Chest pains can also result but the onset of these are usually delayed. Chronic exposures can lead to cardiovascular and kidney diseases, as well as the potential to cause cancer in the respiratory tract[39]. Cadmium is also well documented to be hazardous, in both acute and chronic doses. Inhalation of cadmium contaminated air can lead to shortness of breath, and destruction of mucous membranes. Intake of cadmium contaminated food/water can cause vomiting and diarrhoea when the concentration is at unsafe levels[40]. Chronic exposure to cadmium commonly leads to kidney damage, with a biological half-life of 10 years, it can accumulate in the body over time. Chronic Cd exposure has also been associated with the occurrence of Itai Itai disease, in which patients experience high rates of bone fractures, and intense associated pain. It is thought that the source of this is through cadmium substituting for calcium in the carbonated HAp lattice found in bone materials. It is this same substitution property which is being

exploited when HAp powders are used to remediate water contaminated with cadmium.

Currently, industries treat heavy metal contaminated water through the lime-soda precipitation technique[41]. This however produces a large volume of contaminated sludge material, and the waste water requires further treatment. Due to the stability of hydroxyapatite, it offers an ideal matrix for long term capture of these metals. For this reason, several studies have investigated the potential for the material to be used in treating contaminated waters. Generally, these studies have used synthesised nano-HAp particles, and the adsorption on these particles have been found to follow the Langmuir isotherm model, which allow calculations of adsorptive capacities. Some reported adsorptive capacities of nano-HAp particles for these metals are 46.17[36] mg/g for Ni^{2+} and 142.86[37] mg/g for Cd^{2+}. Once adsorbed to the materials, desorption of the metal back into solution is low. This is an important feature if the materials are to be disposed of, as it will prevent the metals from re-entering the environment.

1.4.3.2.2 Strontium removal

Natural levels of stable strontium in the environment and water systems are generally not harmful to humans. Higher levels of strontium however have been shown to influence the mineralisation of bone materials in animals, through replacement of the calcium ion in the bone mineral[42]. The adsorption of strontium is of interest given the events surrounding the Fukushima Daiichi nuclear power plant following the tsunami incident in March 2011. This area was exposed to significant levels of radioactive nuclides, such as ^{134}Cs, ^{137}Cs and ^{90}Sr. ^{90}Sr is considered a waste product of the nuclear industry, as it has limited uses elsewhere. And due to its radioactive nature, its presence in the environment is considered a risk. In light of this incident, HAp materials have been found to be able to remove more than 90 % of the initial Sr content in laboratory generated samples[38]. These methods involved the generation of a column from the HAp material, through which aqueous strontium samples were passed through. These column adsorption experiments demonstrated an adherence of the system tested to the Langmuir type isotherm model, with an adsorptive capacity of 27 μmol/g being measured. Desorption was also found to be low as observed with the cadmium and nickel-HAp systems in the aforementioned studies, suggesting that that adsorption is strong, which is beneficial if the materials are to be uplifted and disposed of.

1.4.3.2.3 Arsenic removal

Arsenic is commonly found in nature and is a known poison and co-carcinogen in humans. Humans are mostly exposed to arsenic through contamination in drinking waters. The most common source of arsenic contamination in water samples is arsenic leaching from rock formations into water sources[43]. Arsenic can be used in industry to produce paints, pesticides and wood preservation, and it is an essential trace element for some animals, hence it is sometimes included as an additive in animal feed. The speciation of arsenic plays an important role in its toxicity, in foods, it is generally present in organo-arsenic type compounds, these are rapidly exchanged and excreted in urine and are generally considered non-toxic. Inorganic species however, such as the ones which leach from rocks into water samples, are considered highly toxic. Acute exposure to arsenic generally occurs through accidental ingestion of pesticides. Acute exposures can lead to nausea, vomiting, abdominal pain, diarrhoea, and in higher doses, lethal.

Chronic exposure to arsenic has been linked to multisystem diseases. Some of those which can be affected are the gastrointestinal, cardiovascular, neurological and respiratory systems. Long term exposure can also lead to the onset of cancer, as well as changes in the skin of an individual[44].

When arsenic is the anionic form of arsenate (AsO_4^{3-}, As(V)), as it is often found in arsenic contaminated water, there is the potential for it to substitute into the HAp lattice in place of orthophosphate anions (PO_4^{3-}) [45-46]. Other reports[47] have suggested that the method of removal is through co-precipitation as well as ion exchange, however the exchange is with OH^- instead of PO_4^{3-}, and the following reactions are suggested:

Co-precipitation:

$Ca_{10}(PO_4)_6(OH)_2 + Ca^{2+} + HAsO_4^{2-} \rightarrow Ca_{10}(PO_4)_6(OH)_2.Ca(HAsO_4)$

Ion exchange:

$Ca_{10}(PO_4)_6(OH)_2 + HAsO_4^{2-} \rightarrow Ca_{10}(PO_4)_6(HAsO_4) + 2OH^-$

Regardless of the specific mechanism, the materials appear to show great potential as adsorbents for arsenate, which will be investigated as part of this study.

1.4.3.2.4 Fluoride removal

The hydroxide ion component can be replaced by several anionic species, such as Cl^- and F^-[48]. Fluoride substitution is of particular interest as this is commonly found and regulated in drinking water supplies. It is well understood that the addition/regulation of fluoride in drinking waters is beneficial for human health[49].

Some adverse acute effects of fluoride include nausea, vomiting, hypotension, and in extreme cases where the fluoride dosage is high, coma and subsequent death can result. Adverse chronic effects of unsafe fluoride levels include skeletal fluorosis, birth defects, gastric irritation and muscular spasms.

It is therefore important that the level of fluoride in drinking water supplies is monitored and maintained at the safe, beneficial level. There are however areas in the world in which the natural fluoride content is higher than the US EPA recommended safe level of 4 mg/L[50], and drinking water supplies are not regulated. In such areas, access to fluoride removal technologies can be limited due to the associated economic costs. The use of bone-derived materials for this application mitigates this as these should be a low-cost product. Removal percentages of up to 86 % for the fluoride anion have been found using hydroxyapatite materials[48]. Due to the promising results in the literature for similar materials, the materials in this project were subject to similar experiments to determine their suitability as adsorbents for water contaminants.

1.4.3.3 Enzyme Immobilisation

Immobilised enzymes, are enzymes which are physically or chemically bound to a solid support material, ideally with the retention of their catalytic ability, which can be repetitively used, and are generally easier to handle than typical in-solution enzymes[51]. Support surfaces can also increase the lifetime of the enzymes, improve the thermal and pH stabilities[52], increase the availability of the enzyme to the substrate, and enable an easy method of recovery of the enzymes after use[53] which also reduces protein contamination in the final product. Immobilisation also allows for enhanced control over reactions as it allows for on demand arrest of reactions through removal of the immobilised material from the reaction mixture. A variety of techniques to immobilise enzymes can be used, some of these are reversible physical adsorption, ionic linkages, and covalent bonding (irreversible) usually through the use of a coupling reagent which ideally does not negatively impact the enzymes activity[51]. During immobilisation, enzymes will often undergo chemical and physical changes which may vary depending on the immobilisation method used. Some covalent linkages can chemically and physically alter the reactive site of the enzyme, which may lead to decreased catalytic activity. An important factor in the success of an immobilised enzyme is the solid support surface chosen, several factors influence this, such as mechanical stability, non-toxicity, stability in a range

of solutions, and cost. An issue with commonly used materials, such as silica-based carriers, acrylic resins and synthetic polymers is that the cost of production is high, and complex technology is required to carry out the immobilisation methods, leading to an increased cost of the overall final product. It is therefore of particular interest to develop and investigate low-cost solid support materials, which have similar efficiencies to these more expensive materials.

Collagen has been found to be an ideal support surface for enzyme immobilisation through the use of a coupling reagent[9]. The collagen molecule contains many available carboxyl groups, which couple via the free amino groups on the enzyme material. Additionally, as collagen is a hydrophilic structure, it prevents denaturing of the enzymes bound to it, and promotes accessibility to the target molecules. As bone consists of interdigitated collagen inside a relatively insoluble and stable inorganic mineral matrix, it makes for an ideal candidate for enzyme immobilisation. Previous work has identified the potential for bovine bone-derived materials to act as a solid support system for enzymes, when combined with the coupling reagent tris-hydroxymethyl phosphine (THP)[54]. This study outlined the importance of using materials which still contained collagen in the bone matrix, as the collagen molecules were shown to be the reactive site for THP in the bone-derived material. Developing a similar enzyme immobilisation material out of these fish bone materials could be therefore be significantly rewarding, as their low cost and high volume mitigates some of the disadvantages faced by current support surfaces.

1.4.4 Previous animal species studied

Other work from this research group at the University of Waikato has seen extensive characterisation and investigation into bovine bone materials[9, 28].

A range of other species to date have also had their bones characterised. Kano et al, 1992[55] investigated spines extracted from rats, hens, bullfrogs, newts, carp, codfish, parrotfish and a shark. This wide range was selected to gain an idea of the differences between the apatite compounds from a range of different animals.

A number of studies investigating the bone skeletons of fish species have also been reported. Commonly studied species types are salmon[32, 56], cod[57-58], sword fish and tuna[24]. The use of fish bones offers an advantage over larger mammalian bones. These bones are already small and can be reduced to bone-powders with ease. While this makes the materials unsuitable candidates for implant materials, it adds

convenience to the methods required to produce powders from the bone materials. As mentioned earlier, these are also produced in significantly large quantities by the fishing industry in New Zealand, as well as globally. Studies involving New Zealand fish species appear to be less common in the literature, and so this study aimed to add to this knowledge gap by characterising and investigating the uses of bone materials from some New Zealand fish species which are caught in high volumes. Finding any use for such a high volume, low cost product, has the potential to be significantly beneficial for both the NZ environment, and economy.

1.5 Aims and Objectives of the Present Study

The purpose of this study was to extensively characterise the bone-derived powders from four different fish species, which are waste products from the fishing industry, and determine if there are any key differences between the powders from the different species.

The materials would then be subject to a range of processing methods, with characterisation carried out on the products of each method to understand the changes the material as a function of processing.

Once this work had been done, the primary goal was to investigate a few potential applications for the materials, with the focus being on water treatment. A summary of the main objectives investigated in this study are as follows:

- Characterise extensively as received bone-derived materials of four different fish species from Plant and Food, Nelson, and the shell exteriors of four marine shellfish species.

- Subject these materials to several processing techniques, with characterisation, to understand the effects of these processing steps.

- Investigate the potential for a range of as received and processed materials to act as an adsorbent material for the following divalent metal ions, Ni^{2+}, Cd^{2+}, Pb^{2+} and Sr^{2+}, as well as the arsenate and fluoride anions, to provide support for future investigations into the production of an adsorbent product.

- Study the suitability of as received materials as potential solid support surfaces for the immobilisation of enzymes.

1.6 Overview of the Study

As mentioned above, the main aims of this study were to characterise extensively with processing the bone-derived powders from four fish species, and the shell remains of four shellfish species, and to investigate potential applications for these materials. Chapter 2 covers the characterisation and processing techniques of these materials, while chapter 3 focuses on the potential applications for the materials. The final chapter (chapter 4) presents the conclusions drawn by this study, along with recommendations for future research.

References for Chapter One

1. Shahidi, F.; Kim, S. J.; Jung, W.-K., Calcium from Fish Bone and Other Marine Resources. 2007; p 419-430.
2. Arvanitoyannis, I. S.; Kassaveti, A., Fish industry waste: treatments, environmental impacts, current and potential uses. *International Journal of Food Science & Technology* **2008,** *43* (4), 726-745.
3. Malde, M. K.; Bügel, S.; Kristensen, M.; Malde, K.; Graff, I. E.; Pedersen, J. I., Calcium from salmon and cod bone is well absorbed in young healthy men: a double-blinded randomised crossover design. *Nutrition & Metabolism* **2010,** *7*, 61-61.
4. Oshida, Y., *Hydroxyapatite: Synthesis and Applications*. Momentum Press: 2014.
5. Aoki, H., *Medical Applications of Hydroxyapatite: Bone Mineral, Drug Delivery System, Cancer & HIV, IVH & CAPD, Dental Implant*. Ishiyaku EuroAmerica: 1994.
6. Kay, M. I.; Young, R. A.; Posner, A. S., Crystal Structure of Hydroxyapatite. *Nature* **1964,** *204*, 1050.
7. Vallet-Regi, M.; Arcos, D., Silicon substituted hydroxyapatites. A method to upgrade calcium phosphate based implants. *Journal of Materials Chemistry* **2005,** *15* (15), 1509-1516.
8. Astala, R.; Stott, M. J., First Principles Investigation of Mineral Component of Bone: CO3 Substitutions in Hydroxyapatite. *Chemistry of Materials* **2005,** *17* (16), 4125-4133.
9. Johnson, G. S. Characterisation and processing of biological hydroxyapatite. 1998.
10. Hench, L. L., *An Introduction to Bioceramics: Second Edition*. World Scientific Publishing Company: 2013.
11. Buddhachat, K.; Klinhom, S.; Siengdee, P.; Brown, J. L.; Nomsiri, R.; Kaewmong, P.; Thitaram, C.; Mahakkanukrauh, P.; Nganvongpanit, K., Elemental Analysis of Bone, Teeth, Horn and Antler in Different Animal Species Using Non-Invasive Handheld X-Ray Fluorescence. *PLoS ONE* **2016,** *11* (5), e0155458.
12. Tzaphlidou, M., Bone Architecture: Collagen Structure and Calcium/Phosphorus Maps. *Journal of Biological Physics* **2008,** *34* (1-2), 39-49.
13. Feng, X., Chemical and Biochemical Basis of Cell-Bone Matrix Interaction in Health and Disease. *Current chemical biology* **2009,** *3* (2), 189-196.
14. Boskey, A. L., Bone composition: relationship to bone fragility and antiosteoporotic drug effects. *BoneKEy Rep* **2013,** *2*.
15. Viguet-Carrin, S.; Garnero, P.; Delmas, P. D., The role of collagen in bone strength. *Osteoporosis International* **2006,** *17* (3), 319-336.
16. Ricard-Blum, S., The Collagen Family. *Cold Spring Harbor Perspectives in Biology* **2011,** *3* (1), a004978.
17. Shoulders, M. D.; Raines, R. T., COLLAGEN STRUCTURE AND STABILITY. *Annual review of biochemistry* **2009,** *78*, 929-958.
18. Hou, Y.; Shavandi, A.; Carne, A.; Bekhit, A. A.; Ng, T. B.; Cheung, R. C. F.; Bekhit, A. E.-d. A., Marine shells: Potential opportunities for extraction of functional and health-promoting materials. *Critical Reviews in Environmental Science and Technology* **2016,** *46* (11-12), 1047-1116.
19. Vijaya Ramnath, B.; Jeykrishnan, J.; Ramakrishnan, G.; Barath, B.; Ejoelavendhan, E.; Arun raghav, P., Sea Shells And Natural Fibres Composites: A Review. *Materials Today: Proceedings* **2018,** *5* (1, Part 1), 1846-1851.

20. Uster, B.; Trumm, D.; Pope, J.; Weber, P.; O'Sullivan, A.; Weisener, C.; Diloreto, Z., *Waste Mussel Shells to Treat Acid Mine Drainage: A New Zealand Initiative*. 2014.
21. Loftus, E.; Rogers, K.; Lee-Thorp, J., *A simple method to establish calcite: Aragonite ratios in archaeological mollusc shells*. 2015; Vol. 30, p 731-735.
22. Antonakos, A.; Liarokapis, E.; Leventouri, T., Micro-Raman and FTIR studies of synthetic and natural apatites. *Biomaterials* **2007,** *28* (19), 3043-54.
23. Zhou, J.; Zhang, X.; Chen, J.; Zeng, S.; De Groot, K., High temperature characteristics of synthetic hydroxyapatite. *Journal of Materials Science: Materials in Medicine* **1993,** *4* (1), 83-85.
24. Boutinguiza, M.; Pou, J.; Comesaña, R.; Lusquiños, F.; de Carlos, A.; León, B., Biological hydroxyapatite obtained from fish bones. *Materials Science and Engineering: C* **2012,** *32* (3), 478-486.
25. Ozawa, M.; Suzuki, S., Microstructural Development of Natural Hydroxyapatite Originated from Fish‐Bone Waste through Heat Treatment. *Journal of the American Ceramic Society* **2002,** *85* (5), 1315-1317.
26. Venkatesan, J.; Kim, S. K., Effect of Temperature on Isolation and Characterization of Hydroxyapatite from Tuna (Thunnus obesus) Bone. *Materials* **2010,** *3* (10), 4761.
27. Sciadini, M. F.; Dawson, J. M.; Johnson, K. D.; Sciadini, M. F., Evaluation of bovine‐derived bone protein with a natural coral carrier as a bone‐graft substitute in a canine segmental defect model. *Journal of Orthopaedic Research* **1997,** *15* (6), 844-857.
28. Foster, D. L. Studies on calcium phosphates derived from New Zealand animal bone. Thesis (M. Sc. Chemistry)--University of Waikato, 2001., 2001.
29. Allen, T. D., Guist's Bone Spheres. *American Journal of Ophthalmology* **1930,** *13* (3), 226.
30. Mucalo, M., *BOOK: Hydroxyapatite (HAp) for Biomedical Applications*. Woodhead Publishing: 2015.
31. Frayssinet, P.; Rouquet, N.; Mathon, D.; Autefage, A.; Fages, J., Histological integration of allogeneic cancellous bone tissue treated by supercritical CO2 implanted in sheep bones. *Biomaterials* **1998,** *19* (24), 2247-53.
32. Ruthu; Murthy, P. S.; Rai, A. K.; Bhaskar, N., Fermentative recovery of lipids and proteins from freshwater fish head waste with reference to antimicrobial and antioxidant properties of protein hydrolysate. *Journal of Food Science and Technology* **2014,** *51* (9), 1884-1892.
33. Li, Y.; Li, Q.; Zhu, S.; Luo, E.; Li, J.; Feng, G.; Liao, Y.; Hu, J., The effect of strontium-substituted hydroxyapatite coating on implant fixation in ovariectomized rats. *Biomaterials* **2010,** *31* (34), 9006-14.
34. Vincenzini, P., *Ceramics in Substitutive and Reconstructive Surgery: Proceedings of the Satellite Symposium 3 on Ceramics in Substitutive and Reconstructive Surgery of the 7th International Meeting on Modern Ceramics Technologies (7th CIMTEC - World Ceramics Congress), Montecatini Terme, Italy, 27-30 June 1990*. Elsevier: 1991.
35. Habibovic, P.; Barrère, F.; Blitterswijk, C. A.; Groot, K.; Layrolle, P., Biomimetic Hydroxyapatite Coating on Metal Implants. *Journal of the American Ceramic Society* **2002,** *85* (3), 517-522.
36. Mobasherpour, I.; Salahi, E.; Pazouki, M., Removal of nickel (II) from aqueous solutions by using nano-crystalline calcium hydroxyapatite. *Journal of Saudi Chemical Society* **2011,** *15* (2), 105-112.

37. Mobasherpour, I.; Salahi, E.; Pazouki, M., Removal of divalent cadmium cations by means of synthetic nano crystallite hydroxyapatite. *Desalination* **2011,** *266* (1), 142-148.
38. Nishiyama, Y.; Hanafusa, T.; Yamashita, J.; Yamamoto, Y.; Ono, T., Adsorption and removal of strontium in aqueous solution by synthetic hydroxyapatite. *Journal of Radioanalytical and Nuclear Chemistry* **2016,** *307* (2), 1279-1285.
39. Duda-Chodak, A. D. A.; Błaszczyk, U., *The impact of nickel on human health*. 2008; Vol. 13, p 685-696.
40. Godt, J.; Scheidig, F.; Grosse-Siestrup, C.; Esche, V.; Brandenburg, P.; Reich, A.; Groneberg, D. A., The toxicity of cadmium and resulting hazards for human health. *Journal of Occupational Medicine and Toxicology (London, England)* **2006,** *1*, 22-22.
41. Kurniawan, T. A.; Chan, G. Y. S.; Lo, W.-H.; Babel, S., Physico–chemical treatment techniques for wastewater laden with heavy metals. *Chemical Engineering Journal* **2006,** *118* (1), 83-98.
42. Cohen-Solal, M., Strontium overload and toxicity: impact on renal osteodystrophy. *Nephrology, dialysis, transplantation : official publication of the European Dialysis and Transplant Association - European Renal Association* **2002,** *17 Suppl 2*, 30-4.
43. Tyler, C. R.; Allan, A. M., The Effects of Arsenic Exposure on Neurological and Cognitive Dysfunction in Human and Rodent Studies: A Review. *Current Environmental Health Reports* **2014,** *1* (2), 132-147.
44. Ratnaike, R. N., Acute and chronic arsenic toxicity. *Postgraduate Medical Journal* **2003,** *79* (933), 391-396.
45. Young Lee, P. S., Yuanzhi Tang, Wei Li, Brian L. Phillips, John Parise, Richard Reeder, Arsenate substitution in hydroxylapatite: Structural characterization of the Ca5(PxAs1–xO4)3OH solid solution. *American Mineralogist* **2009,** *94* (5-6), 666-675.
46. Mahsa, M.; Esmaeil, B.; Keivan, S., Removal of Arsenic from Drinking Water by Hydroxyapatite Nano Particles. *Current World Environment 26* (28), 331-338.
47. Chen, Y.-N.; Chai, L.-Y.; Shu, Y.-D., Study of arsenic(V) adsorption on bone char from aqueous solution. *Journal of Hazardous Materials* **2008,** *160* (1), 168-172.
48. Mourabet, M.; El Rhilassi, A.; El Boujaady, H.; Bennani-Ziatni, M.; El Hamri, R.; Taitai, A., Removal of fluoride from aqueous solution by adsorption on hydroxyapatite (HAp) using response surface methodology. *Journal of Saudi Chemical Society* **2015,** *19* (6), 603-615.
49. Ullah, R.; Zafar, M. S.; Shahani, N., Potential fluoride toxicity from oral medicaments: A review. *Iranian Journal of Basic Medical Sciences* **2017,** *20* (8), 841-848.
50. Fawell, J.; Bailey, K.; Chilton, J.; Dahi, E.; Fewtrell, L.; Magara, Y., *Fluoride in Drinking-water*. IWA Publishing: 2006.
51. Mohamad, N. R.; Marzuki, N. H. C.; Buang, N. A.; Huyop, F.; Wahab, R. A., An overview of technologies for immobilization of enzymes and surface analysis techniques for immobilized enzymes. *Biotechnology, Biotechnological Equipment* **2015,** *29* (2), 205-220.
52. Datta, S.; Christena, L. R.; Rajaram, Y. R. S., Enzyme immobilization: an overview on techniques and support materials. *3 Biotech* **2013,** *3* (1), 1-9.
53. Sheldon, R. A., Enzyme Immobilization: The Quest for Optimum Performance. *Advanced Synthesis & Catalysis* **2007,** *349* (8‐9), 1289-1307.

54. Johnson, G. S.; Mucalo, M. R.; Lorier, M. A.; Gieland, U.; Mucha, H., The processing and characterization of animal-derived bone to yield materials with biomedical applications. Part II: milled bone powders, reprecipitated hydroxyapatite and the potential uses of these materials. *Journal of materials science. Materials in medicine* **2000,** *11* (11), 725-41.
55. Seisuke Kano, A. Y., Ryohei Otsuka, Masataka Ohgaki, Satoshi Nakamura, Masaru Akao, Hideki Aoki, X-Ray Diffractometry and Thermal Analysis of Several Vertebrate Animals' Biological Apatites. *Apatite* **1992,** *1*, 91-95.
56. Malde, M. K.; Graff, I. E.; Siljander-Rasi, H.; Venäläinen, E.; Julshamn, K.; Pedersen, J. I.; Valaja, J., Fish bones - a highly available calcium source for growing pigs. *Journal of Animal Physiology & Animal Nutrition* **2010,** *94* (5), e66-e76.
57. Piccirillo, C.; Silva, M. F.; Pullar, R. C.; Braga Da Cruz, I.; Jorge, R.; Pintado, M. M. E.; Castro, P. M. L., Extraction and characterisation of apatite- and tricalcium phosphate-based materials from cod fish bones. *Materials Science and Engineering C* **2013,** *33* (1), 103-110.
58. Mkukuma, L. D.; Skakle, J. M.; Gibson, I. R.; Imrie, C. T.; Aspden, R. M.; Hukins, D. W., Effect of the proportion of organic material in bone on thermal decomposition of bone mineral: an investigation of a variety of bones from different species using thermogravimetric analysis coupled to mass spectrometry, high-temperature X-ray diffraction, and Fourier transform infrared spectroscopy. *Calcified tissue international* **2004,** *75* (4), 321-8.

Chapter Two: Characterisation of As Received and Processed Materials

2.1 Methodology

2.1.1 Source of bone-derived materials

The cleaned fish bone-derived powders of four species, snapper, hoki, gurnard and flounder were provided by Dr Matthew Cummings, Plant and Food, Nelson. These materials were isolated and cleaned by Plant and Food using the following methods.

2.1.1.1 Preparation of snapper and gurnard

The heads and frames of the fish were left to soak in water heated to 50 ^{o}C and left overnight. The materials were rubbed by hand and washed using high pressure cold tap water to remove flesh materials. The materials were then frozen at -40 ^{o}C for 5 days, prior to freeze drying for 22 hours. The bones were then ground and freeze dried for a further 20 hours.

2.1.1.2 Preparation of hoki and flounder

The heads and frames of the fish were agitated by hand in heated water (55 ^{o}C) for 15 minutes. The bones were rubbed by hand and washed with high pressure cold tap water to remove flesh materials. The materials were then frozen at -40 ^{o}C for 3 days. The same freeze-drying processes were then employed as with the snapper and gurnard materials.

2.1.2 Source of shell-derived materials

The mineral exteriors of four marine shell species were sourced from Sanford LTD in Tauranga, and were provided by Professor Chris Battershill, and Mr David Culliford from the University of Waikato's Tauranga Branch. Some of these materials had residual flesh attached to the mineral components, so these were all subject to the same cleaning methods.

2.1.2.1 Preparation of shell materials

Shell materials were boiled for two hours in a pressure cooker. The materials were then rubbed by hand to remove any residual flesh and washed with type 1 water. These were dried in an oven overnight at 80 ^{o}C. The dried shells were broken down to smaller sizes by hand using a hammer, followed by milling using a ring mill for 1 minute to produce a fine shell powder.

2.1.3 Solvents and reagents

Table 2-1 below displays the sources of the chemical reagents used in the characterisation section of this study.

Table 2-1: Solvents and reagents used in this study

Chemical Name	Grade	Brand
Sodium hydroxide pellets		EMSURE™
Potassium bromide	IR spectroscopy grade	Merck
Hydroxyapatite	>90% purity	Fluka
Tri-calcium phosphate	>99% purity	Fluka
Methyl acetate	Analytical grade	Merck
Sodium hypochlorite	15%	Andrew Industrial Ltd
Nitric acid	For analysis, 65%	EMSURE™
Hydrochloric acid	Fuming, for analysis 37%	EMSURE™

2.1.4 Processing methods

2.1.4.1 Thermal treatment of materials

A high temperature furnace was used to treat as received bone and shell derived materials at the following range of temperatures: 300 ^{o}C, 500 ^{o}C, 600 ^{o}C, 700 ^{o}C, 800 ^{o}C and 1000 ^{o}C. Each sample was weighed out into an alumina crucible using 2 d.p. scales. These crucibles were placed in the furnace at the desired temperature for approximately 2 hours. After processing, the crucibles were re weighed to track the weight loss as a result of the treatment. The samples were then characterised using a suite of analytical techniques.

2.1.4.2 Chemical treatment of materials

Chemical treatments were only performed on the bone derived powders as these materials were the main focus of the study.

2.1.4.2.1 Soaking of materials in NaOCl

As received bone materials (1 g) were placed in a 250 mL conical flask, to which a solution of NaOCl was added (100 mL, 15%). These solutions were stirred thoroughly using a magnetic stir-bar for an hour and were left to sit overnight.

2.1.4.2.2 Refluxing of materials in different solutions

As received bone materials (1 g) were placed in a round bottom flask with type 1 water (40 mL). The solutions were heated to boiling and were left under reflux for an hour. The resulting solutions were decanted and washed with cold type 1 water, this was repeated three times.

This same general method was also employed for the other refluxing solutions trialled, which were NaOH (1 $molL^{-1}$) and ethyl acetate. In some samples, the entire refluxing process was repeated a second and third time to further clean the materials.

2.1.4.2.3 Digestion in acid and reprecipitation by base

Bone materials were weighed out to 4 d.p. into a round-bottom flask with three necks. HNO_3 (1 M) was added with swirling until the solid had just dissolved. This solution was heated to 80 ^oC with stirring, the temperature was maintained between 70 ^oC and 90 ^oC, as measured by a thermometer. Once at temperature, NaOH was added dropwise to the solution until a precipitate had formed and the pH had risen to above 9, measured using pH 1-14 and pH 8-10 indicator paper. The solution was stirred for 3 hours with temperature being maintained between 70 and 90 ^oC, the pH was maintained above 9 using NaOH (2 $molL^{-1}$) and measured using narrow range indicator paper (pH 8-10).

The solutions were transferred into 50 mL centrifuge tubes for washing. The initial suspensions were centrifuged followed by discarding of the supernatant. Type 1 water was added to each of the tubes and mixed well. These were centrifuged and again the supernatant was discarded. This was repeated until no further pH change was observed in the washings (usually 3 repeats were deemed sufficient).

2.1.5 Instrumentation and sample preparation

2.1.5.1 Fourier-Transform Infrared Spectroscopy (FT-IR)

Infrared spectra of the ground bone and shell derived materials were added to analytical grade KBr in a sample:KBr ratio of approximately 1:10. These were ground to a fine homogeneous powder using an agate mortar and pestle. The powder was then pressed into a disc to be analysed using a Perkin Elmer 400 FT-IR/FT-FIR spectrometer. The spectra were obtained between 450 and 4000 cm^{-1}, with a resolution of 4 cm^{-1}, with 3 scans. A background spectrum was recorded before each analysis of an empty sample holder in the chamber. Base-line corrections were applied to every spectrum recorded, which were performed by an automatic function in the Spectrum software.

2.1.5.2 Solid State Nuclear Magnetic Resonance Spectroscopy (SS-NMR)

Ground samples were packed into ZrO_2 rotors (4 mm outer diameter), ensuring even and homogenous sample distribution inside the rotor. These were stoppered with

'Kel-F' caps. These were then spun at 5 kHz using a magic angle spinning unit (the magic angle was set using KBr, at 54.74^{o} with respect to the magnetic field).

The NMR spectra were recorded using a Bruker Avance-III 300 mHz spectrometer, with a Bruker 4 mm H/X CP-MAS solids probe. Reference standards were as follows:

For ^{31}P – $(NH_4)H_2PO_4$ with a standard ^{31}P shift of 0.8 ppm

For ^{13}C – COO signal from alpha-glycine, with a ^{13}C shift of 176.5 ppm.

Spectra of these standards were run prior to analysis of the unknown samples for providing a spectral reference (SR) value which was applied to each sample spectrum run for the respective nuclei.

2.1.5.3 Powder X-Ray Diffraction (pXRD)

Prior to pXRD analysis samples needed to be ground using a ring mill for 60 seconds. These powders were then packed into sample holders with even distributions to ensure the sample had a flat surface in the holder. The diffractograms of these samples were recorded using a Panalytical Empyrean Series 2 diffractometer, with the following instrument parameters:

Anode Material: Cu

Divergence slit: Fixed, 0.5 r

Receiving slit: 0.1

Monochromator used: No

Generator voltage: 45 mV

Tube current: 40

Scan range: 5.021 – 99.999

Scan step size: 0.026

Time per step (ms) 236.64

2.1.5.4 Scanning Electron Microscopy (SEM)

Thin layers of samples were spread and adhered to double-sided carbon tape on the surface of 15 mm aluminium sample holder stubs. These were then sputter-coated in platinum and analysed using a Hitachi S-4700 Field Emission Scanning Electron Microscope, using a voltage of 5 kV.

2.1.5.5 Inductively Coupled Plasma Mass Spectrometry (ICP-MS)

Raw samples were weighed out to 4 d.p. (~0.2000g) into plastic tubes and digested in nitric acid (20 mL, 68%). These were sealed and heated in a water bath (at 80 ^{o}C) to aid digestion. Usually 30 minutes was sufficient. Some of the raw samples required the addition of more acid (a further 20 mL), and longer periods of heating (2 hours). The digested samples were then passed through at 0.45-micron syringe filter, before being diluted by a factor of 1000 with type 1 water. The diluted samples were submitted to Steve Cameron, University of Waikato, for analysis in triplicate on an Aligent 8900 ICP/MS Triple Quad. The samples were run on a single quad, with high purity helium gas tuning to reduce interferences.

2.2 Characterisation of As Received Materials

2.2.1 Characterisation of bone-derived materials

Before any processing treatments were carried out, the as received materials needed to be characterised to confirm the nature of the material, and to understand the effects of each processing technique.

2.2.1.1 Appearance of materials

Figure 2-1 below contains images of the materials as received by Plant and Food, Nelson.

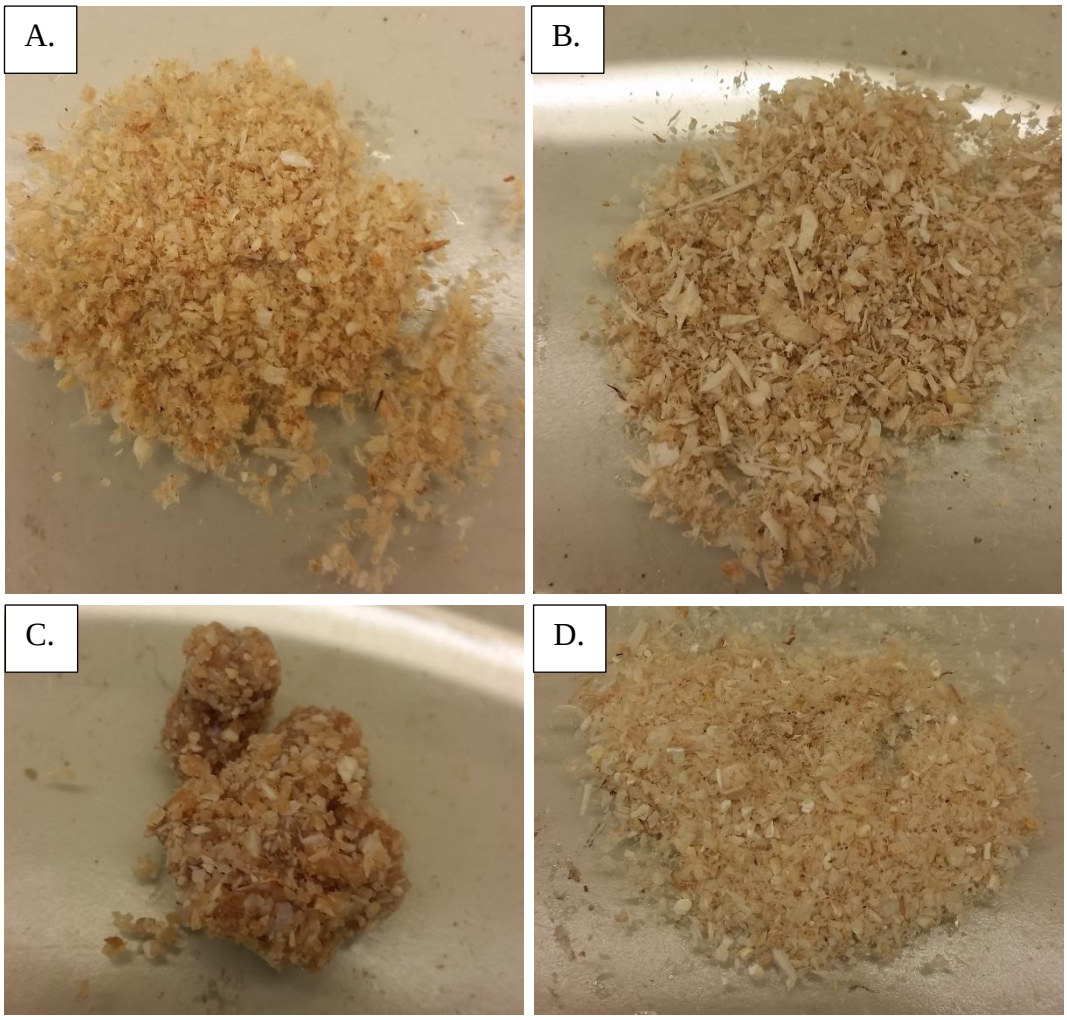

Figure 2-1: Images of ground fish bone materials, as received by Plant and Food, Nelson. A) Gurnard bones. B) Hoki bones. C) Snapper bones. D) Flounder bones.

The flounder, gurnard and hoki bones all appeared reasonably similar, with a mix of white, cream, and brown coloured flakey solids that had a range of particle shapes and sizes. The snapper bones differed from the others in that they retained a high 'waxy/fatty' content after the processing done by Plant and Food. This gave them

a more agglomerated appearance. As expected, all of the bones contained a slight distinct fish-like odour.

2.2.1.2 Fourier transform infra-Red spectroscopy (FT-IR)

Table 2-2 below contains assignments of infra-red peaks which were commonly found in this study.

Table 2-2: Common peak assignments in the IR spectrum for this study. (b) and (s) denote broad and sharp respectively and describe the shapes of the peaks in the spectra.

Species	Position in IR spectrum (cm^{-1})
H_2O (moisture)	3400 (b), 1640 (b),
CO_3^{2-}	1450 (b)
PO_4^{3-}	1050 (b), 560 (b)
Collagen i.e. (C=O)	~1600 region, i.e. 1650, 1550
Nitrate	1380 (s)
-OH	3400 (s)

Figure 2-2 below illustrates the labelled IR spectra (with peak assignments) of the hoki and flounder bone materials, as received by Plant and Food Research, Nelson. In general, the FT-IR spectra of all four species showed peaks characteristic of carbonated hydroxyapatite, (CO_3^{2-} at 1450 cm^{-1}, PO_4^{3-} at 1050 and 560 cm^{-1}) with collagenous contributions through the amide I peak being at approximately 1650 cm^{-1} (combined peak with O-H bond) and an amide II peak at 1550 cm^{-1}.[1]

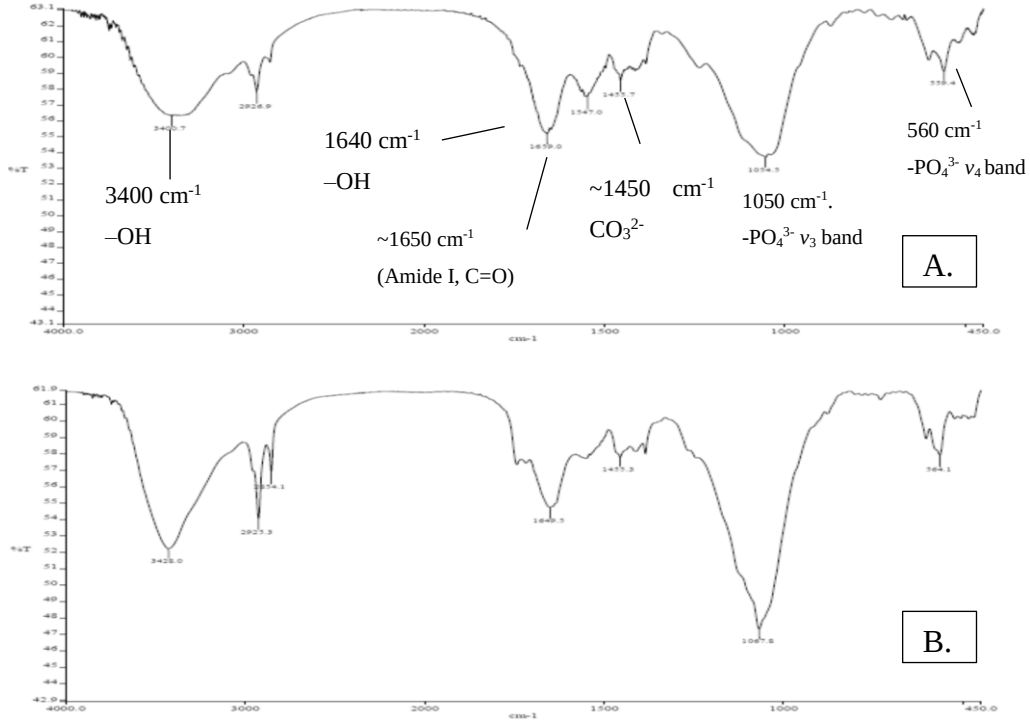

Figure 2-2: FT-IR spectra of A) As received hoki bones and B) As received flounder bones.

The IR spectra of the four fish species had different intensities in their peaks which are likely to be the result of the different levels of oils and other organics remaining after the initial processing of the materials by Plant and Food. The differing intensities observed were the result of the physical nature of the as received materials. It was found that the materials were difficult to grind down to fine powders due to the toughness of the bone materials. While a ring mill grinding step was used to achieve fine powdered materials, the level of oils in the material made this difficult as the solids would clump together. This caused the ground samples to remain quite heterogeneous in nature and appearance so that creating the KBr discs with a uniform distribution of analyte for spectral investigation was challenging at times, leading to spectra which were occasionally weak in terms of the signal intensity and resolution from the baseline.

2.2.1.3 Solid State Nuclear Magnetic Resonance Spectroscopy (SS-NMR) Characterisation

Figure 2-3 below contains the ^{13}C MAS NMR spectrum of the hoki bone material.

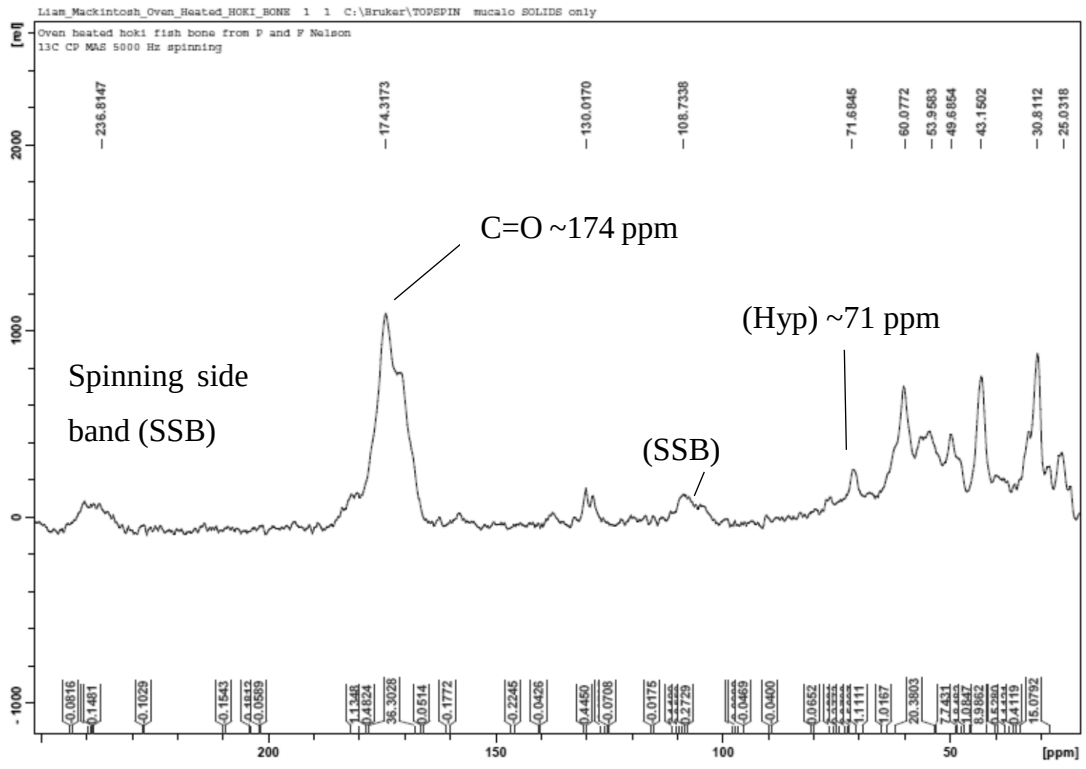

Figure 2-3: ^{1}H - ^{13}C Cross Polarised Magic Angle Spinning (CP MAS, 5000 Hz) of raw snapper bone dried in oven.

The above spectrum appears to be dominated by a pattern resembling a collagenous material, (174 ppm – C=O from amino acids 25-80 ppm CH_3, CH_2 groups) with other smaller peaks scattered throughout likely to be the result of oils and organics in the material. One peak of interest is the peak with a chemical shift of ~71 ppm.

This peak is understood to correspond with the Cγ (CHOH) carbon in hydroxyproline[2] (hyp), an amino acid which is almost exclusive to the collagen protein[3]. Hence the presence of hyp is generally deemed as an indicator of the presence of collagen. Spinning side bands are also visible in the spectrum at 110 and 210 ppm and these are a consequence of spinning the sample at 5000 Hz. For comparison, a ^{13}C CP-MAS spectrum of collagen foam, which had been recorded for an earlier project in the research group, is given below in Figure 2-4

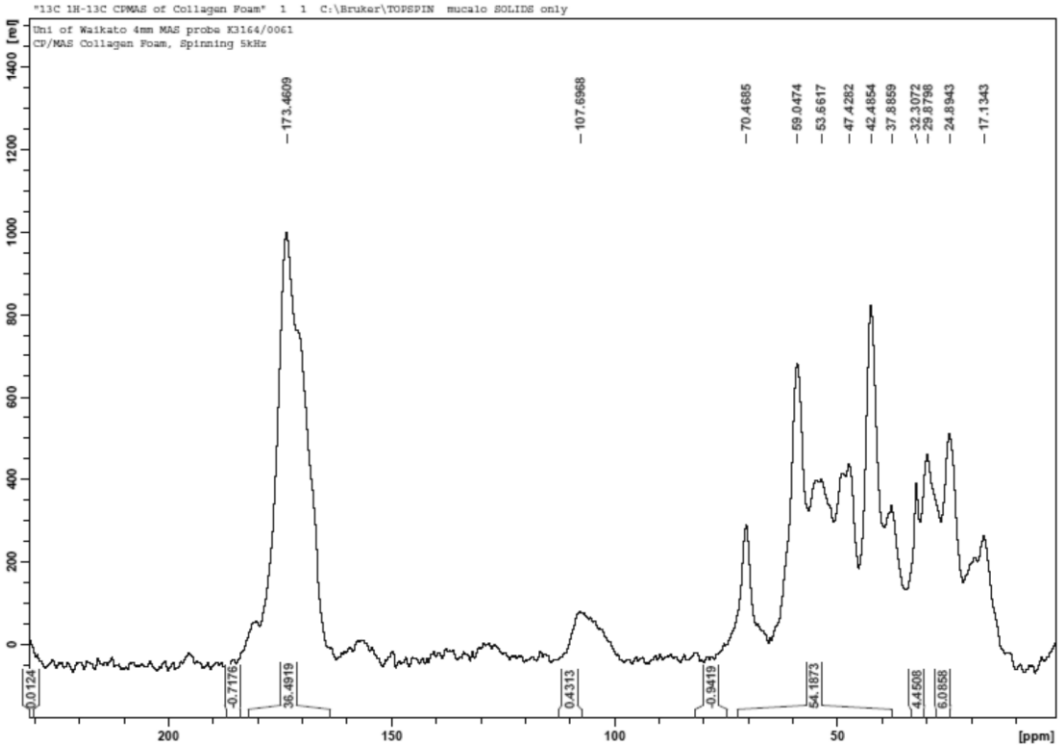

Figure 2-4: ^{13}C ^{1}H CP MAS NMR spectrum of collagen foam.

The peak patterns in these two NMR spectra show a strong resemblance to each other, both of which also contain the 70 ppm ^{13}C peak characteristic of hyp, confirming that the collagen protein is indeed present in the snapper bone sample. A comparison of the NMR spectra from the raw bone materials, and the collagen foam is given below in Figure 2-5.

The bone materials from the different species are all quite similar, they show the same dominating collagen spectral pattern. Their differences arise from small peaks scattered throughout which are likely to be the result of different levels and types of residual oils/hydrocarbon compounds. All spectra contain the aforementioned Cγ carbon shift of 70 ppm, confirming that collagen is present in all of the as received bone-derived materials from the four fish species characterised in this study.

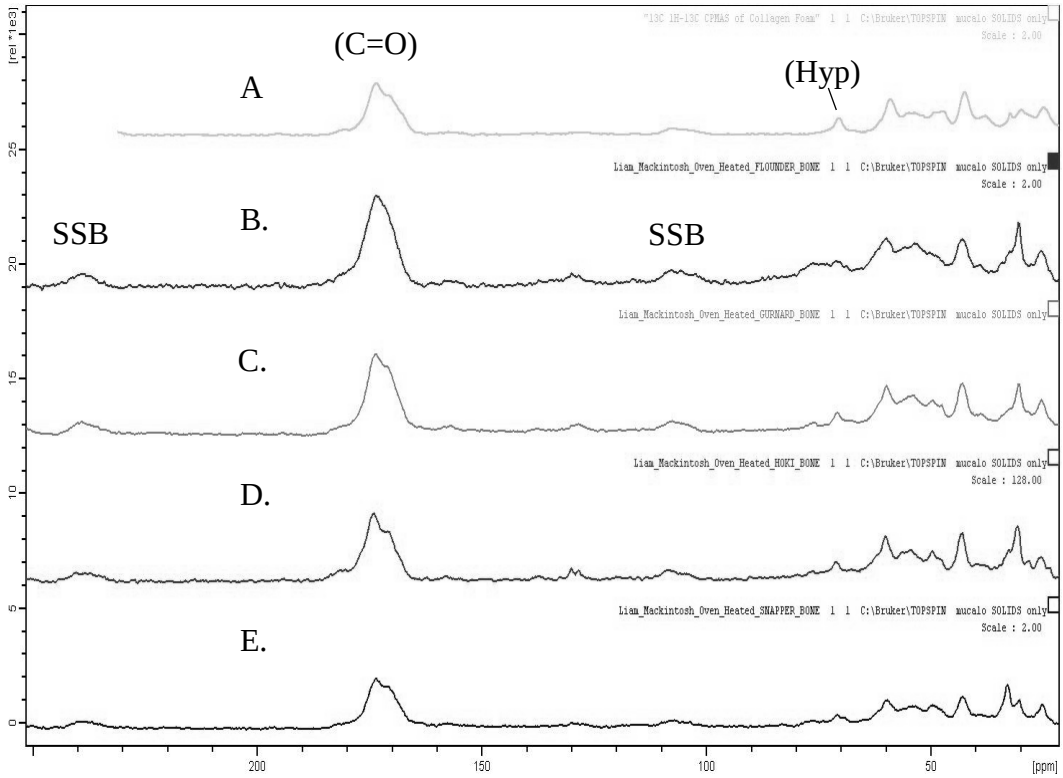

Figure 2-5: ^{1}H - ^{13}C CP-MAS combined spectra comparing all raw species to collagen foam. A) Collagen foam. B) Raw flounder. C) Raw Gurnard. D) Raw Hoki. E) Raw Snapper.

2.2.1.4 Scanning Electron Microscopy with Energy Dispersive X-Ray Spectroscopy (SEM/EDX)

Figure 2-6 below contains scanning electron microscope images of the raw bone materials

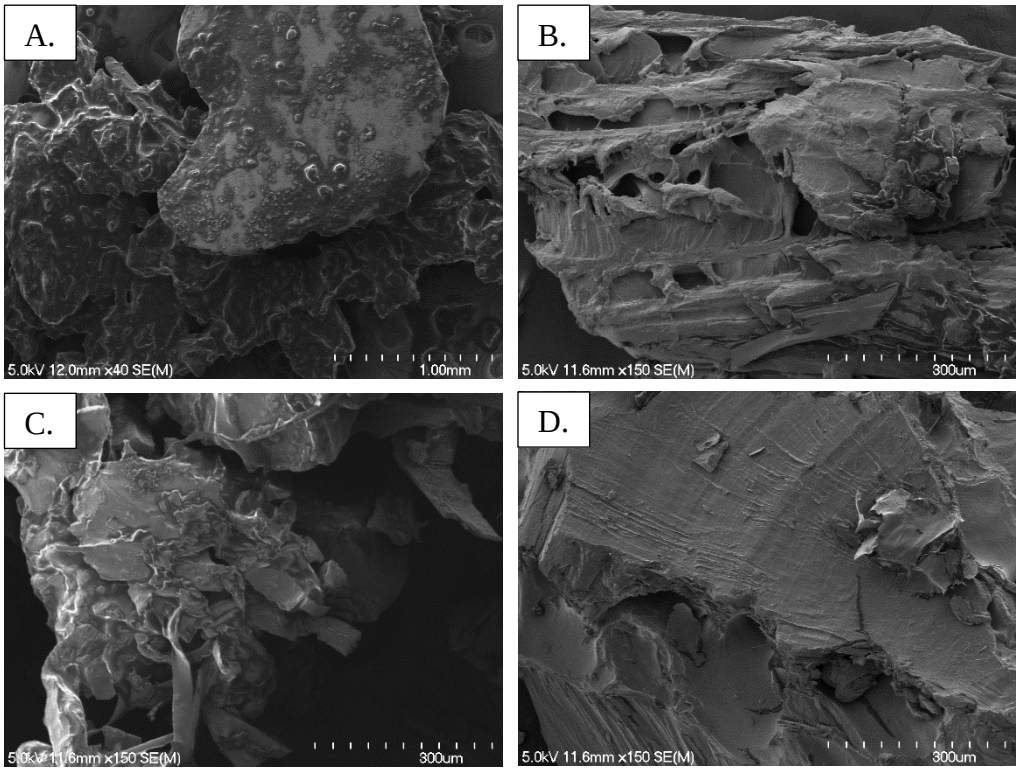

Figure 2-6: Scanning Electron Microscope images of raw fish bone materials. A) Snapper bones. B) Hoki bones. C) Gurnard bones. D) Flounder bones.

These images show that the materials are similar in appearance to each other with all appearing to contain porous bone material and incorporated/interdigitated oils/collagen. These results agree with the initial appearances of these solids, in that the snapper bones appear much oilier in nature than the other species bones ('shiny' areas in image are likely the result of the presence of organics and oils coating surfaces). The snapper sample was also problematic to image due to the presence of these oils as some of the material appeared to be volatilising under the influence of the electron beam. This led to issues with focussing and acquiring a still image. This problem was mostly confined to snapper bones because of the oil content and did not present itself as so much of an issue for the other species materials.

2.2.1.5 Powder X-Ray Diffraction (pXRD) characterisation

Powder X-Ray diffractograms were recorded for these samples to gain an idea of the phases and crystallinity present in the materials. Due to the agglomerated nature of the snapper sample, the diffractogram of this sample was unable to be recorded. The diffractograms of the hoki, gurnard and flounder samples are displayed in Figure 2-7 below.

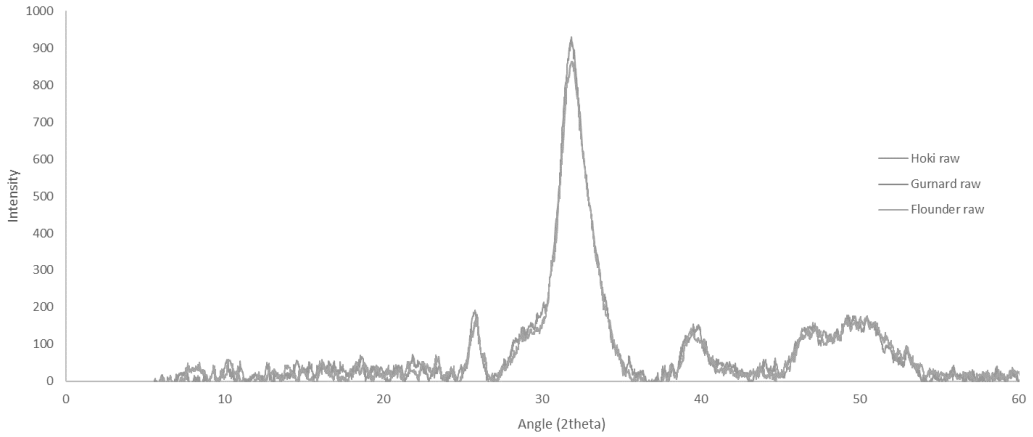

Figure 2-7: XRD diffractograms of as received bone powder samples from Plant and Food.

For comparison, the diffractogram of pure HAp (Fluka brand) is overlaid on the raw hoki diffractogram in Figure 2-8 below.

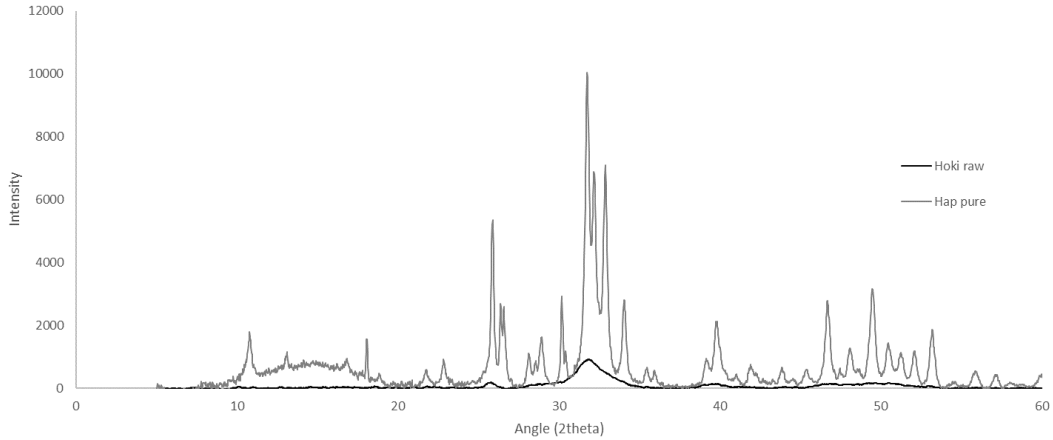

Figure 2-8: XRD diffractograms of as received hoki bone powder (black) with pure HAp (red).

Differences between the raw samples in the diffractograms are small, they are almost perfectly overlapping each other. Their peaks are all broad, suggesting low crystallinity, which is in agreement with the FT-IR data. The diffractograms of the raw samples have low intensities relative to the pure hydroxyapatite sample, however the broad peaks do appear to follow the same pattern given by the pure HAp sample. This further confirmed the presence of hydroxyapatite in the as received bone powders.

2.2.1.6 Inductively Coupled Plasma Mass Spectrometry (ICP-MS)

In general, the samples digested without too many issues, however, digestion of the samples in HNO_3 presented some challenges as an orange coloured material was found adhering to the side of the plastic tubes. This is likely the result of the formation of coloured xanthoproteic species which arise from the nitration of certain amino acids by nitric acid[4]. This was overcome by the addition of stirring during the digestion, which prevented the species from aggregating and sticking to the sides of the vessel. Table 2-3 presents the results of the elemental analyses of the as-received fish bone samples from Plant and Food.

Table 2-3: ICP-MS results for the raw fish bone samples.

	Concentration (ug/g bone, ppm)					
Element	**Snapper**	**Gurnard**	**Flounder**	**Gurnard #2**	**Gurnard #3**	**RSD %**
B 10	13.644	20.688	21.747	13.919	23.115	15.50
Na 23	6110.8	355877.8	6745.1	8285.4	72926.5	0.87
Mg 24	2749.4	3311.2	2907.7	2743.9	2648.1	4.69
Al 27	110.34	298.93	133.73	170.65	184.93	0.19
P 31	86892.4	100277.4	73918	83373.9	78581.2	0.11
K 39	1113.9	4455.1	3789.1	3328.9	3381.5	3.12
Ca 43	206216.6	215067	163688.3	189654.7	176460.6	0.01
V 51	1.9317	2.1668	4.4613	2.6062	2.7054	0.62

Cr 52	6.823	8.581	8.249	7.377	8.239	1.58
Fe 54	-1327	-1416	-1403	-1344	-1384	-
Mn 55	27.413	50.097	25.421	33.92	40.827	0.05
Ni 60	398.804	599.082	415.382	460.147	436.792	0.02
Cu 65	16.111	46.24	25.968	24.538	16.396	0.53
Zn 66	220.69	343.45	208.29	105.68	136.16	0.13
As 75	0	5.589	12.939	3.615	11.543	0.55
Sr 88	906.65	948.549	741.546	791.041	797.595	0.86
Ag 109	0.86	1.38	1.8	1.514	2.036	2.89
Cd 111	0.324	1.067	0	0.275	0.16	6.54
Ba 137	9.611	5.29	1.654	1.375	1.242	1.34
Hg 202	0.681	0.544	0.524	0.114	0.077	4.56
Pb 207	0.041	9.101	1.768	1.163	1.066	0.90

Due to the labile nature of the HAp lattice, a wide range of species can substitute in with ease[5]. Some of these include Na^{+}, Mg^{2+}, K^{+}, Sr^{2+}, Zn^{2+} Ba^{2+}, Cd^{2+} and Al^{3+}. The extent to which these are found in natural bone materials depends on the environment from which the bones were sourced. For example, it is not surprising that these marine species have significant levels of sodium. Additionally, due to the presence of Mg^{2+}, K^{+} and Sr^{2+} in the oceans, it is not surprising this has appeared in all of the samples. The relative concentrations of these metals appears to follow closely the naturally occurring concentrations of these elements in sea water[6] (i.e. $Na^{+} > Mg^{2+} > K^{+} > Sr^{2+} > Al^{3+} > Cu^{2+} > Ba^{2+}$). An exception to this is the presence of nickel in the samples. This is unusually high compared to the usual concentration in sea water. It is possible that this nickel content is introduced due to the grinding process, using stainless steel ring mill equipment. There are also a few trace levels of some heavy metals, and as these are able to substitute for Ca^{2+} in the HAp lattice, and are moreover found in sea water samples, in low concentrations, it is not overly surprising that these were found in these samples. Negative values for iron are reported as these samples had Fe concentrations lower than the calibration blanks. Correction algorithms are used in the calculations of concentrations for ICP-MS, and it is likely that these have over-compensated for the very low Fe values giving negative values. It is therefore safe to assume that the samples are low in Fe and are below detection limits.

The raw gurnard sample shows some interesting differences from the other materials. It has larger concentrations of both lead and sodium. The source of this is not known. It was thought that potentially the tap water at Plant & Food, Nelson (used in the initial processing of the fish samples) may have had some influence on this, so a sample of water from a hot and cold tap water was taken for analysis. The

elemental results of these samples returned concentrations much lower than those observed in the bone samples. It is therefore unlikely that the use of tap water at Plant and Food has significantly influenced the elemental results obtained for the bone materials.

From the results in Table 2-3, it was possible to calculate the Ca:P mole ratio for comparison to stoichiometric hydroxyapatite, this provides information on the nature of the phases present in the materials. These values are given below in Table 2-4.

Table 2-4: Ca:P mole ratios for raw fish bone samples.

Sample	Ca:P mole ratio
Snapper Raw	1.83
Flounder Raw	1.71
Gurnard Raw #2	1.76
Gurnard Raw #3	1.74

Stoichiometric hydroxyapatite has a Ca:P ratio of 1.67 (10 Ca atoms to 6 P atoms in $Ca_{10}(PO_4)_6(OH)_2$). Hence, values for the ratio above this value, could suggest that carbonate has been incorporated into the HAp lattice in place of phosphate ions, hence mathematically raising the ratio. This is typical of natural bone samples[7]. The Ca:P mole value is easily influenced, for example a sample with the empirical formula of $Ca_{10}(PO_4)_5(CO_3)(OH)_2$ which is quite similar to stoichiometric HAp, would have a Ca:P ratio of 2.0. This observation is supported by the FT-IR spectra (Figure 2-2) which show significant carbonate peaks. It is more difficult to demonstrate in the solid-state NMR spectra as the carbonate peak in this is overlaid by that due to collagen impurities.

As the FT-IR spectra show significant carbonate peaks (see Figure 2-2), this supports the observation of the non-stoichiometric Ca:P mole ratios from ICP-MS.

2.2.2 Characterisation of shell-derived materials

Although not the main focus of the project, it was of interest to investigate marine shells in a similar manner to what was done with the fish bone materials as the generation of these from processing can constitute an environmental problem in terms of its disposal. As with the bone-derived materials, prior to any processing techniques, the materials first needed to be characterised spectroscopically.

2.2.2.1 Appearance of materials

These shell materials (cockle, oyster, mussel and scallop shells) were provided as whole shells, some of which appeared to still have small amounts of flesh attached, and so these were boiled in a pressure cooker for two hours. This successfully cleaned up any remaining fleshy attachments on the materials. Crushing, and subsequent milling of the shells generated a granular sand-like powder for all of the species investigated.

2.2.2.2 FT-IR characterisation

It was expected that these materials would be primarily composed of calcium carbonate. Normally in nature, $CaCO_3$ is found as two common polymorphs, calcite and aragonite, and these polymorphs can be distinguished by differences in their FT-IR spectra. The spectra of mussel and oyster shells are given in Figure 2-9 below.

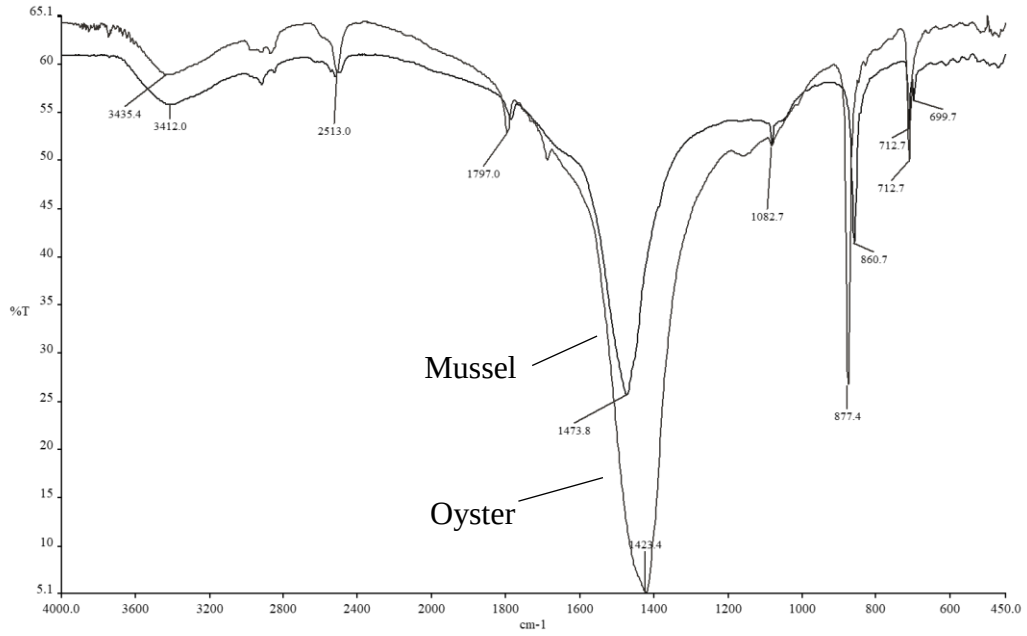

Figure 2-9: FT-IR spectra of ground raw mussel and oyster shells.

As evident in Figure 2-9 above, the two spectra are broadly similar in appearance, however they can be distinguished by small differences in the peaks. The oyster material contains a much more intense, and broad CO_3^{2-} peak (~1400 cm^{-1}), these also have a slightly different maximum peak value, in the oyster it is 1423 cm^{-1} and in the mussel it is 1473 cm^{-1}. These two also differ in the shapes of the peaks in the 2500 cm^{-1} and the 2800 cm^{-1} region. These differences suggest that these are two different forms of calcium carbonate. Separate standards of calcium carbonate polymorphs were not available to compare these to, however comparison to literature[8] shows that the aragonite form of $CaCO_3$ has two peaks in the 700 cm^{-1} region, at 700 and 713 cm^{-1}. This matches what is found in the mussel spectrum.

Calcite only has the single 713 cm^{-1} peak, which matches the oyster spectrum. So, it is likely that the mussel shells are predominantly made up of the aragonite form, while the oysters are made predominantly from calcite. The IR spectrum of cockle shells matched closely to the mussel spectrum, and so it is likely that cockle is also made mostly from aragonite. Likewise, the scallop shells matched the oyster IR spectrum, so these are most likely calcite in nature, literature has shown that scallops are typically composed of mostly calcite[9].

An IR spectrum of a commercial calcium carbonate sample also had its spectrum recorded, it was not stated on the bottle what polymorphs were presented in this sample. A comparison of this with some ground shell materials is given in Figure 2-10.

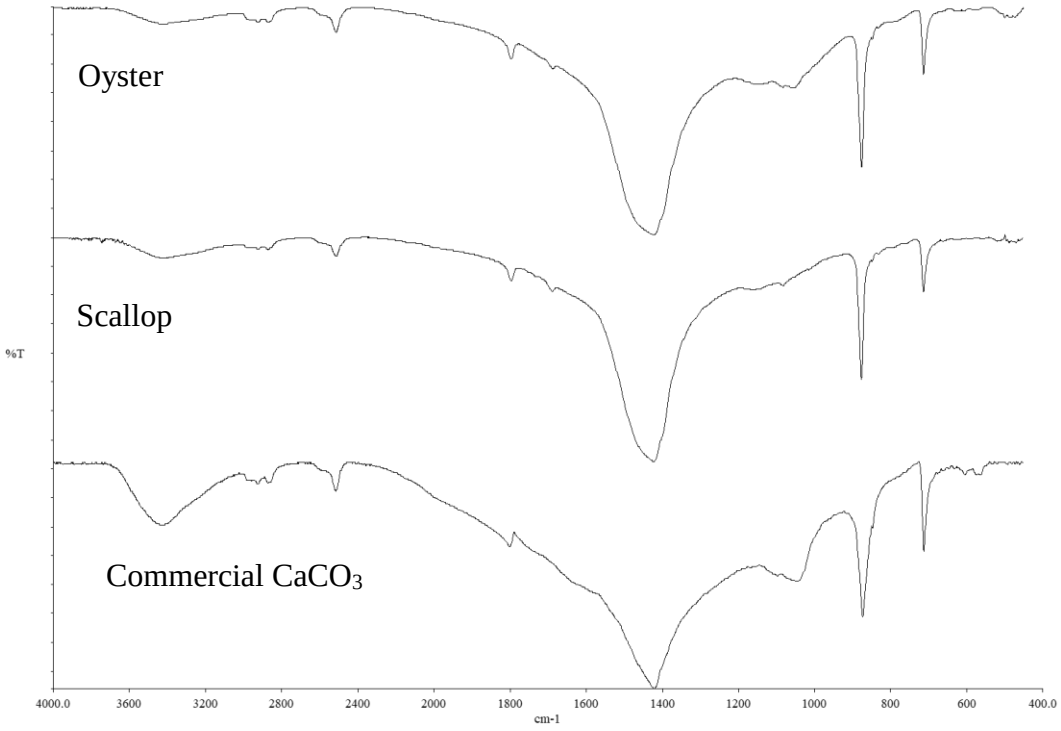

Figure 2-10: FT-IR spectra of ground shell materials and commercial $CaCO_3$.

These spectra show similar dominating peaks as the commercial $CaCO_3$. There are small differences. These spectra however confirm that the shells are composed from some form of calcium carbonate.

2.2.2.3 SS-NMR characterisation

A ^{13}C SS-NMR spectral comparison is given in Figure 2-11 below.

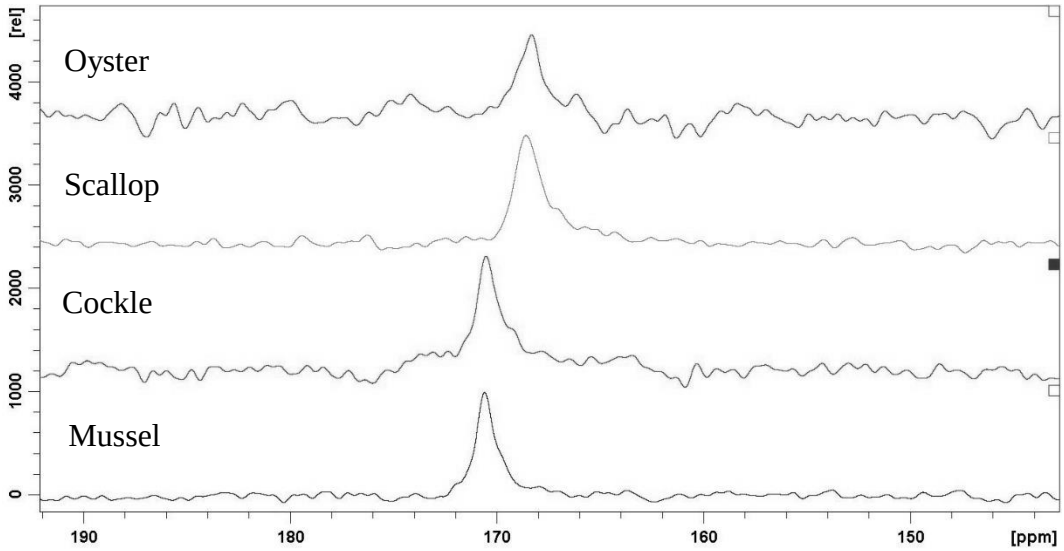

Figure 2-11: ^{13}C NMR spectra of ground raw shell materials.

The peaks between ~168-170 ppm are characteristic of the carbon in CO_3^{2-}[10]. The mussel and cockle shells both have similar shifts of 170.7 ppm and 170.6 ppm respectively. These differ from the scallop and oyster shells, which have shifts of 168.7 ppm and 168.6 ppm respectively. This difference between the two sets of species suggests the carbon nuclei in each exist in slightly different chemical environments, and supports the FT-IR data in suggesting that these sets may be two different polymorphs of calcium carbonate. Previous studies have suggested that $CaCO_3$ materials with carbon chemical shifts *ca*. 168 ppm are primarily composed of calcite, while shifts *ca.* 170 ppm suggest the materials is composed of aragonite. When fitting these observations to the data above, it shows that the mussel and cockle shells are composed of aragonite, while the oyster and scallop shells are composed of calcite, consistent with the results found by the FT-IR studies above.

2.2.2.4 pXRD characterisation

Diffractograms of the raw mussel, cockle and scallop shells are given in Figure 2-12 below.

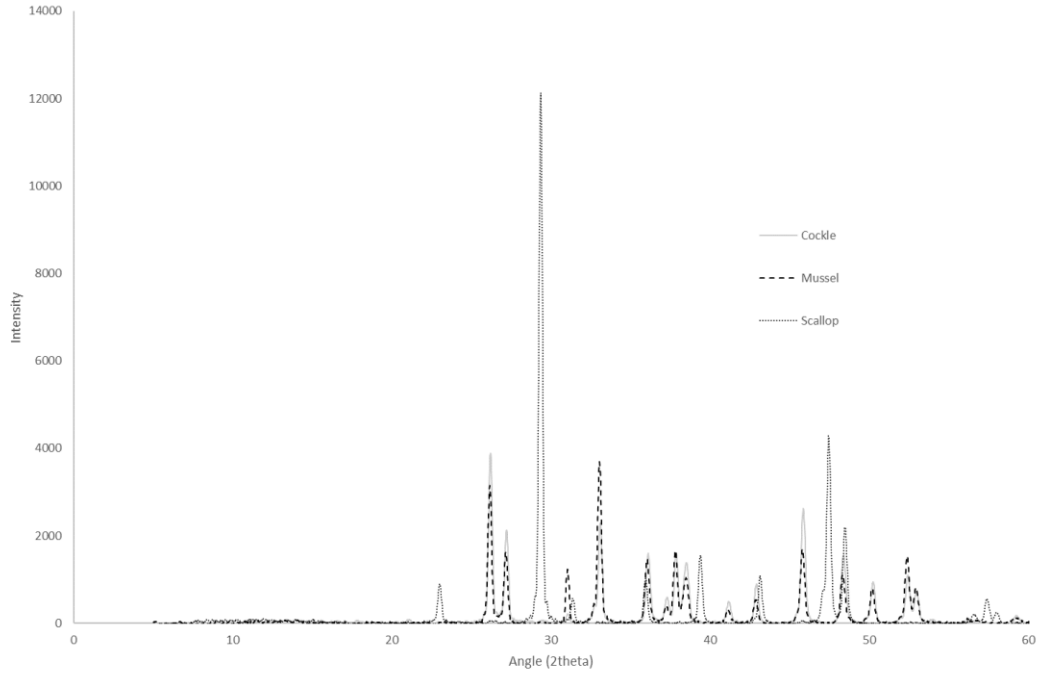

Figure 2-12: pXRD diffractograms of cockle, mussel and scallop ground shell materials.

The cockle and mussel patterns match each other, while the scallop appears quite different. Although the scallop does share some of the same peaks with the other two samples, it has unique intense peaks, for example the peak at 2θ angle 29. These are consistent with the other techniques, showing that the mussel and cockle shells share the same $CaCO_3$ polymorph, while the oyster and scallops share a different polymorph. Using the database search in the HighScorePlus® software on the XRD computer, the cockle and mussel samples were confirmed to match aragonite, while the scallop matched a calcite pattern. These results are consistent with the FT-IR, and SS-NMR results and confirm with confidence the different polymorphs are present in the shells.

2.2.3 General findings from the characterisation of as received materials

2.2.3.1 Fish bone-derived material characterisations

Characterisation of the as received materials from Plant and Food, Nelson showed that the bone-derived powders were principally composed of carbonated hydroxyapatite, with interdigitated collagen and other organics/oils. Differences between natures of the bones from different species were small and were mostly due to varying levels of oils remaining in the materials. The results from the elemental analysis on the materials were mostly as expected, and the metals which were detected were correlated back to the natural concentration of these metals in the oceans from which the fish originated. The results were mostly as expected and

served as a reference point for understanding the changes to the nature of the materials investigated as varying processing techniques were applied.

2.2.3.2 Shell-derived material characterisations

The shell-derived powders were confirmed to be primarily composed of different polymorphs of $CaCO_3$. The oyster and scallop shells consisted of the calcite polymorph, while the mussel and cockle shells were composed of the aragonite polymorph. This was confirmed by the comparison of IR spectra to the literature, and the use of pXRD with ancillary evidence provided by solid state NMR spectra. As there was a cost involved in using ICP-MS, elemental analyses were not performed on these shell materials, as these were only intended to be a small part of the project, with phase characterisation and determination of applications for the bone-derived materials being the primary focus.

2.3 Thermal Treatments

2.3.1 Thermal treatment of fish bone materials

Thermal treatments were carried out on the bone materials in attempts to remove/reduce the collagen/oils content of the bones, with the ideal intent being to produce a mostly phase pure HAp powder. A range of treatments were used, with extensive characterisation of the products to understand the changes occurring within each material as a result of the treatment temperatures they were exposed to.

2.3.1.1 Observations

Table 2-5 below contains the observations, and weight loss values for the fish bones processed via thermal treatments.

Table 2-5: Observations from thermal treatment experiments.

Sample	T (°C)	%Mass Loss	Appearance
Hoki	300	24.4	Blackened brittle flakes
Hoki	500	50.2	Dark brown brittle flakes
Hoki	600	49.8	Grey brittle flakes
Hoki	700	50.5	White brittle flakes, some grey/brown remaining
Hoki	800	50.2	White brittle flakes
Hoki	1000	51.7	White brittle flakes
Flounder	300	24.1	Blackened brittle flakes
Flounder	500	46.1	Dark brown brittle flakes
Flounder	600	40.5	Grey brittle flakes
Flounder	700	39.7	White brittle flakes, some grey/brown remaining
Flounder	800	44.3	White brittle flakes

Flounder	1000	40.3	White brittle flakes
Snapper	300	21.6	Blackened brittle clumps
Snapper	500	55.7	Dark brown brittle flakes
Snapper	600	51.4	Grey brittle flakes
Snapper	700	52.8	White brittle flakes, some grey/brown remaining
Snapper	800	58.5	White brittle flakes
Snapper	1000	57.5	White brittle flakes
Gurnard	300	20.7	Blackened brittle clumps of flakes
Gurnard	500	47.5	Dark brown brittle flakes
Gurnard	600	44.7	Grey brittle flakes
Gurnard	700	46.3	White brittle flakes, some grey/brown remaining
Gurnard	800	50.0	White brittle flakes
Gurnard	1000	52.9	White brittle flakes

These results showed that the behaviour of the bones across each of the species was relatively similar for the thermal treatments which indicated that the materials were broadly similar in compositional character to each other with only differences of scale of (components present) being the contrast. For instance, the thermal treatment product of snapper bones being treated at 300 ^{o}C was different from the others as it was initially a more agglomerated solid due to its greater fat content. Higher temperature treatments on the snapper bones broke these clumps apart and produced the more brittle flakes. The appearances of these materials match closely to what can be found in the literature for similar studies using *Thunnus obesus* bones (a species of tuna)[11].

Weight changes after thermal treatment gave some interesting albeit variable results. In all cases, the bones treated at 300 ^{o}C had a mass loss of about 20%. It was expected, that increasing the temperature would then lead to further mass loss. This was true for the 500 ^{o}C cooked samples, however the trend did not continue past this. The % mass loss between 600 and 1000 ^{o}C appears random. This could be a result of the accuracy of the balance used, a 2 d.p. balance was used instead of a 4 d.p. as the crucibles were too heavy to be measured using 4 d.p. These experiments were also not done in duplicate, and the weight of the sample was small relative to the weight of the crucible. Positioning in the muffler furnace could also have had an influence on these results, however this was not monitored.

To gain a better understanding of the weight loss as a function of temperature, samples were submitted to be analysed using a thermal gravimetric analyser (TGA), which measures the mass change of a sample across a temperature gradient program. The results of this are given in Figure 2-13 below.

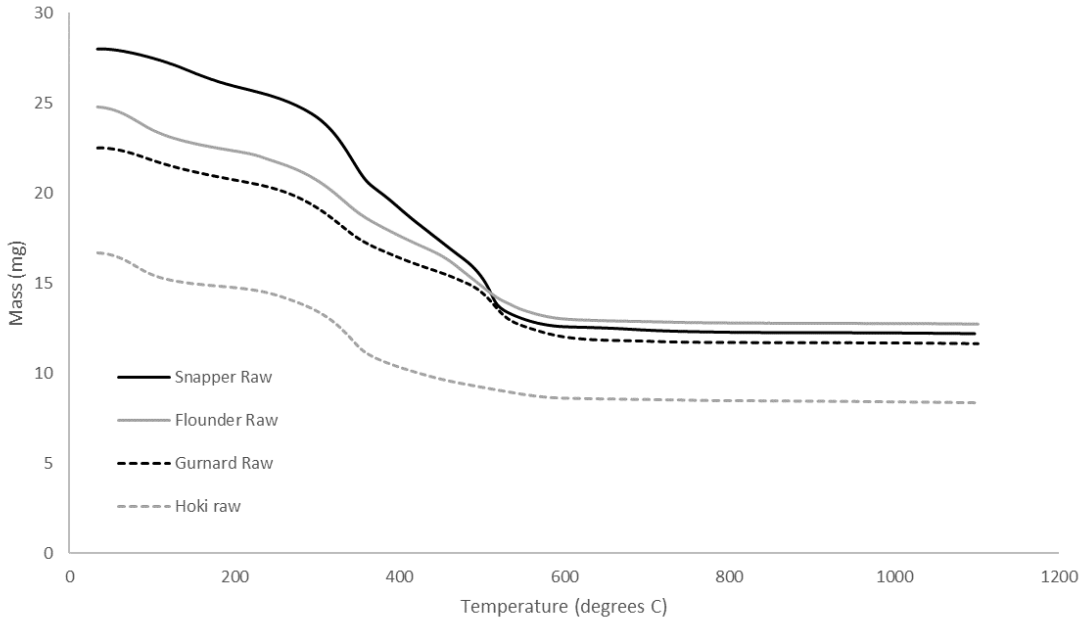

Figure 2-13: TGA results for the fish bone materials.

It was also possible to calculate the % mass loss at any given temperature, and so this was calculated for samples at 300 ºC and at 600 ºC. The values at 300 ºC agree with the earlier method, in that approximately 20% of the materials mass is lost at 300 ºC. Also, at 600 ºC, the % weight loss values were between 40 and 60 %, dependent on species. These agree with the initial weight tracking experiment (Table 2-5). These TGA results however do show, as expected, that the increase in treatment temperature leads to a decrease in weight across the entire temperature range (20 ºC – 1100 ºC). This decrease in mass is gradual between 20 ºC – 300 ºC, between 300 and 550 ºC the decrease is faster, and above 600 ºC there is no significant loss. This is also consistent with data available in the literature, bones from tuna (*Thunnus obesus*)[11], were also analysed through the use of TGA, with the results given in Figure 2-14 below.

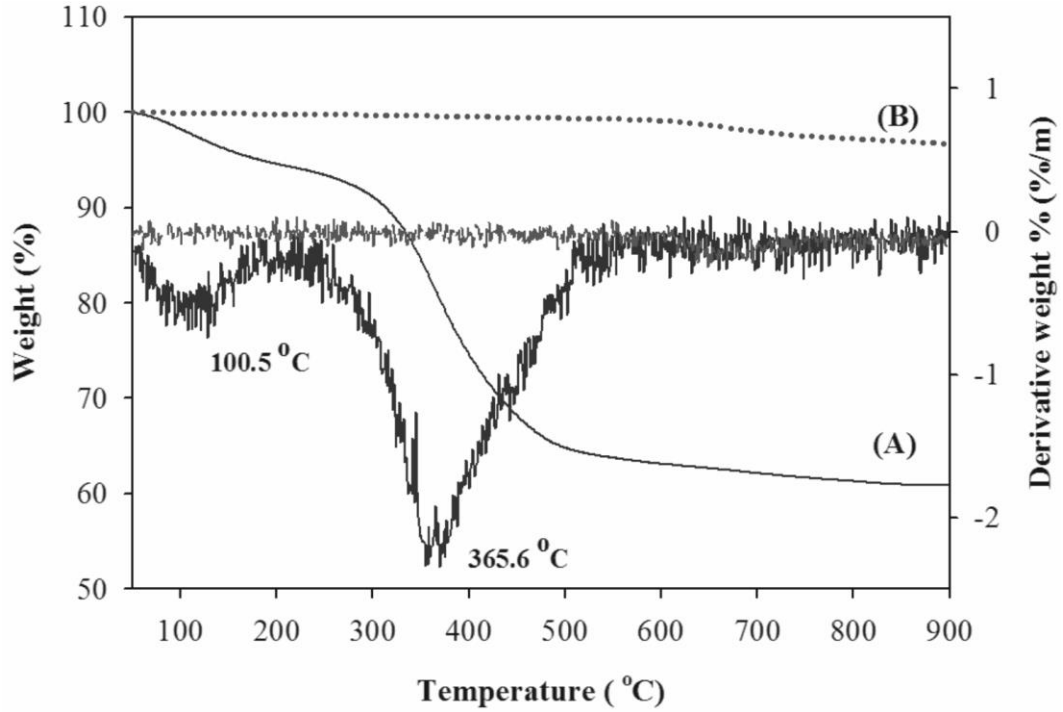

Figure 2-14: TGA curves of (A) raw fish bone and (B) thermal treatment at 900 ºC from literature[11].

Although the scale of the curve in Figure 2-14 is different to the scale presented in Figure 2-13, the trends of the curve A, and all curves in Figure 2-13 are similar.

The raw fish bone in this analysis, depicted by (A) in the figure above, appears to match closely to the mass loss trends found in the TGA analysis for this study. As observed in the present study, weight loss changes observed above 600 ºC are small, hence material in this region would be inorganic in nature without any tendency to decompose further, at least in that temperature range.

The weight changes observed, and molecular or physical processes attributed to them are as follows: The initial mass loss at 100 ºC is attributed to the loss of moisture from the sample, as water will boil off at 100 ºC. Further gradual loss past this point is assumed to be due to the burn off of the volatile fats/oils present in the sample. The sudden increase in mass loss between 300 ºC and 500 ºC is likely the result of the loss of further organic carbon groups through combustion as the samples were heated in air in the muffler furnace. Gradual loss above 600 ºC can be attributed to the slow decomposition of carbonate in the material, through Equation 2-1 below.

Equation 2-1: Thermal decomposition reaction of $CaCO_3$

$CaCO_{3\,(s)} \rightarrow CaO_{\,(s)} + CO_{2\,(g)}$

The calcium oxide formed is then prone to adsorb moisture from the atmosphere, to form $Ca(OH)_2$ which can induce alkalinity in certain media.

2.3.1.2 FT-IR characterisation

FT-IR spectra were useful in tracking the phase changes for the materials as they were processed. Figure 2-15 below contains the spectrum of the snapper bones, treated at 300 ºC, as an example of the spectra obtained.

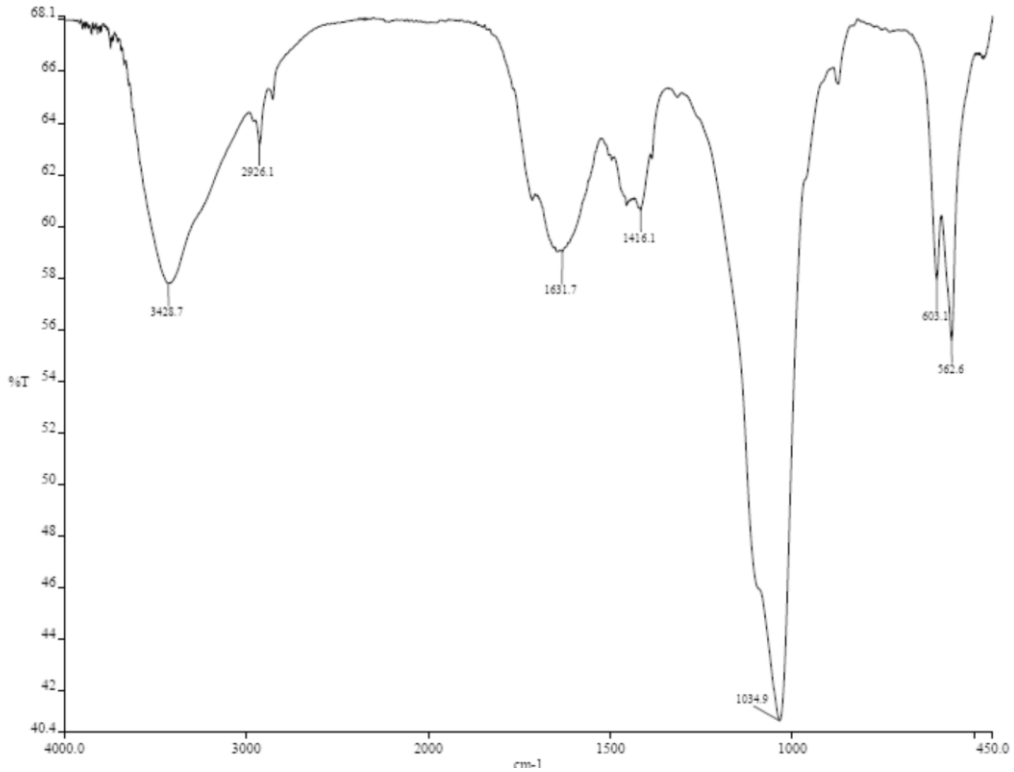

Figure 2-15: FT-IR spectrum of hoki bones thermally treated at 300 ºC.

The spectrum in Figure 2-15 has similar features to the spectra presented earlier in Figure 2-2, with the main differences being the sharpness of the peaks, and the size of the organics region (1650 – 1200 cm^{-1}) compared to the phosphate ν_3 band (1050 cm^{-1}). This is as expected, as mentioned earlier, there is an approximately 20% reduction in the mass of the material, and it is likely that this is a result of the burning off of some organics in the material.

Figure 2-16 below contains the spectra obtained for the snapper bones treated at a range of temperatures. The same comparison spectra were generated for the other species bones also, and these all generally follow the same trend displayed by the snapper bones below.

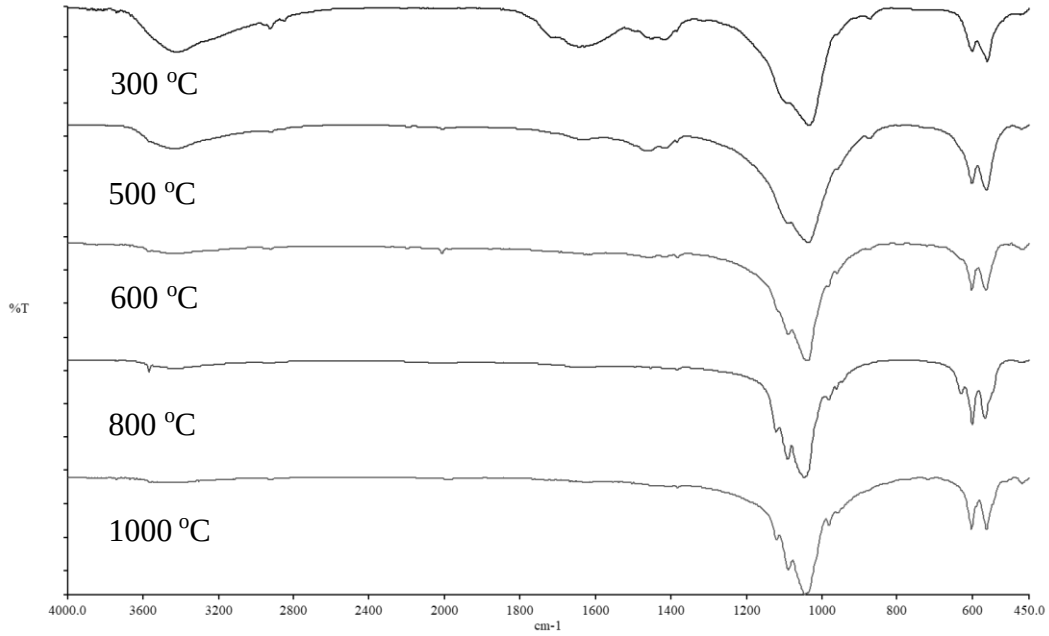

Figure 2-16: FT-IR spectra comparison of the snapper bones thermally treated at different temperatures.

These series of spectra show that the peaks become sharper as the treatment temperature increases to 700 ºC, past this point the peaks appear unchanged in terms of sharpness. As expected, the region of peaks originating from the organic content become smaller as temperature increases, up until 700 ºC. In the 600 ºC spectrum there are traces of these peaks remaining, however these are small.

It is noticed that at a treatment temperature of 500 ºC, a small sharp peak in the -OH region begins to appear. This peak, at 3571 cm^{-1} becomes increasingly resolved as the treatment temperature increases to 800 ºC. It is believed that this is the result of stretching of the O-H bond in the hydroxide component of HAp. There is also a small peak at 632 cm^{-1} which appears as though it is part of a group of three peaks. This peak is believed to be the result of the same OH species, only it is caused by a "librational" mode involving the O-H bond instead. It is likely that these two peaks were present in the raw materials, and the materials treated at lower temperatures, however they are shadowed by the large broad peaks nearby to them.

The sizes of these two OH peaks are reduced in the sample treated at 1000 ºC, suggesting there could be a phase change occurring in the material between 800 and 1000 ºC. It is thought that this change may be caused by the dehydration of HAp to form tricalcium phosphate. For comparison, IR spectra of commercial β-TCP and

HAp samples were measured. Figure 2-17 below presents a comparison of the snapper bones sintered at 1000 ºC with β-TCP.

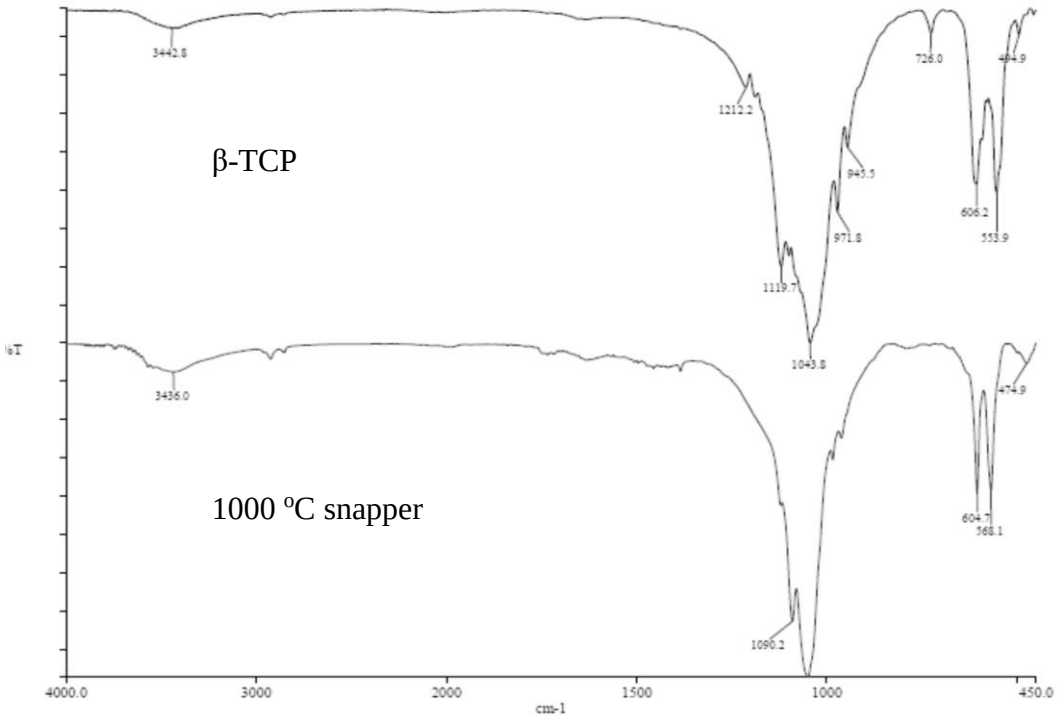

Figure 2-17: IR spectra comparison of snapper sintered at 1000 ºC with commercial β-TCP.

A similar comparison spectrum was generated with commercial HAp and is given in Figure 2-18 below.

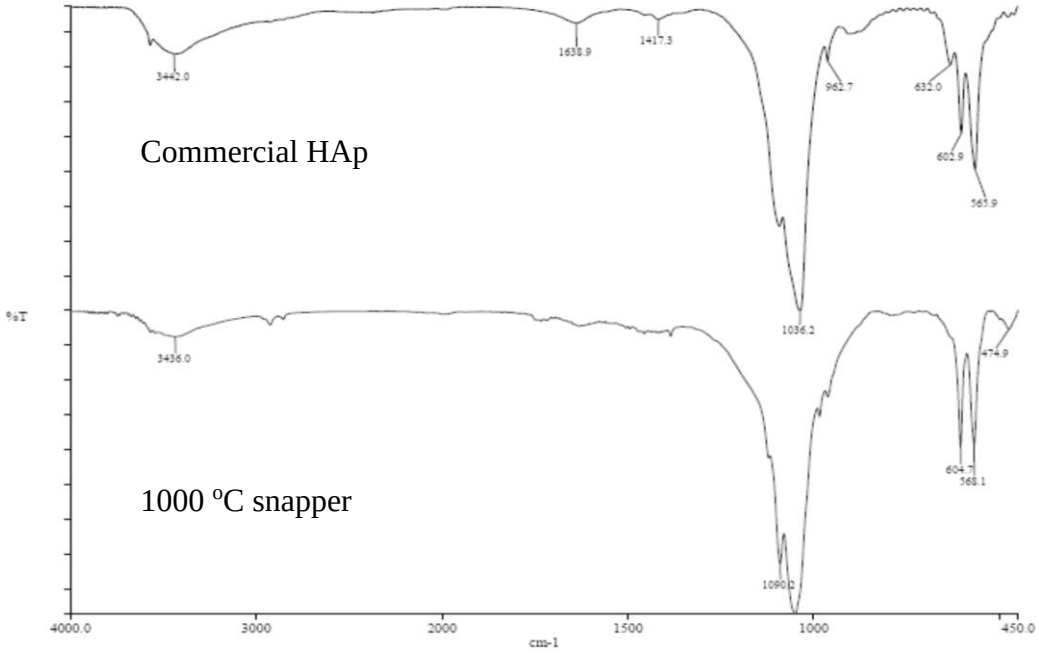

Figure 2-18: IR spectra comparison of snapper cooked at 1000 ºC with commercial Hap.

These spectra show that the 1000 ºC treated sample has similarities with both the commercial β-TCP and HAp. However it most closely matches to the HAp spectrum. It is possible that at this temperature, the material is beginning to undergo a change to the TCP phase, however the predominant phase is still HAp.

While the literature agrees that treatments of 600 ºC and above are completely free from any organic components, there are varied results on the phases present at the higher temperatures.

Some studies report that for their fish bones, a treatment temperature of 1000 ºC was optimum for producing pure HAp[12]. The FT-IR spectra presented in their work shows that the bone samples treated to 1000 ºC still contain the sharp resolved OH peak mentioned earlier. No mention is made of the formation of TCP in their products. Their methods are slightly different however as the bones in this referred study were treated at the desired temperature for four hours, while the materials in the current study were only treated for two hours.

Another study, agrees more closely with the results found[13] in the present study, in that fish bones which had been treated at 950 ºC for 12 hours, had a smaller OH peak than the sample treated at 600 ºC. They also concluded that, while HAp made up the majority of the sample, low levels of TCP had begun to form. This is consistent with the results in the present study, despite the fact that samples were treated at 1000 ºC, for a much shorter length of time. It is therefore possible, that increasing the length of treatment may not have affected a significant increase in formation of TCP, and the rate of this formation is more dependent on treatment temperature than treatment time. Another study[14] supports the hypothesis that it is TCP forming at temperatures above 800 ºC in which the OH peaks in the IR spectrum of their bone materials are reported to decrease in intensity with increasing temperature, between 850 ºC and 1000 ºC, and where it is stated that HAp is dehydroxylated to form β-TCP. The reaction driving this change is described below in *Equation 2-2*

Equation 2-2:

$$Ca_{10}(PO_4)_6(OH)_2 \rightarrow 3\beta - Ca_3(PO_4)_2 + CaO + H_2O$$

2.3.1.3 SS-NMR characterisation

Of the samples treated at 300 ºC and 500 ºC, only the snapper samples had their ^{13}C and ^{31}P spectra recorded. This was due to concerns that the potential carbon black

content of these blackened materials would cause arcing in the NMR solids probe during acquisition of cross polarised solid-state NMR spectra.

The ^{13}C NMR spectrum of the snapper treated at 300 ^{o}C is given below in Figure 2-19.

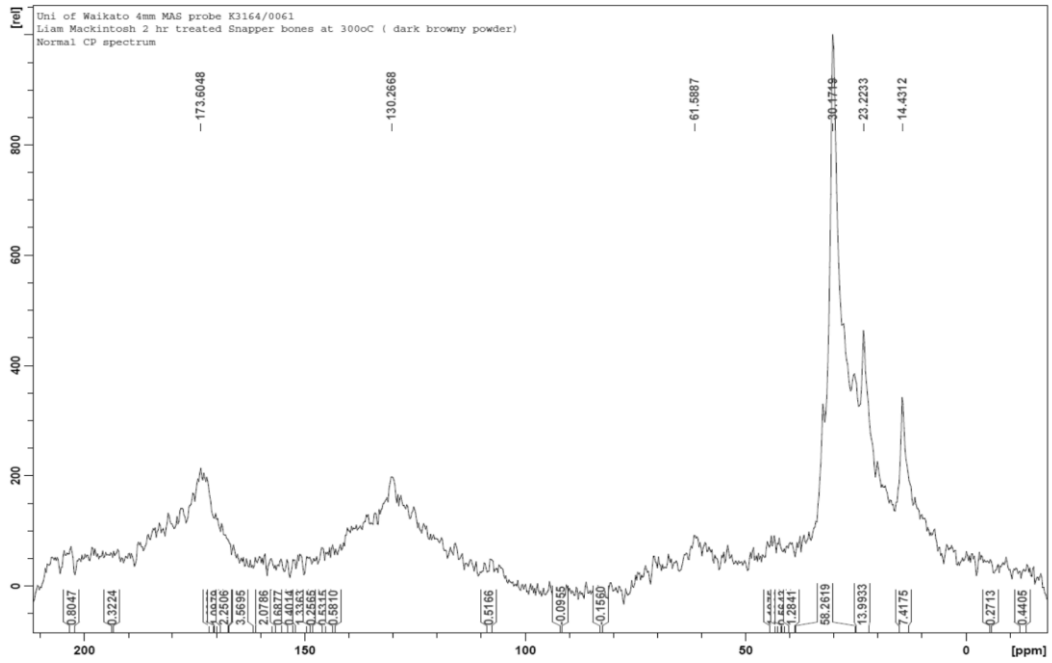

Figure 2-19: ^{13}C SS-NMR spectrum of snapper bones treated thermally at 300 ^{o}C.

The spectrum shows that there is still carbon material present, however the collagen structure has been decomposed and only a few carbon signals remain, such as the C=O peak. Figure 2-20 below shows a comparison of the ^{13}C SS-NMR spectra from the raw (unheated), 300 ^{o}C and 500 ^{o}C samples.

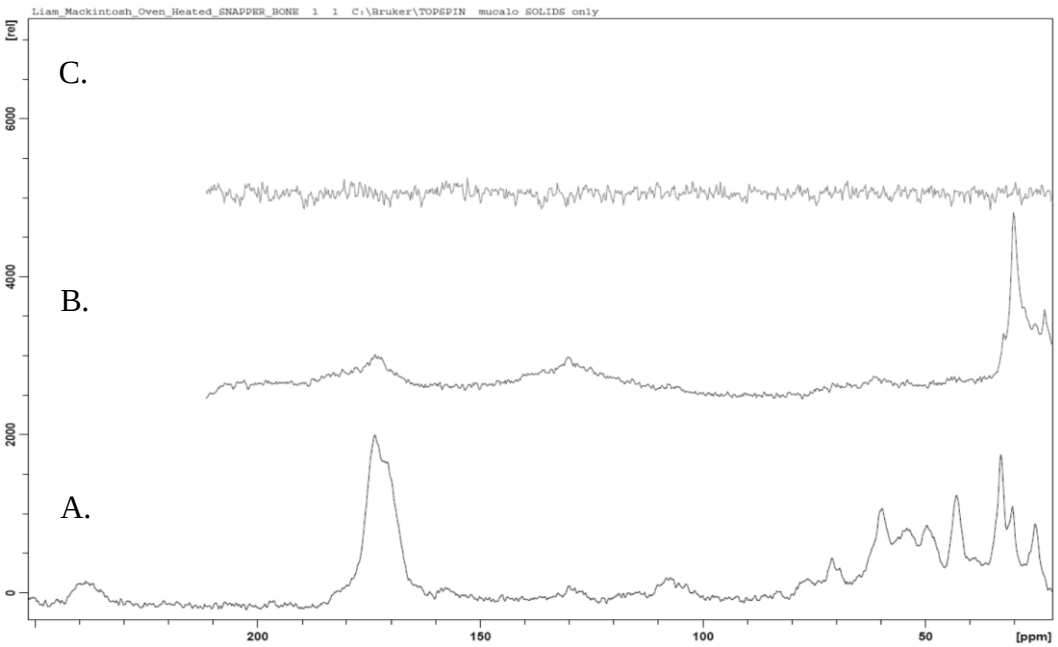

Figure 2-20: 13C SS-NMR spectral comparison of snapper bones (A) Unprocessed, (B) Treated at 300 ^{o}C, (C) Treated at 500 ^{o}C.

The spectrum of the sample treated to 500 ^{o}C shows no carbon signal resolving from the noise. As expected this was also found with the samples treated at temperatures above 500 ^{o}C. While this suggests that there is no carbon content remaining in the sample treated to 500 ^{o}C, the IR spectrum, and the actual appearance of the sample suggests otherwise. This is due to the lack of sensitivity in the NMR technique as there still may be carbon present in the materials, however because of it being at such a low level, it cannot be detected using NMR.

SS-NMR was also used to study the nature of the ^{31}P content in the processed samples. A spectral comparison of these samples is given in Figure 2-21 below.

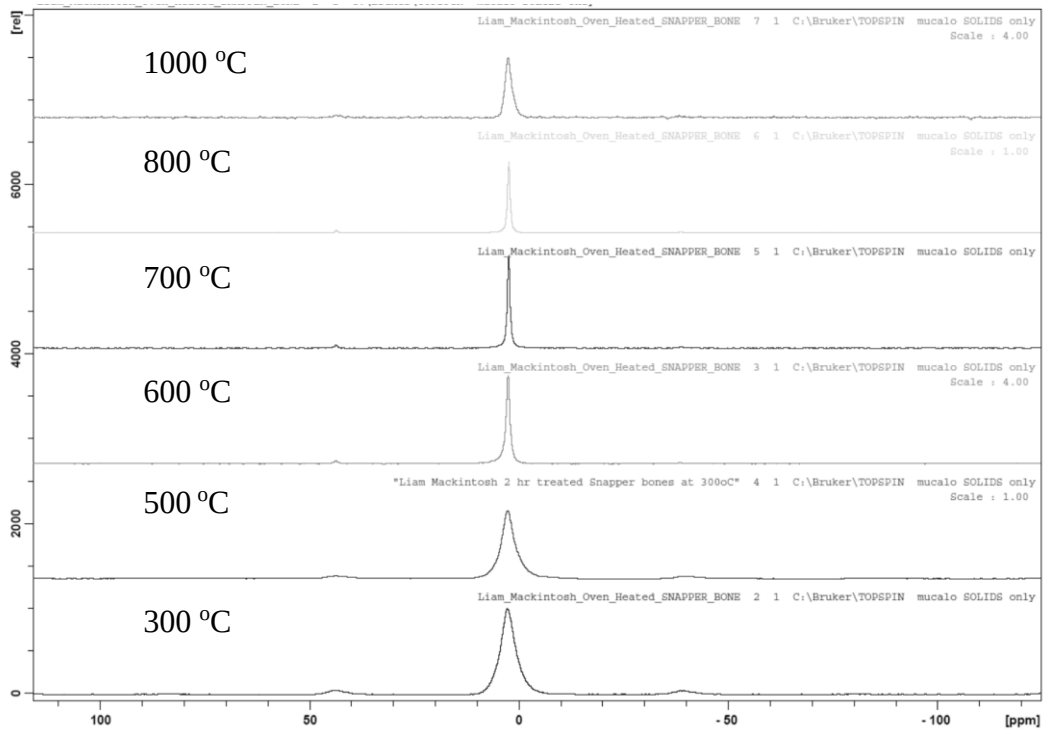

Figure 2-21: ^{31}P SS-NMR spectra of snapper bones treated at different temperatures.

As expected, a single ^{31}P peak was detected in the spectra (with spinning side bands), which can be assigned to the one phosphorus chemical environment found in the HAp structure (i.e. orthophosphate). This ^{31}P peak, appears to become sharper as the treatment temperature increases. As the carbonate, collagen and hydrocarbon-based fats are decomposed, there is likely an increase in purity and crystallinity, and this is commonly accompanied by an increase in the sharpness of peaks. The reference-corrected chemical shifts obtained here range between 2.4 ppm and 2.8 ppm, which are similar to what is reported in the literature for HAp[15]. The other trend observed was that the broadness appears to return in the samples treated at 1000 ^{o}C. When this peak is expanded, as shown in Figure 2-22 below, it becomes

apparent that a shoulder begins to emerge, with the peak losing symmetry. This could provide support for the possibility of low levels of a TCP phase forming due to dehydration of HAp at higher treatment temperatures.

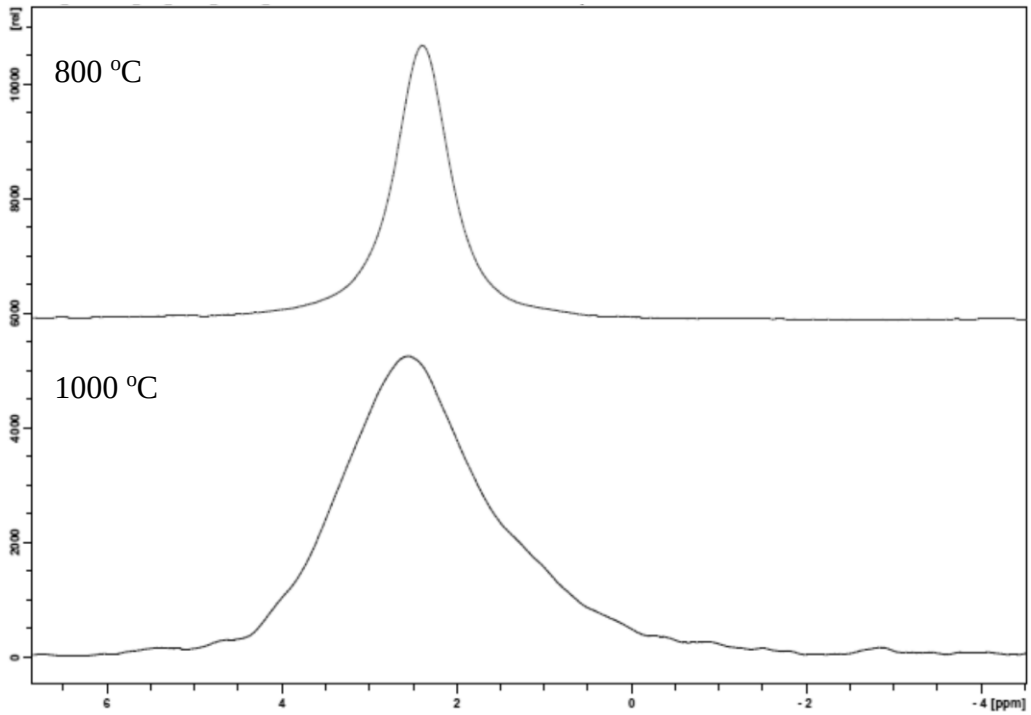

Figure 2-22: Expanded view of ^{31}P NMR spectrum for thermally treated snapper bones.

2.3.1.4 SEM characterisation

SEM images of the fish bone derived powders subjected to the thermal treatment processes are given in Figure 2-23 below.

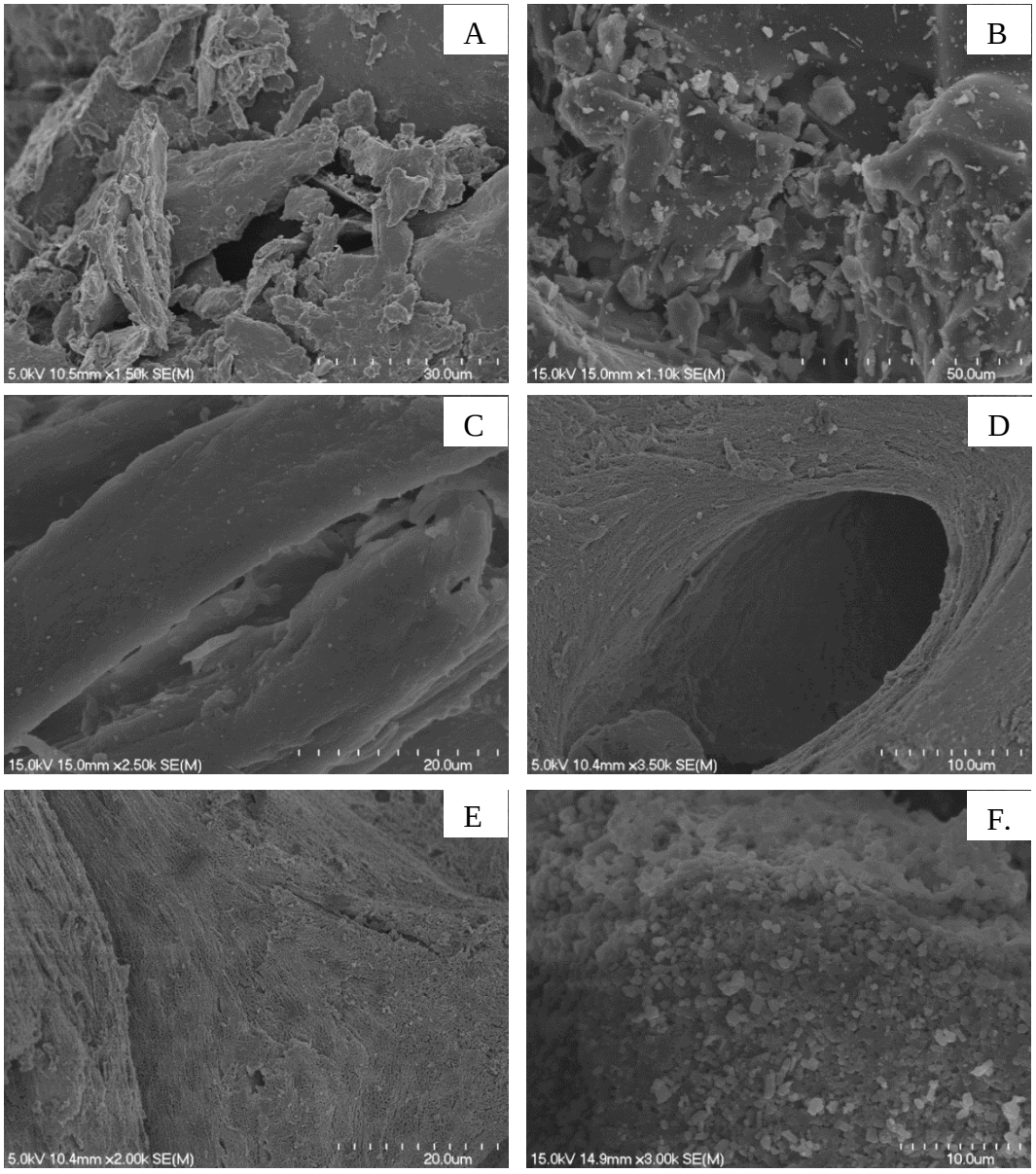

Figure 2-23: SEM images of bone materials processed at differing temperatures: **(A)** Raw **(B)** 300 ºC **(C)** 500 ºC **(D)** 600 ºC **(E)** 800 ºC **(F)** 1000 ºC.

As can be seen in the micrographs, the 'shiny' regions on the surfaces of the materials appear to have all reduced in size as the treatment temperature increases, to the extent that in the material heated to 600 ºC, they are completely absent. These areas as mentioned earlier are associated with the organic content, so it is expected that these would become less prominent in the samples. These results are consistent with the other analytical techniques in that the organics are almost completely removed after heating at 600 ºC. It was also noted that a distinct surface morphological change appeared to occur in samples heated at temperatures of 800 ºC and 1000 ºC, as shown in Figure 2-24 below.

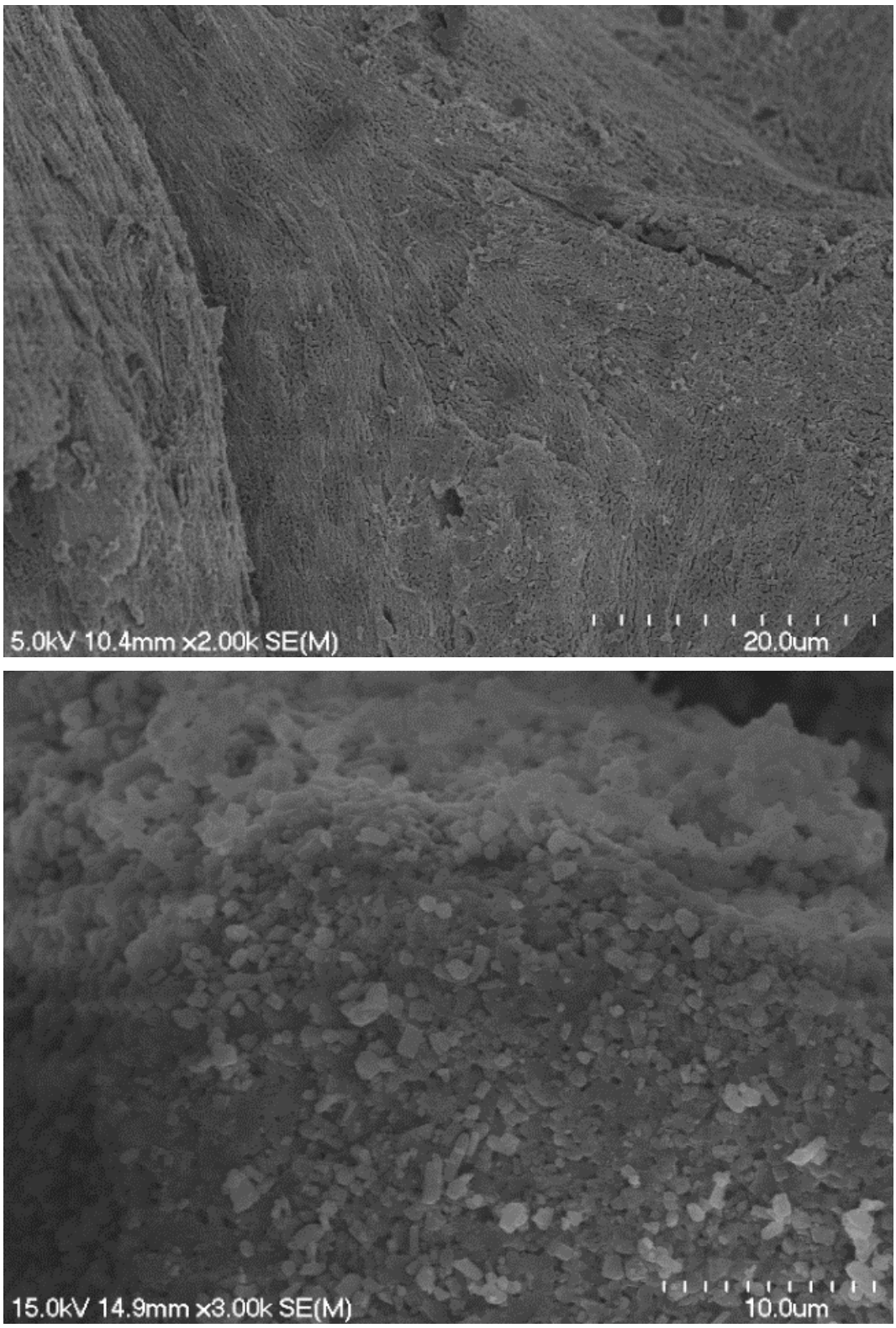

Figure 2-24: Expanded SEM images of bone materials treated to 800 and 1000 ^{o}C.

The bones treated to 800 ^{o}C have a similar appearance to the products of the lower temperatures, a smooth like surface with high porosity. The materials treated to 1000 ^{o}C however appear as though crystals have formed, this has also been found in previous studies and is likely a result of the re-formation of apatite crystals on the surface of the materials[16].

2.3.1.5 pXRD characterisation

XRD analyses were carried out on the samples to gain an idea of the phase changes occurring as a function of processing temperature. The hoki bone powders heated to 300, 500, 600, 800 and 1000 ^{o}C are given in Figure 2-25 below, also compared with the pure HAp (Fluka) diffractogram.

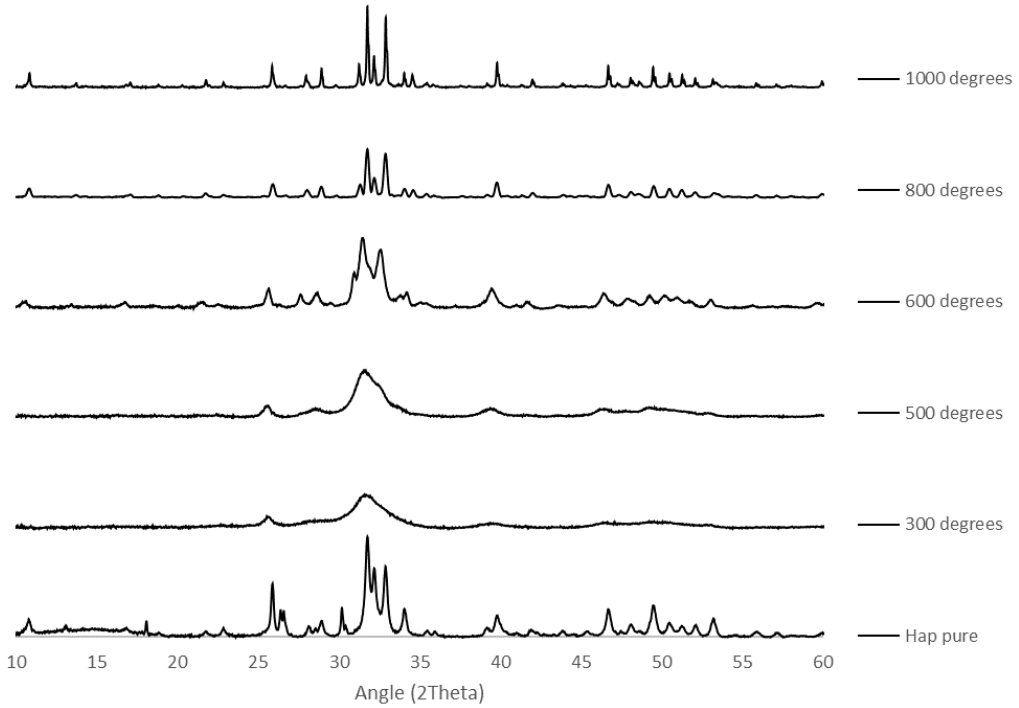

Figure 2-25: XRD diffractograms of thermally treated hoki materials.

As is evident, all of the thermally treated samples follow the same HAp pattern. As treatment temperature increases, there is an increase in peak sharpness, and intensity. This is likely a result of the burning off of the organic impurities, resulting in an increase in hydroxyapatite crystallinity. The sharpening of peaks continues to increase up until being treated to 800 ^{o}C, at this point all residual organic matter has been completely burned off, and the carbonate component is beginning to decompose.

There are however a few peaks in the HAp diffractogram which are not present in the two thermally treated samples, one at 30.2 degrees 2theta, and the other two at 26.4 and 26.5 degrees 2theta. This is suggestive of the decomposition of some of the HAp lattice. As the formation of a TCP phase was suspected to occur at these higher temperatures, a diffractogram of a sample of pure TCP was also recorded and compared to the thermally treated samples as well as to pure HAp. This is given in Figure 2-26 below.

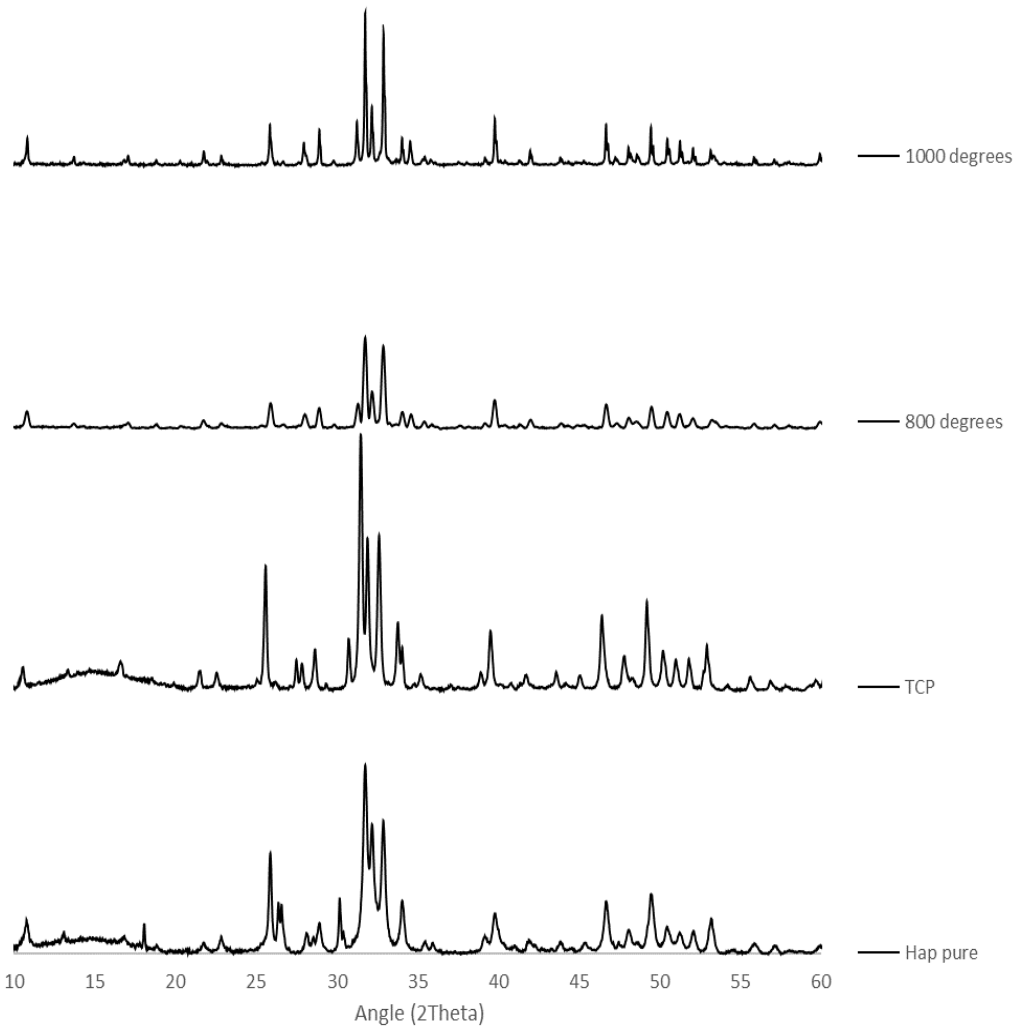

Figure 2-26: XRD diffractograms of thermally treated samples compared with pure TCP (Fluka) and pure Hap (Fluka).

The diffractograms of HAp and TCP have certain peaks which overlap each other. They do however differ in a few peaks. The HAp peaks mentioned above that are absent in these heated samples, (26.4 and 26.5) are also absent in the TCP spectrum. The diffractograms of the heated samples overlap and match the HAp pattern more closely, however small matchings to the TCP spectrum suggest the material is still predominantly composed of HAp, but also contains low levels of TCP due to the decomposition of HAp.

2.3.1.6 ICP-MS characterisation

ICP-MS analyses were also carried out for the thermally treated samples. The results of these are given in Table 2-6 below.

Table 2-6: ICP-MS data for thermally treated snapper bones. RSD values were of similar magnitude to those presented in Table 2-3 earlier.

Concentrations in ug element / g of bone (ppm)					
Element	**Snapper 300 °C**	**Snapper 500 °C**	**Snapper 600 °C**	**Snapper 800 °C**	**Snapper 1000 °C**
11 B	0	0	0	0	0
23 Na	24175.3	38480.3	41989.5	85125.4	65724.5
24 Mg	15418.3	30882.7	33213.6	68651.3	66907.6
27 Al	1313.24	959.66	1276.37	1410.38	974.07
31 P	378230.1	805480.3	878050.6	1834826.6	1800276.3
39 K	5538.81	12187.62	12914.56	21370.23	356.56
44 Ca	942894.1	2017533.8	2125437.7	4486600.4	4510278.0
51 V	0.9132	8.4428	12.2058	21.5475	24.3112
52 Cr	21.918	18.762	21.796	38.198	177.472
55 Mn	168.95	354.60	417.61	765.92	836.30
56 Fe	0	0	0	125.37	12.16
59 Co	3.653	20.638	6.103	293.830	4.862
60 Ni	0	0	0	0	0
63 Cu	14.612	42.214	40.976	84.231	51.053
68 Zn	621.92	272.98	13172.62	3640.55	427.88
75 As	0	0	0	0	0
88 Sr	4564.38	9908.07	10636.44	21667.97	22960.29
107 Ag	0	0	0	0	0
111 Cd	31.963	26.266	28.771	52.889	38.088
121 Sb	0	0	0	0	0
137 Ba	99.543	131.332	141.238	226.249	267.423
201 Hg	0	0	0	0	0
207 Pb	0	0	0	0	0
238 U	0.913	0.938	0.872	1.959	1.621
Ca:P mole ratio	1.93	1.94	1.87	1.89	1.94

Due to costing limitations, it was not deemed necessary to analyse the other species samples through ICP-MS. As seen with the unprocessed samples, these processed samples have a number of metals present. It is expected that the metal of these would be similar to the original samples, the only difference between the materials is the thermal processing, and this should not influence the concentrations of these metals. One difference of interest however, is the lack of nickel in these samples compared to the unprocessed samples. It was assumed that the presence of nickel was from the grinding step, but these thermally samples were also processed using the same stainless-steel grinding equipment. It was noted, that these materials were much more brittle than the unprocessed materials, so it is possible that this has led to less abrasion of the stainless steel during the grinding process, and therefore a lower concentration of nickel would be observed.

The main intention for ICP-MS on these samples was to be able to calculate the Ca:P ratios for each of the materials, which are given at the bottom of Table 2-6 above. These mole ratios do not appear to follow any particular trend, it was expected that these would remain relatively constant, as the absolute values of Ca and P should not be influenced by these treatment temperatures as these were not washed prior to analysis, hence any CaO which may have formed would still be present. It is possible, that the variation observed is a result of heterogeneity in the original samples used in the thermal treatments.

2.3.2 Thermal treatment of shell materials

As with the bones, the shells were subjected to a range of treatment temperatures with characterisation of each sample produced. The intention, as with the bone samples, was to produce materials which could be assessed for their potential to have an industry/environmental application.

2.3.2.1 Observations

Figure 2-27 below shows the appearances of the mussel shells after exposure to a range of treatment temperatures. A summary of the other species studied is given in appendix 2.

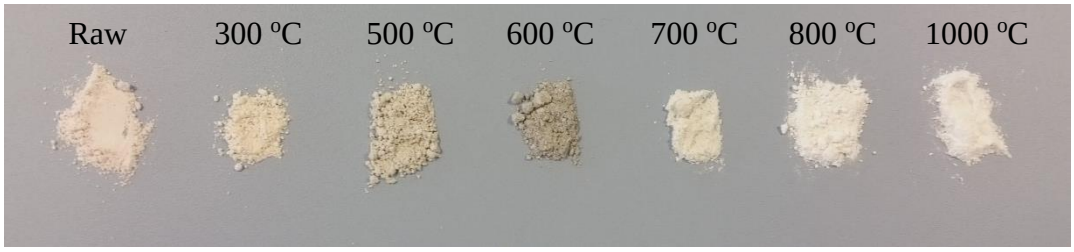

Figure 2-27: Appearances of shell materials as a function of thermal treatments

The weights of these samples were not tracked as carrying out a thermogravimetric analysis was shown earlier to be the most effective way of tracking the weight changes. The results of the TGA on shells are given below in Figure 2-28.

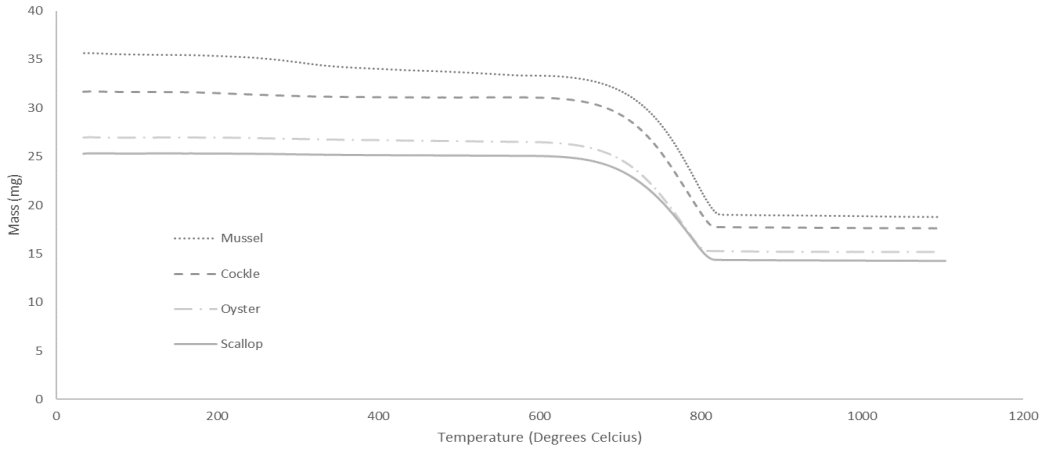

Figure 2-28: TG analysis on shell materials.

The results show gradual weight loss in all samples over the range of 20 °C to 600 °C, however after this point rapid loss occurs. The traces look mostly consistent with each other across all shellfish species studied. This suggests a significant phase change is occurring here, likely a result of the decomposition of a $CaCO_3$ phase.

2.3.2.2 FT-IR characterisation

The two pairs of materials showed slightly different trends in the IR spectrum as they were thermally treated. The first of these trends is given below in Figure 2-29, a spectral comparison of thermally treated oyster shells.

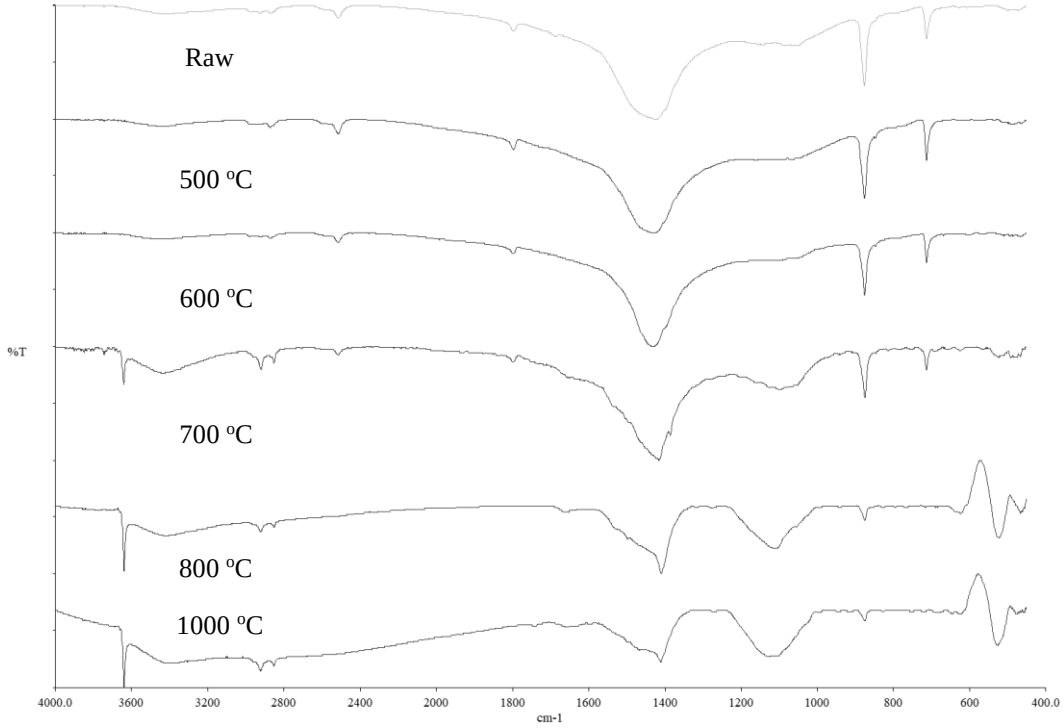

Figure 2-29: FT-IR spectra of thermally treated oyster shells.

The spectra remain mostly unchanged until being treated to 700 °C. At this point, a sharp peak in the OH region begins to appear, which becomes more intense with increasing treatment temperature. As this is also the temperature at which the majority of the weight loss occurred in the TGA, it is likely these changes are associated with a phase change in the material, and that the 700 °C sample is a mixture of the calcium carbonate phase, and a new phase. It has been shown in the literature that treatment of shell materials to between 700 and 1000 °C, can produce calcium oxide[17], through the reaction presented in Equation 2-1 earlier. It is likely that this same process is occurring in these shell materials.

The aragonite material behaved slightly different under these treatment conditions. An IR spectral comparison of the cockle shells is given below in Figure 2-30.

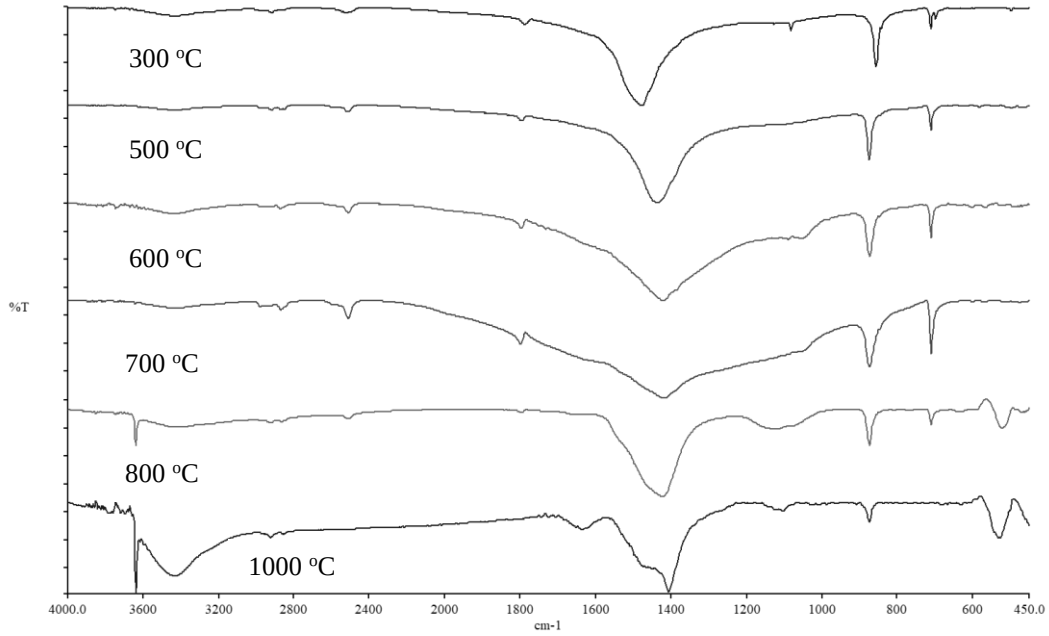

Figure 2-30: FT-IR comparison of thermally treated cockle shells.

The main point of difference in these spectra is that the shells treated to 500 ºC differ slightly from the 300 ºC sample, and hence the raw sample also. The double peak mentioned earlier being characteristic of aragonite changes to a single peak at 713 cm^{-1} when treated to 500 ºC. The rest of IR spectrum for this sample also appears to match closely to the raw oyster and scallop samples. It is therefore likely that the original aragonite polymorph in the cockle shells is converting to the calcite polymorph when treated to 500 ºC. This observation is backed up a previous study[18] which confirms the phase transformation, accompanied by a small weight loss (~1.2 %) occurs at 450 ºC. The same trends were observed in the thermally treated mussel samples. When heated to 700 ºC and above, the samples behaved in the same manner as the oyster and scallop samples.

An IR spectrum of CaO was recorded to confirm the formation of this phase at the high temperatures. This is compared with the cockle sample treated to 800 ºC, and a commercial sample of $Ca(OH)_2$, in Figure 2-31 below.

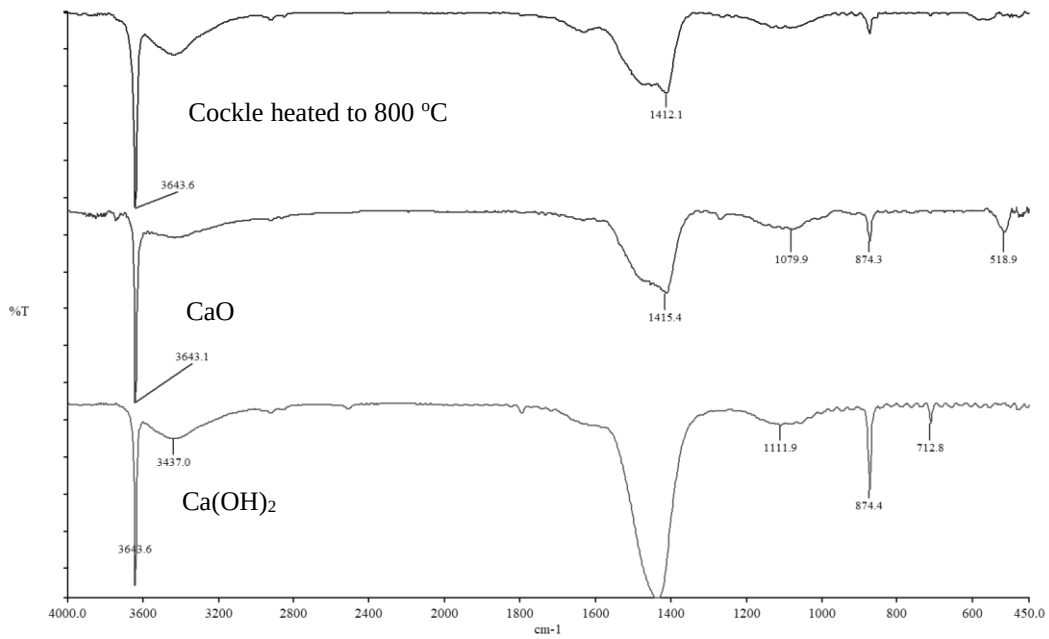

Figure 2-31: IR spectra of processed shells and pure mineral standards.

In theory, CaO should not produce an infrared spectrum as the only bond present is that between Ca and O, and this is not known to produce a stretch in the infra-red region. It is however likely that the material has adsorbed moisture during the disc formation and produced small amounts of $Ca(OH)_2$, sufficient to be detected by the spectrometer. Preventing exposure to moisture during the formation of these discs was not possible as there was no way to isolate the equipment from the atmosphere. The sample treated to 800 ^oC appears to match almost perfectly to the CaO IR spectrum. It is therefore likely that this hydrolysis has also occurred to a similar extent in the heated material, hence CaO is likely to be the main phase present in these samples with some $Ca(OH)_2$ also present.

2.3.2.3 SS-NMR characterisation

^{13}C SS-NMR spectra were attempted for shells which had been thermally treated, however these resulted in spectra which had no signal isolated from the baseline. Figure 2-32 below contains the ^{13}C NMR spectrum of mussel shells treated to 300 ^oC.

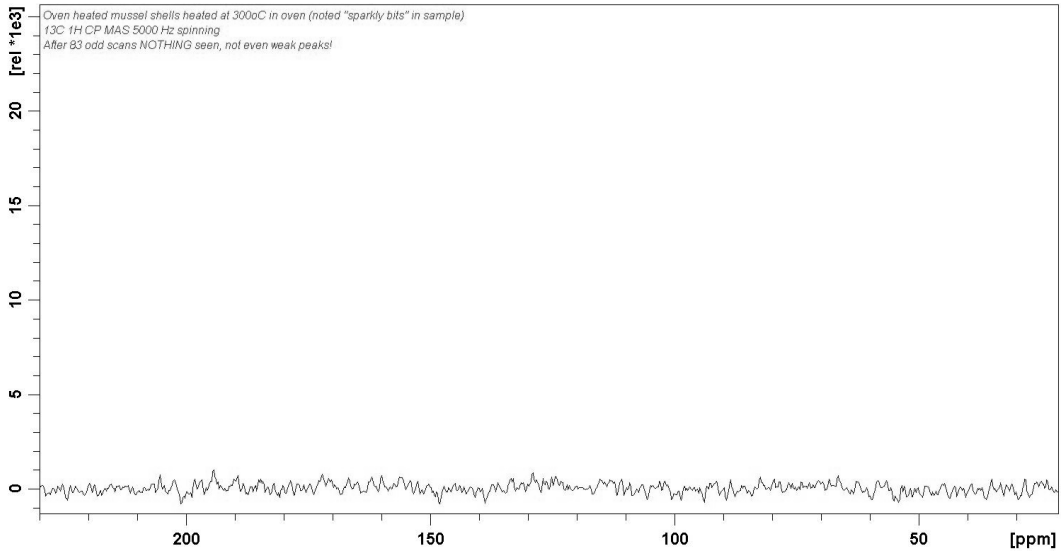

Figure 2-32: CP ^{13}C SS-NMR of mussel shells treated to 300 ^{o}C.

The lack of signal is likely due to a lack of protons in the ceramic/mineral nature of the materials, which prevents cross polarisation occurring. High power decoupling was also used, which is a direct polarisation technique. It was hoped that this would produce a single peak in the carbonate region as seen in the raw samples, however this was not the case. These were repeated for a sample treated to 500 ^{o}C, however the same result was observed. For a carbon atom to have a signal in the ^{13}C CP-MAS NMR spectra, there needs to be nearby protons[19]. Thermally treating the materials to 300 ^{o}C has reduced the already low organic and water content in the shell materials to an extent where there are no longer protons in the structures, and hence no signal is observable for these samples. It was concluded that NMR would not be a useful technique to characterise these materials, FT-IR produced much more valuable information on the phases in the samples, with the benefit of a quick results turnaround time, compared to the use of SS NMR.

2.3.2.4 SEM characterisation

Figure 2-33 presents SEM micrographs of the treated cockle shell materials.

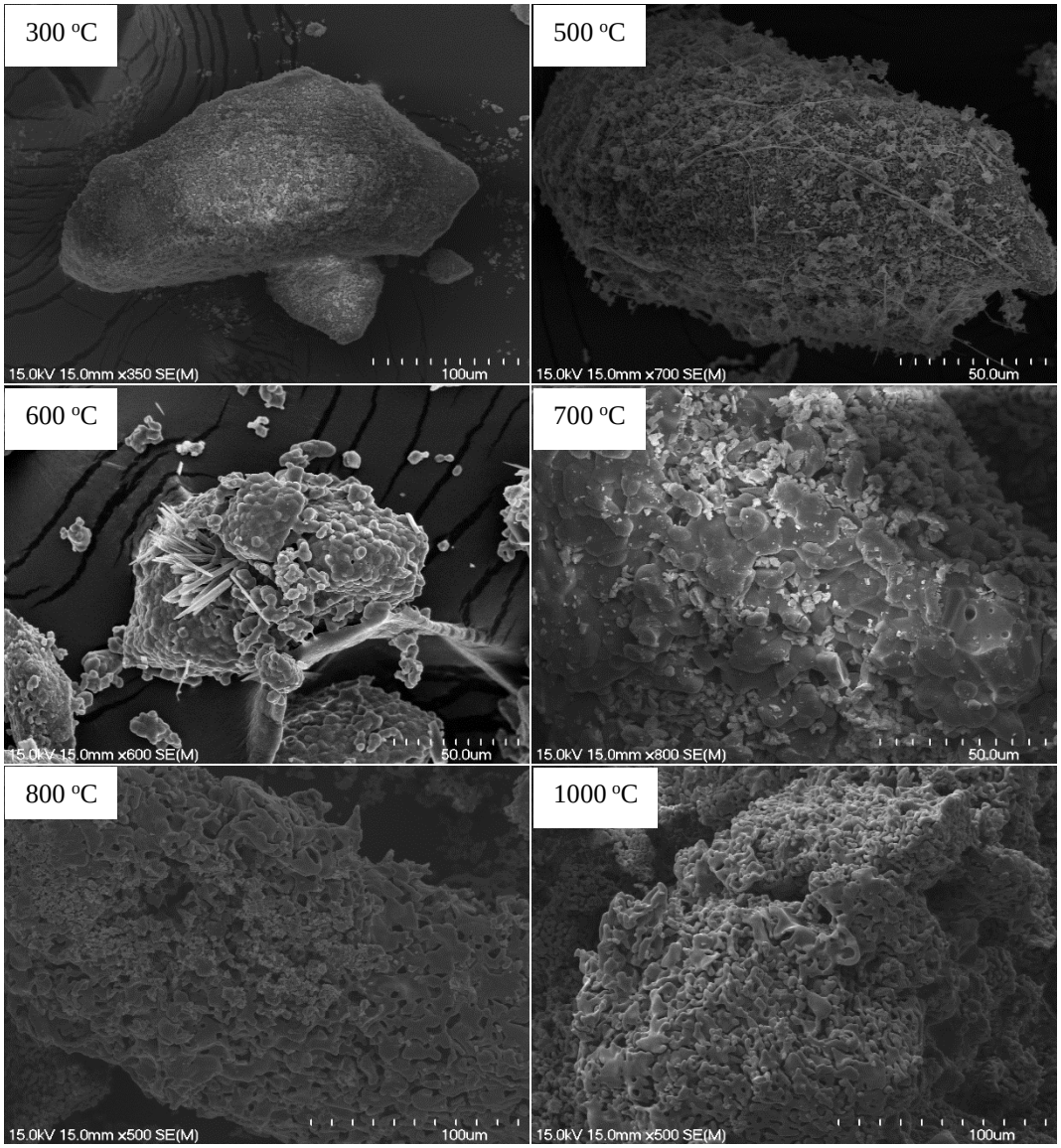

Figure 2-33: SEM micrographs of thermally treated cockle shell derived powders.

The micrographs show distinct surface morphology changes occurring at a few of the treatment temperatures. The shells treated to 300 ºC appear to have a solid crystallising on the surface of the material. This crystallisation appears to be more intense in the sample treated to 500 ºC, with the additional formation of long string like crystals on the surface. As this material was the cockle shells, which were found to be naturally aragonite, which transforms into calcite between 300 and 500 ºC, it is possible that the surface crystallisation in these samples is a result of this conversion of the aragonite to calcite, similar observations can be found in literature[20]. In the 600 ºC micrograph, needle like crystals can be seen on the surface. This provides further evidence of crystallisation of the new phase. It was shown in the FT-IR spectra that heating the materials to 700 ºC causes the formation of CaO

in the material. This is reflected in the micrograph also, it appears as though there is a new material crystallising on the surface of this mater compared to the sample treated at 600 ^{o}C. This new surface type becomes increasingly prominent in the 800 ^{o}C micrograph. It is understood that at this temperature, the material has almost completely converted to CaO. The surface of the material treated to 1000 ^{o}C appears unchanged from the 800 ^{o}C sample. This is consistent with the IR also, as there are few differences between the two samples, both appearing to be predominantly CaO (with some presence of $Ca(OH)_2$).

2.3.2.5 pXRD characterisation

Cockle shells were chosen for the XRD comparison as these were shown to be aragonite in the raw materials. Diffractograms showing the differences between samples treated at 300, 500, 600, 700, 800 and 1000 ^{o}C are given in Figure 2-34 below.

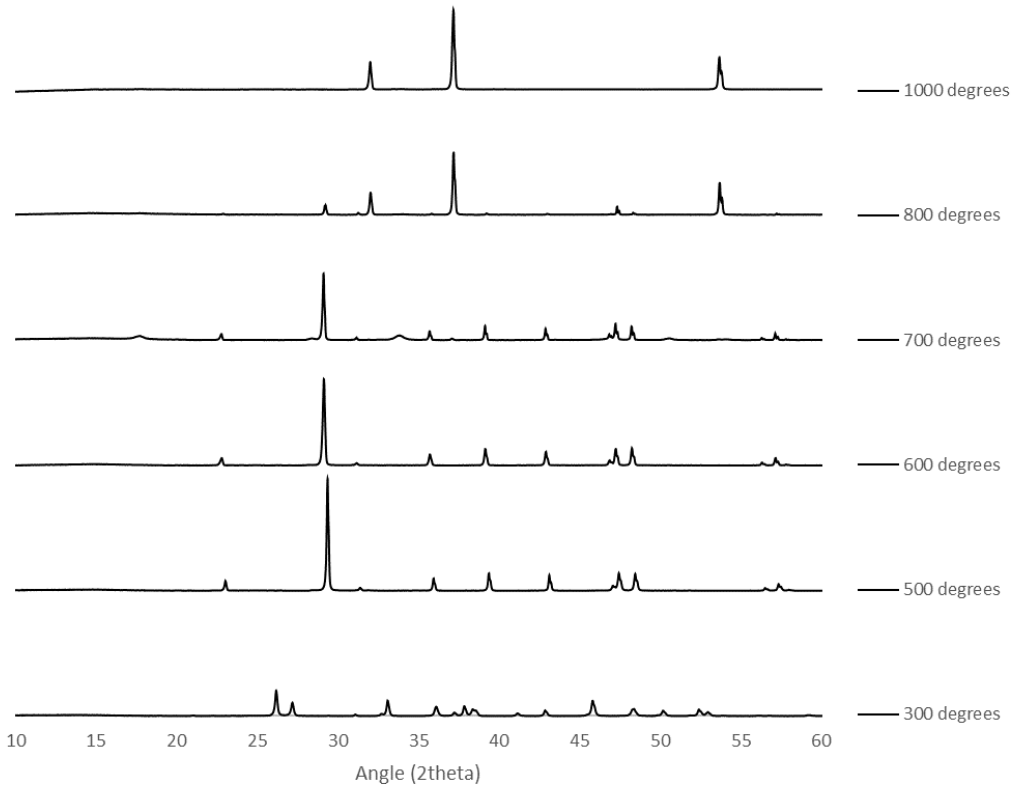

Figure 2-34: XRD diffractogram of thermally treated cockle shells.

The sample treated to 300 ^{o}C has a distinctively different pattern compared to the 500 and 600 ^{o}C samples. Matching these patterns to the pattern database on the XRD instrument showed that the samples treated at 300 ^{o}C are still primarily composed of aragonite, where as those treated at 500 and 600 ^{o}C have converted to the calcite polymorph of $CaCO_3$. This is consistent with the FT-IR spectra for these

materials. The phase change appears to occur between 300 ºC and 500 ºC, with literature suggesting this occurs at 450 ºC[18]. As with the IR spectra, when treated between 500 and 600 ºC, the cockle and mussel samples have diffractogram which match the raw samples of the oyster and scallop shells, which provides further support for the phase change of aragonite to calcite at these temperatures.

Comparison of the higher temperature samples shows a phase change beginning to occur at 700 ºC and becoming much more intense at 800 ºC. The 600 and 700 ºC sample show a lot of overlapping peaks, while the 800 ºC sample is distinctively different.

Diffractograms were recorded of pure samples of CaO and $Ca(OH)_2$ for comparison with these treated samples, given in Figure 2-35.

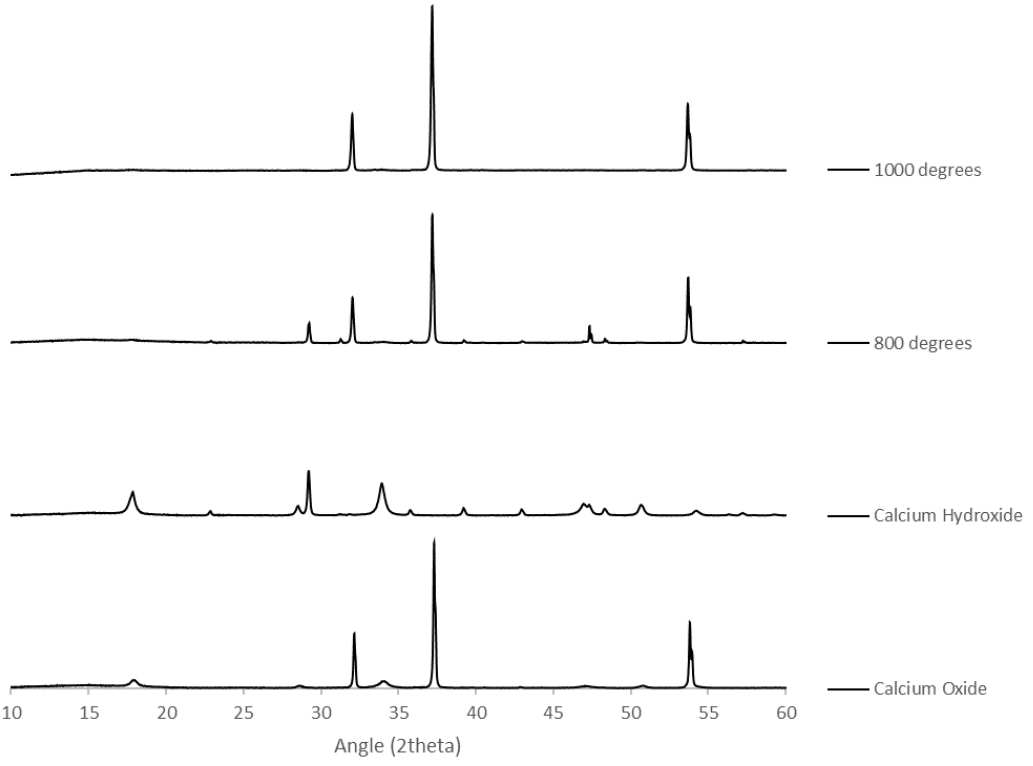

Figure 2-35: XRD diffractograms of cockle treated to 800 and 1000 ºC, compared with diffractograms of CaO and $Ca(OH)_2$.

The 800 ºC sample appears to show similarities to both CaO and $Ca(OH)_2$, however it is clear that CaO gives the dominating pattern. This observation is the same for the 1000 ºC treated sample. It is therefore likely that treating the samples to 800 ºC produces a sample with a dominant CaO phase, but with some $Ca(OH)_2$ presence also, while treating all the way to 1000 ºC generates a sample which appears to be almost pure CaO. This observation was consistent for all four of the shell species.

The presence of $Ca(OH)_2$ is understood to be due to the hydrolysis of CaO from moisture in the atmosphere.

2.3.3 General findings from thermal processing techniques

2.3.3.1 Thermal treatment of bone materials

The general trend observed in the thermal treatment of these bone materials is that the organic matter burns off between 300 ^oC and 500 ^oC. Between 500 and 800 ^oC there is an increase in the crystallinity of the HAp material, shown by the increase in sharpness of the peaks in the ^{31}P SS NMR spectra and XRD diffractograms. At temperatures above 700 ^oC the carbonate content is believed to burn off through conversion to CO_2 (g) and CaO (s), which can be washed away from the rest of the material with water. This was only done prior to the materials being used in application studies and not prior to characterisations.

Increasing the temperature past 800 ^oC (to 1000 ^oC) appears to induce the conversion of some of the HAp content to TCP, through loss of OH in the HAp lattice. This is accompanied by a reduction in the intensity of the OH peak in the IR spectra, as well as the change of the single ^{31}P peak in the NMR from symmetrical at 800 ^oC, to asymmetrical at 1000 ^oC, suggesting a new P chemical environment is being produced admixed into the existing and predominant HAp phase. Because of the above, the ideal treatment temperature in terms of HAp production for these bone materials, would be 800 ^oC, however if the material is to be used in biomedical applications, it would need to be washed thoroughly with water to remove any CaO which may be present, as this can induce alkalinity when the HAp is exposed to body fluids which has cytotoxic effects[21].

2.3.3.2 Thermal treatment of shell materials

Table 2-7 below summarises the results from the analyses on the thermally treated shell materials.

Table 2-7: Summary of predominant phase changes in shell materials as a function of treatment temperature.

Treatment temperature	Species	
	Cockle and Mussel	**Scallop and Oyster**
Raw	Aragonite	Calcite
300 ^oC	Aragonite	Calcite
500 ^oC	Calcite	Calcite
600 ^oC	Calcite	Calcite
700 ^oC	Calcite/CaO/$Ca(OH)_2$	Calcite/CaO/$Ca(OH)_2$

800 °C	$CaO/Ca(OH)_2$	$CaO/Ca(OH)_2$
1000 °C	CaO	CaO

The presence of $Ca(OH)_2$ was noticed in some of the samples, this is likely to be the result of CaO in the sample absorbing moisture from the atmosphere (despite being kept in air tight containers) to form $Ca(OH)_2$. This is typical of CaO[22], it occurs through the following exothermic reaction $CaO + H_2O \rightarrow Ca(OH)_2$.

Treating the materials to 1000 °C appears to create a sample which is composed primarily of CaO, with no detectable $Ca(OH)_2$, however it is not known what other impurities may be present. It is possible that $CaCO_3$ may be reformed on the surface of the material as a result of the formation of $Ca(OH)_2$. Of course, these CaO reactions which occur from the adsorption of moisture could be avoided through the careful handling of the materials ensuring they do not come in contact with the atmosphere. Thermally treating $CaCO_3$ to these high temperatures is the typical method of creating CaO[22], usually using limestone or seashells as the source of $CaCO_3$, and so these findings were expected from the chemistry of these materials.

2.4 Chemical Treatments of the bone powders

A range of chemical treatments were carried out in attempts to process and produce a hydroxyapatite powder which was free from organic residues. This was done as the intention was for these to be used in the water treatment applications, in which hydroxyapatite is the desired material, while the organic residues are considered impurities. The presence of organic material in HAp if used in biomedical applications can also lead to infections or the spread of diseases, so the organic material needs to be removed before these can be implanted into bodies.

2.4.1 Refluxing in type 1 water

2.4.1.1 Observations

The first material trialled in these experiments was the snapper bones. Initially the suspension of the bone materials in the water produced no visible change to the solution, however once the boiling point was reached, the water quickly changed its appearance to that of a brown “sludge”. The resulting solids suspended in the water were of similar colour. After decanting off the water, the materials were washed and refluxed again, with the same outcome as the first attempt. This was repeated a third time, however on this occasion no significant change to the solution

was observed. The resulting material, however was ultimately converted into a pale orange powder as a result of being washed/refluxed in triplicate in water.

2.4.1.2 FT-IR

Figure 2-36 below shows the FT-IR spectrum of the hoki bones processed through this water reflux technique.

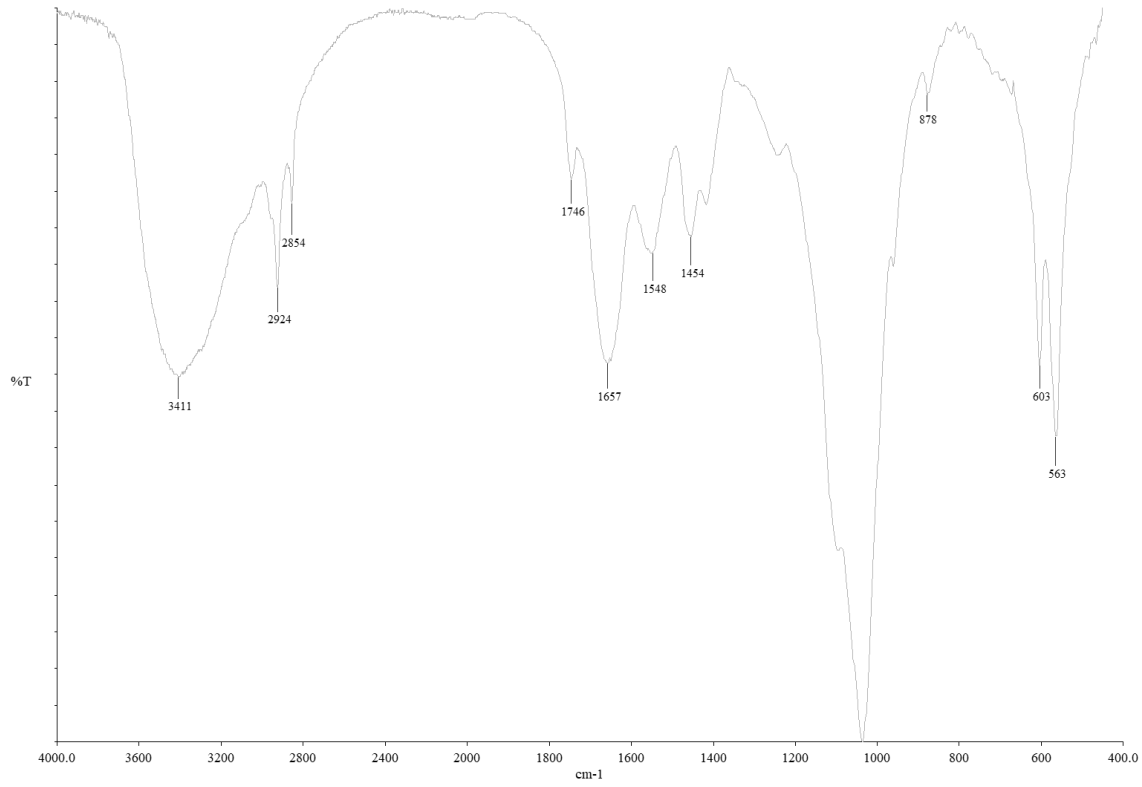

Figure 2-36: FT-IR spectrum of hoki bones processed through refluxing in water in triplicate.

Compared with the (as received) raw bones IR spectrum (Figure 2-2), the group of peaks associated with the organics content was observed to decrease in intensity relative to the PO_4 stretching peak, however these were still a prominent feature in the spectrum, suggesting that the process has not removed a significant level of the organics. This is consistent with the appearance of the material, still being an orange colour indicates these have still retained a significant organic content, including the collagenous component.

2.4.2 Refluxing in NaOH

It was clear from the above that refluxing in water was not an aggressive enough method to remove the organic content, and so NaOH was trialled instead. Firstly, the materials were soaked in NaOH overnight, to ascertain if the application of heat and stirring was necessary. This method produced materials with a distinct orange colour. The same orange colour was found in the solutions which the bones were

immersed in. It was clear that soaking alone would not have a significant effect on the organics content of the bone, and so reflux (heating) experiments were carried out instead, with stirring.

2.4.2.1 Observations

Raw hoki and flounder bones:

With these bone powder samples, the solution was initially cloudy with a pale green tinge. Once heated the solution had turned a deep brown, with the bone materials appearing as a white solid at the bottom of the solution. The starting material was a flaked bone material, however the product appeared as a fine white powder, indicating the material had been broken down during the reflux process.

Raw gurnard and snapper bones:

Immersion of the as received gurnard and snapper bones in NaOH led to a deeply orange coloured solution being formed immediately. The solution became more intensely coloured after heating was commenced with, the resulting solids becoming slightly yellow, and remaining as mainly intact bone shards. These were refluxed a second time in NaOH with the resulting solution, this time, becoming cream in colour, and the solid materials being converted to a fine white powder.

The differences in results of these treatments is likely a result of the different levels of organics i.e. oils, fats, remaining in the materials. It is possible, that these are species specific differences, as all four species bones were processed using the same methods prior to being received.

2.4.2.2 FT-IR characterisation

The infrared spectrum of the flounder bones refluxed in NaOH is given below in Figure 2-37.

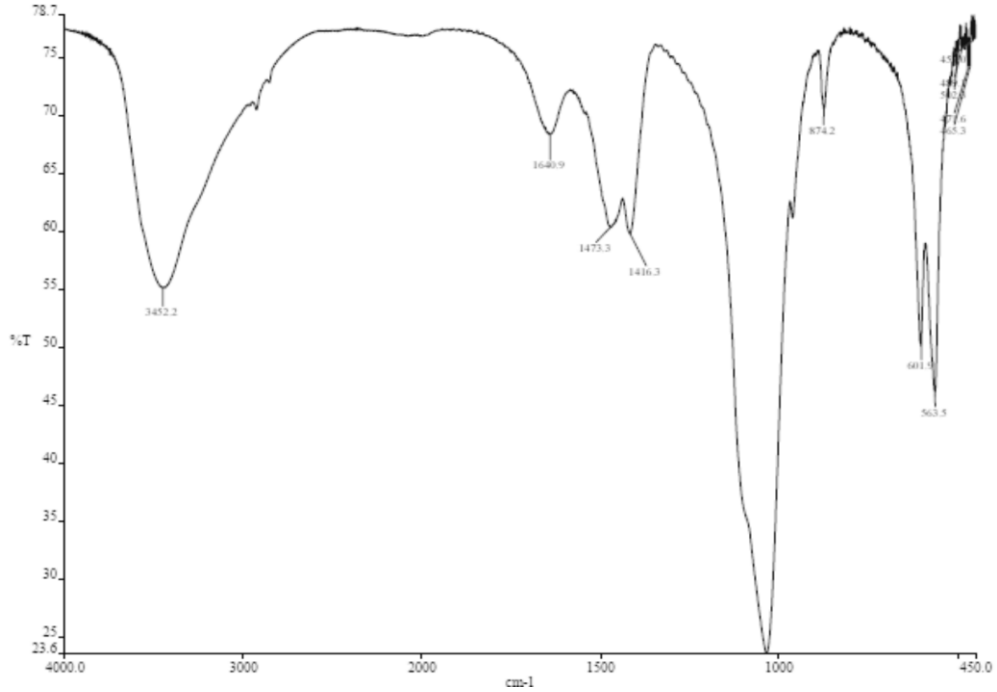

Figure 2-37: FT-IR spectrum of flounder bones refluxed in NaOH.

The phosphate peak at ~1000 cm^{-1} is now the dominating peak in the spectrum. The region between 1400 and 1600, associated with organics and carbonate, is now much smaller relative to this phosphate peak. This suggests that the levels of organics have dropped significantly from the treatment. The sharp -OH peak is not obviously present in this spectrum. This is understood to be due to carbonate species substituted for OH in the HAp lattice, close inspection does suggest a shoulder is present on the left side of the broad OH peak, which could correspond to the sharp peak.

2.4.2.3 Washing products in acetic acid

These materials were soaked in acetic acid, to determine if they could be further cleaned and purified after the NaOH treatment, the idea behind this being that any organics that were not soluble in base, may be soluble in acid. Weak acetic acid was used as it is known that the inorganic mineral content of the bone, i.e. the HAp will dissolve in low pH (< 4) solutions.

The solution appeared unchanged after the bones had been immersed, and the bones themselves also appeared unchanged by the process. An infrared spectrum of this product, compared with NaOH refluxed product is given below in Figure 2-38.

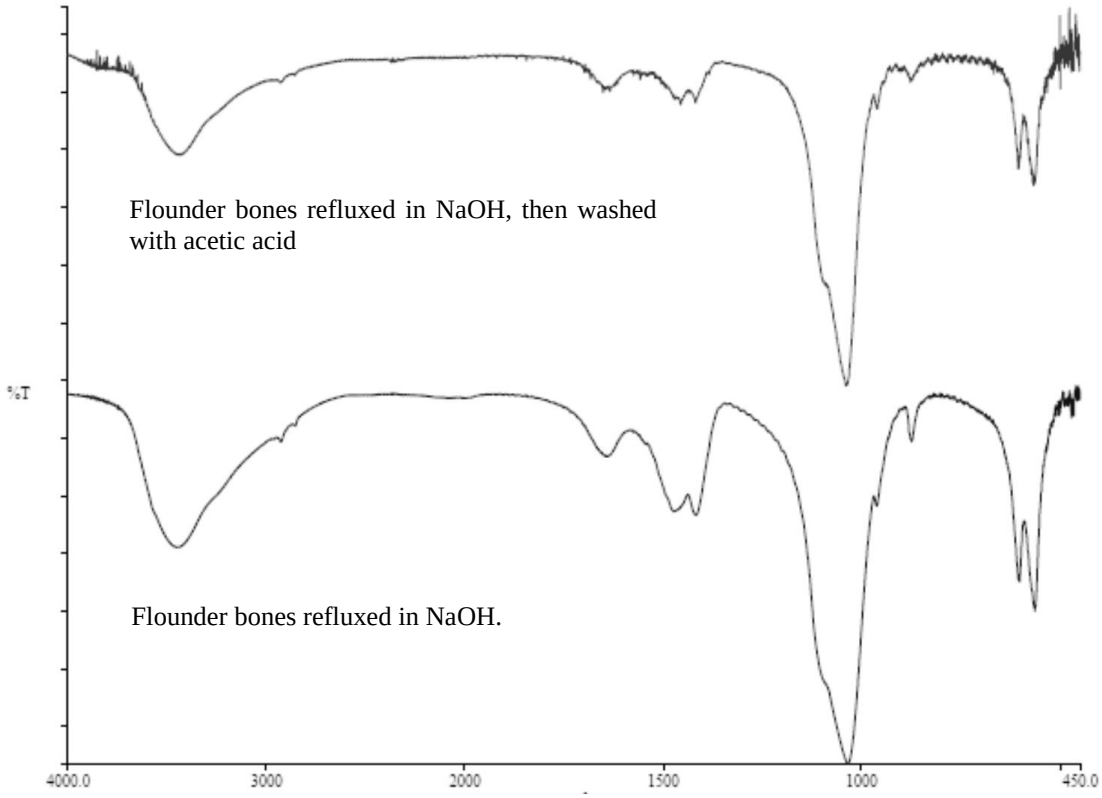

Figure 2-38: Infrared spectral comparison of chemically treated materials.

The carbonate peak (~1450 cm^{-1}) appears to have decreased in intensity, this is expected due to the instability of carbonate in acidic solutions. This however was the only noticeable change in the material, and so the need to carry out this extra step is not justified.

2.4.3 Refluxing of the as received bone samples in ethyl acetate

2.4.3.1 Observations

Ethyl acetate has been previously used as a solvent for treating natural bones materials[23]. It was used in this study as it is a relatively weak polar substance, and so it may target any organic residues that are poorly soluble in the strongly polar NaOH and H_2O (such as the fatty components of the material). The ethyl acetate solution appeared to turn slightly cloudy during the reflux process, however did not adopt that same orange colour that the NaOH solutions did. The bones after the treatment appeared relatively unchanged but did have a slightly lighter colour with their shape being unaffected.

2.4.3.2 FT-IR

The IR spectrum of these materials is given in Figure 2-39 below.

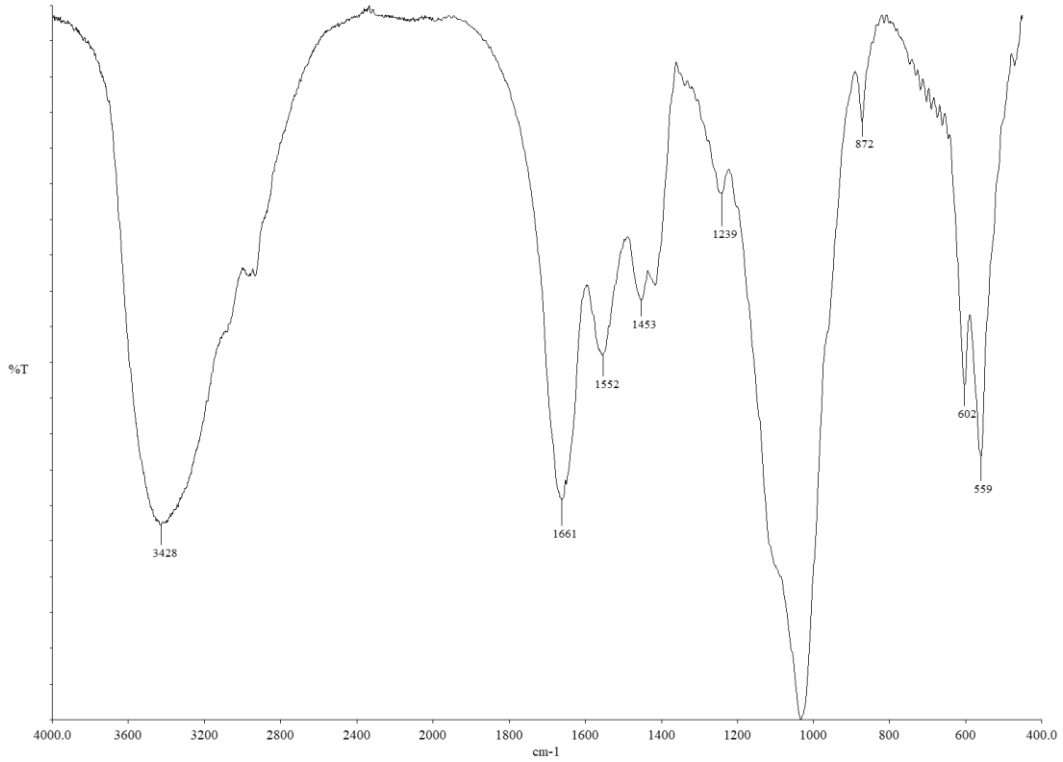

Figure 2-39: FT-IR spectrum of hoki bones refluxed in ethyl acetate.

The relative sizes of the peaks have not been significantly affected by this treatment, again indicating the levels of the organics have not been significantly reduced. This could be due to the solubility of the oils in this solvent. As mentioned earlier, it is possible that the use of this solvent would be more effective when used on materials which had previously been heated with NaOH and washed (with type 1 water) extensively. It is understood that ethyl acetate would target the lipid/fat content in the bone materials, but would not influence the other components of the material, i.e. collagen, carbonate etc.

2.4.4 Soaking in NaOCl

Stirring these materials in a 15% NaOCl solution caused the solutions to become a cloudy light brown colour. The resulting solid materials were slightly lighter in colour, however the change was not as significant as the changes observed when the materials were treated with NaOH and heat. The infrared spectrum of the hoki bone-derived powder, compared with a sample treated with bleach, is given below.

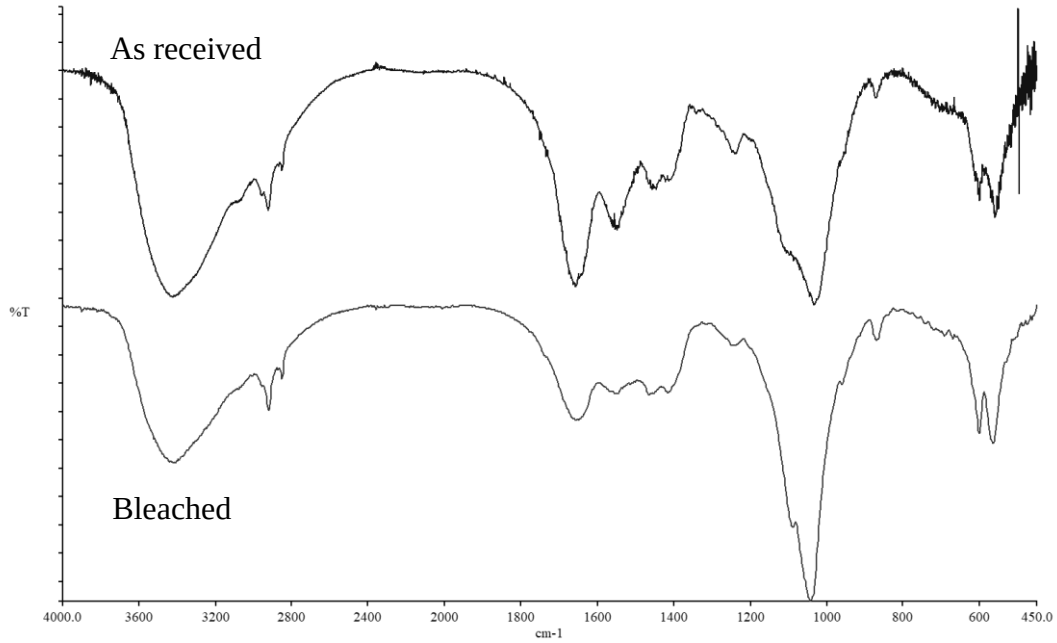

Figure 2-40: As received and bleached hoki bone-derived powder IR spectral comparison.

It is clear from the above spectra that the organic content in the bone materials have been significantly reduced. The collagenous peaks (1650-1550 cm^{-1}) have been reduced in size relative to the phosphate peaks. The carbonate peaks are unaffected by this treatment, due to its stability in NaOCl.

2.4.5 Digestion and reprecipitation of bone materials

Digestion and reprecipitation experiments were carried out with the intention of generating a fine crystalline and homogeneous hydroxyapatite powder. These digestion and reprecipitation processes were also coupled with some pre-treatment techniques for improving the quality of the product.

2.4.5.1 Observations

The first step for this processing technique was the digestion of the bone materials. This was done with either nitric acid or hydrochloric acid. When digesting with HNO_3, samples which had a residual organic content formed a variety of orange/yellow coloured solutions. This is understood to be due to the occurrence of some xanthoproteic reactions[4], a well-known phenomenon which occurs when nitric acid reacts with certain amino acids within collagen proteins, such amino acids are likely to be present in this raw bone material[4]. This colour led to a precipitated powder which also had a yellow/orange colour. To prevent this, and achieve a more aesthetically acceptable white product, it is necessary to remove the organic species before digestion. This was partially achieved through chemical

methods, such as refluxing in the presence of NaOH. Heating the materials to 700 ^{o}C however was guaranteed to remove all organic content. Alternatively, hydrochloric acid could be used as the digesting acid as this discolouration due to xanthoproteic reactions do not occur in concentrated HCl solutions. The disadvantage to the use of HCl, is that the presence of Cl^- in solution can lead to the incorporation of Cl into the apatite lattice in place of OH during reprecipitation[24]. Nitrate does not have this same affinity to replace OH, so the use of nitric acid, with bone materials free of organic materials is the preferred method.

The second step to this process was the reprecipitation of the HAp. Gradual successive addition of NaOH to the digest caused the formation of a precipitate. These were mostly white in colour, again except for the orange coloured digests from HNO_3. These solid materials were found to be fine in nature, and caused blockages in the filter paper when attempting to vacuum filter them from their mother liquors. For this reason, these were instead washed with water by repeat centrifugation and decanting off of the mother liquors. The dried products were hard in nature but could still be ground down using a mortar and pestle.

A range of products was produced using the above techniques, which are summarised below in Table 2-8.

Table 2-8: Summary of materials produced through chemical reprecipitation methods.

Sample name	Treatment
HRr	Raw hoki bones, digested in HNO_3 and reprecipitated using NaOH
H8r	800 degree treated hoki, digested in HNO_3 and reprecipitated using NaOH
H10r	1000 degree treated hoki, digested in HNO_3 and reprecipitated using NaOH
HNr	Hoki bones refluxed in NaOH, digested in HNO_3 and reprecipitated using NaOH
HRrCl	Raw hoki bones, digested in HCl and reprecipitated using NaOH
H6rCl	600 degree treated hoki, digested in HCl and reprecipitated using NaOH
H8rCl	800 degree treated hoki, digested in HCl and reprecipitated using NaOH
H10rCl	1000 degree treated hoki, digested in HCl and reprecipitated using NaOH

2.4.5.2 FT-IR

Figure 2-41 below contains the IR spectra of the raw hoki bones reprecipitated using HNO_3 and HCl as the digesting acids, compared with the spectrum of pure (Fluka brand) HAp.

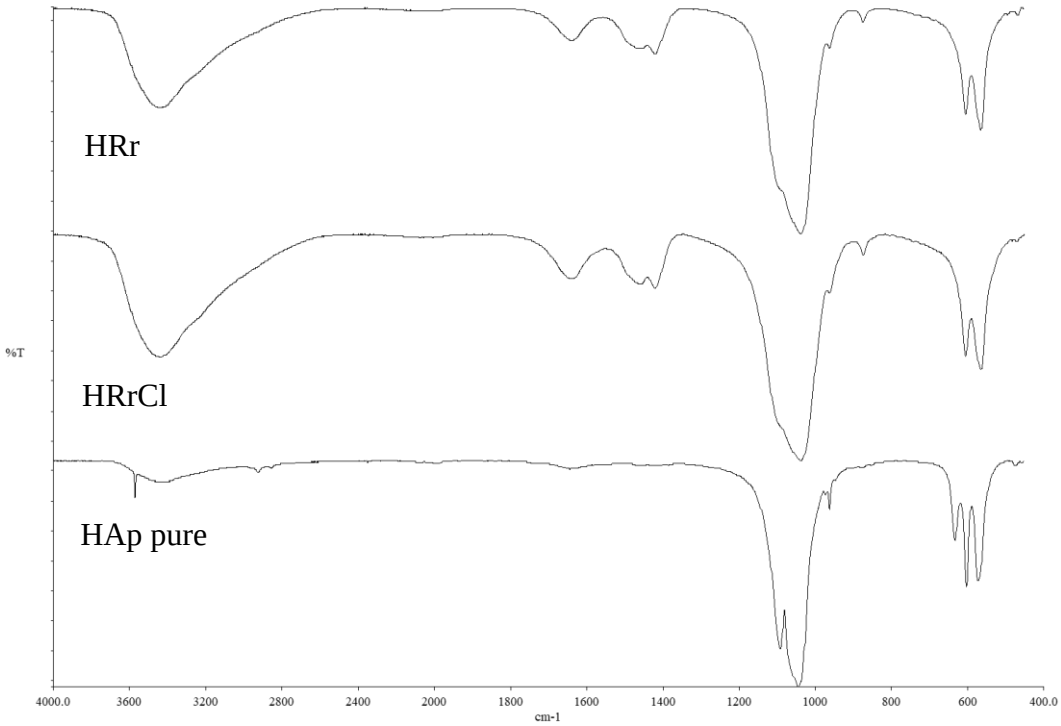

Figure 2-41: FT-IR spectra of reprecipitated materials and pure HAp.

The reprecipitated products appear to be free from any residual organics. There are however still contributions from carbonate (~874 and 1450 cm^{-1}), and from moisture (~3400 cm^{-1}, and 1640 cm^{-1}).

Infrared spectral differences between the materials digested using different acids appear to be small, the spectra have similar peaks in terms of the shapes, size and positions. And so, it is likely that there is little difference between the materials, other than the orange discolouration mentioned earlier for the materials digested using HNO_3. Both of these materials have the characteristics of the pure hydroxyapatite spectrum, however their peaks are broader, and possibly contain significant water contamination. The broadness and decreased resolution of some peaks suggests these processed materials are poorly crystalline, compared to the pure HAp material.

Attempts were then made to decrease the organics content of the materials prior to digestion, so that nitric acid could be used as the digesting acid with the avoidance of any orange colouration. The IR spectrum of the hoki bones treated with NaOH prior to digestion is given below in Figure 2-42 below.

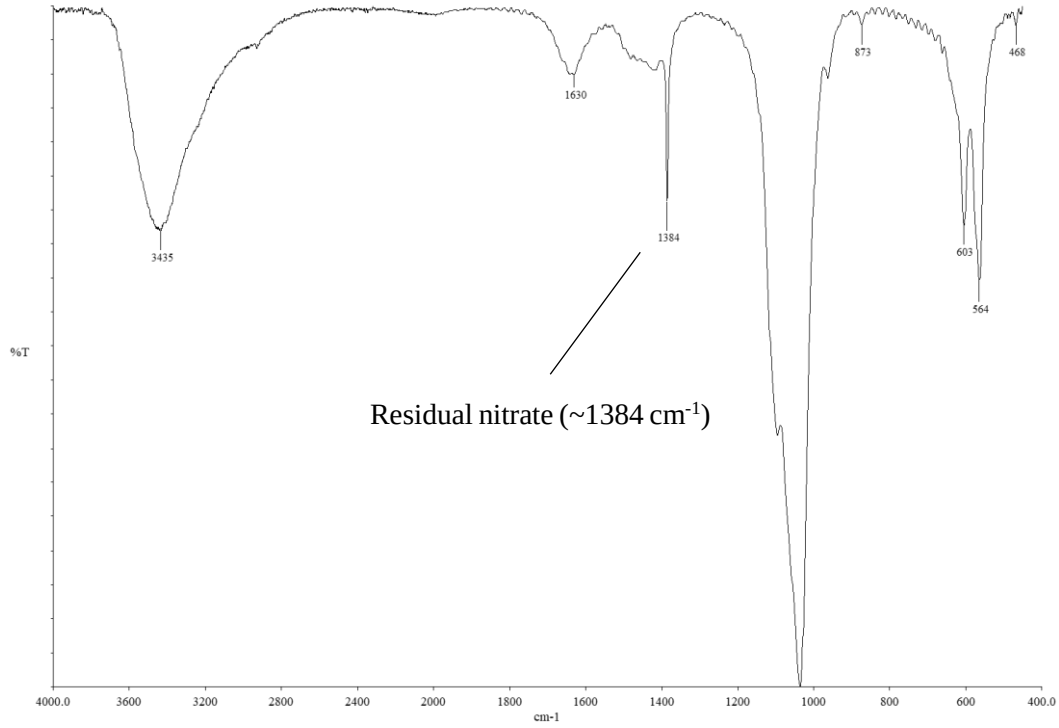

Figure 2-42: FT-IR spectrum of sample 'HNr'.

The appearance of these materials was an off-white cream colour, indicating that the removal of organics was sufficient that the strongly coloured xanthoproteic species were not present. Comparing this spectrum with the spectra presented in Figure 2-41 above, it is apparent that pre-treating these materials with base has reduced the residual organic content in the final product. There is a strong sharp peak at 1384 cm^{-1} which does not appear in the other samples. This is indicative of a nitrate presence in the powder. As nitric acid was used as the digesting acid for this sample, it is possible that this has left traces of nitrate in the sample. It is possible that this particular sample, although washed thoroughly, was not washed sufficiently to remove the nitrate content.

It is highly likely that the carbonate presence in these samples is a result of the atmospheric CO_2 forming carbonates in the alkali solution[25] during the reprecipitation. It is understood that this can be avoided by purging the reaction medium with N_2, however this was not done for these experiments. The final material appeared as a slightly off-white finely divided powder. This pre-treatment was therefore successful in reducing the organic content such that the orange discolouration does not occur. As shown earlier, refluxing in NaOH was the most

effective chemical method trialled to reduce the organic content and prevent xanthoproteic reactions, and so it is unlikely that the other chemical treatments would perform any better, so these were not trialled in these reprecipitation experiments.

Thermal pre-treatments were however trialled, as these had been shown to produce materials completely free from organic residues. Figure 2-43 below contains an IR spectral comparison of the effects of thermally treating the materials at a range of temperatures before digestion and reprecipitation.

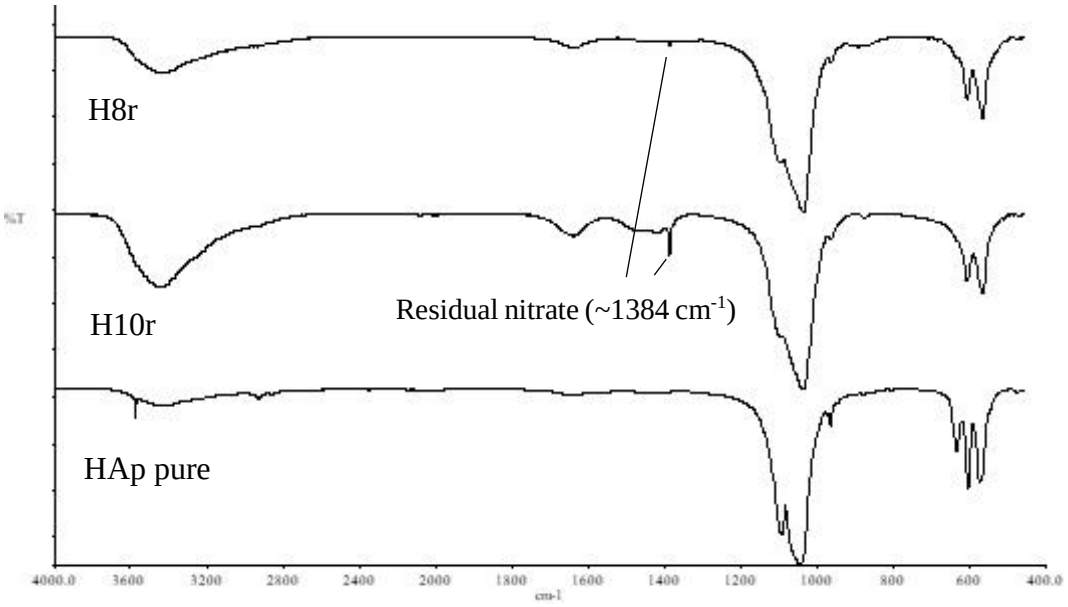

Figure 2-43: FT-IR spectra of reprecipitated materials compared with pure HAp.

The materials thermally treated at 800 and 1000 ^{o}C prior to digestion appear to be quite similar. These materials do have slightly different sizes of carbonate and moisture peaks, however the differences are small and likely insignificant. Compared with the pure HAp spectrum, these materials all have an obvious broad –OH peak. These samples were dried overnight at 100 ^{o}C, however it is possible that these were not sufficiently dried, or the KBr may have absorbed moisture during the disc generation. All three of these products were fine white powders, even though HNO_3 was used, suggesting all organics had been removed prior to digestion. This was as expected, as it was shown earlier that the organics content was completely absent at 800 ^{o}C. Because of this, and the small differences between these spectra, it is possible that it is not necessary to heat these materials all the way to 1000 ^{o}C to achieve an aesthetically acceptable pure white reprecipitated material as 800 ^{o}C appears to be sufficient. One notable peak is nitrate peak in the H8r and H10r samples (1384 cm^{-1}). This peak is also present in the HNr infrared spectrum

(Figure 2-43). Nitric acid was the digestant in these samples and so these materials have therefore not been sufficiently washed to remove these nitrates.

There are no significant differences in the IR spectra of the sample 'HNr' (Figure 2-42), and the samples thermally treated prior to digestion. These all appear to be poorly crystalline hydroxyapatite materials with low levels of carbonate. As the base treated materials only caused a slight discolouration with HNO_3, it is possible that this pre-treatment method is sufficient for producing a pure HAp material, and could obviate the need for extreme thermal conditions.

Figure 2-44 below compares the sample 'H8r' with hoki bones thermally treated to 800 ^oC.

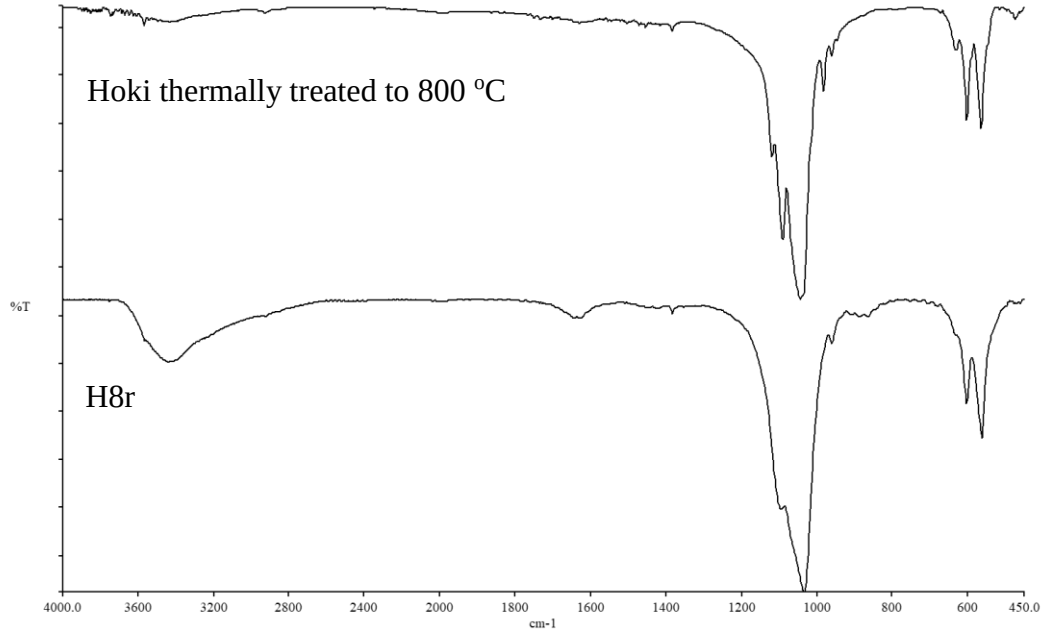

Figure 2-44: FT-IR spectral comparison of processed materials.

This comparison shows that the materials are quite similar in terms of composition. However the bones which have been reprecipitated have much broader peaks, and are likely to be more poorly crystalline that the products of the thermal treatment alone.

2.4.5.3 pXRD

Given the observations made above based on spectral evidence, pXRD characterisations were subsequently carried out on some of the materials to confirm the presence of the hydroxyapatite phase, and to check the crystallinity of the materials. Figure 2-45 below contains a comparison between a thermally treated sample, two reprecipitated samples, and pure HAp.

The patterns of these diffractograms confirm that both materials contain a predominantly hydroxyapatite phase. The reprecipitated sample however has more

broad peaks. This is consistent with the IR results presented above, providing further support to the low crystallinity achieved from these reprecipitated products. One notable observation is the appearance of a peak at 30.2 degrees 2theta, this peak is not present in the thermally treated sample but is present in the HAp pattern.

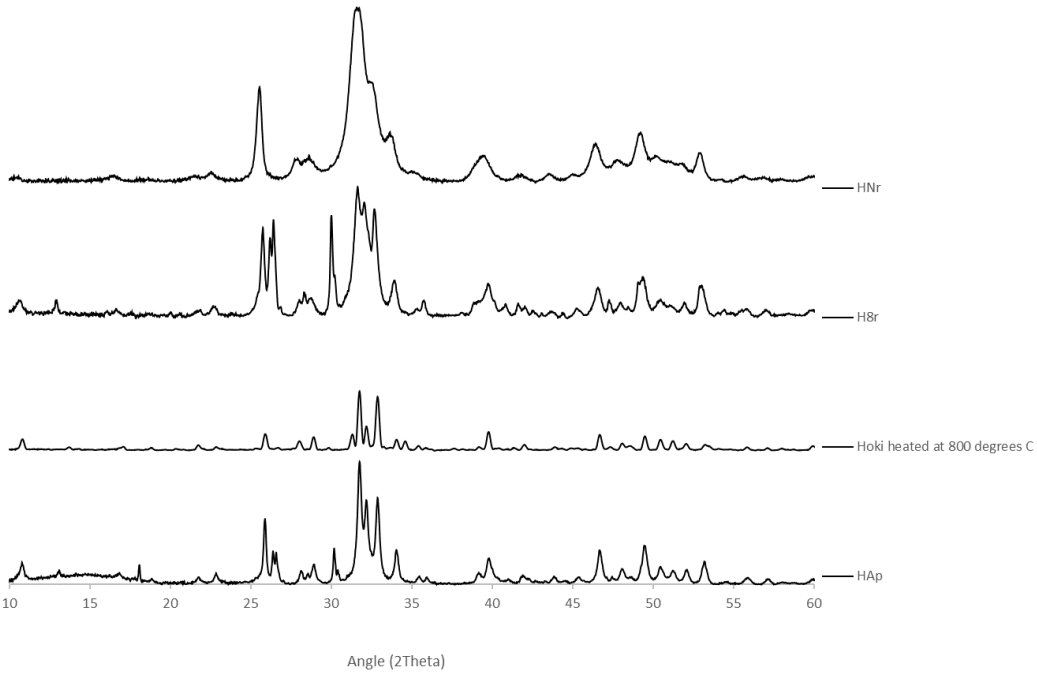

Figure 2-45: XRD diffractograms of reprecipitated materials, bones heated at 800 °C, and pure HAp (Fluka)

The reprecipitated sample appears to match almost perfectly with the Fluka pure HAp pattern. This gives strong support for the material being predominantly composed of HAp.

The broadness of the two reprecipitated materials is similar, and so the low crystallinity is likely a result of the reprecipitation process itself and does not depend on the material which is used in the initial digestion. Poor crystallinity is something which has been found in previous studies also[4], so it was suspected that this would be a feature of these materials. Interestingly, the peak at 30.2 degrees 2theta mentioned above is only present in the H8r sample, not in the HNr sample.

2.4.5.4 SEM

While it is clear that the crystallinity of the reprecipitated materials is lower than that of the thermally treated materials, the reprecipitated materials were expected to have a more uniform and smaller particle size, giving them potential biomedical advantages. To confirm this, an SEM analysis was carried out, some images from this analysis are given in Figure 2-46 below.

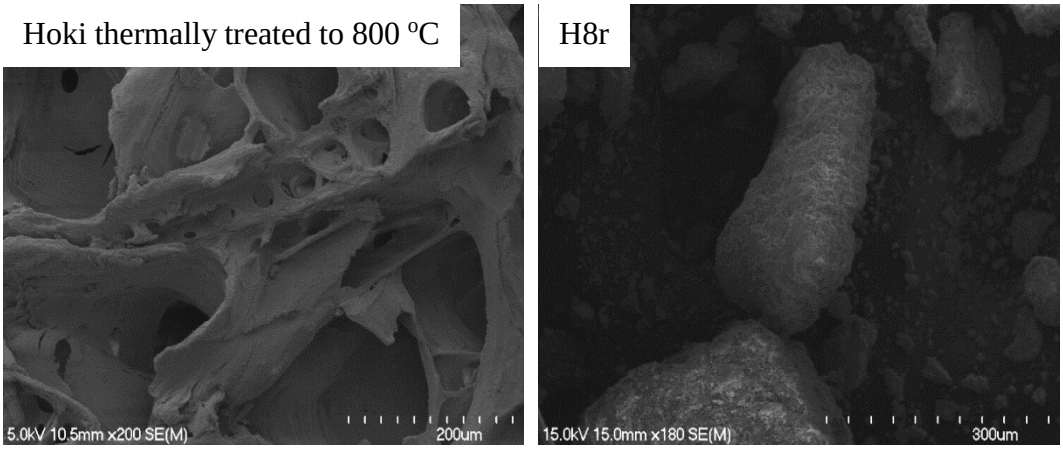

Figure 2-46: SEM images of processed bone materials.

The thermally treated materials, though ground to a powder in the ring mill, still retain the characteristic porous structure of the original bone material. There is a wide range of shapes and sizes of particles in this material. In the reprecipitated material however, the particles appear much more homogeneous and finely divided. Elemental analysis was carried out through ICP-MS to check for any possible concerning levels of elements, the results of this are given in Table 2-9 below.

Table 2-9: ICP-MS results for 'H8r', again RSD values similar to those in Table 2-3.

Element	ug element/g bone (ppm)	Element	ug element/g bone (ppm)
B	87.71	**Ni**	0
Na	9261.3	**Cu**	6.037
Mg	2004.8	**Zn**	112.62
Al	219.10	**As**	2.305
P	196715	**Sr**	1340.9
K	1523.49	**Ag**	2.195
Ca	435390	**Cd**	7.135
V	3.952	**Sb**	0
Cr	8.782	**Ba**	30.52
Mn	88.47	**Hg**	0.4391
Fe	33.37	**Pb**	2.086
Co	33.70	**U**	0.329

The Ca:P mole ratio was calculated from these results, and was found to be 1.71, slightly above that of stoichiometric hydroxyapatite. Previous studies[4, 26] have allowed the material, once reprecipitated, to sit (in solution) for periods as long as 2-3 days to 'age' through the aid dissolution-reprecipitation processes. It is possible that doing this may have driven a decrease in the Ca:P mole ratio. Additionally, as the reaction was carried out in the presence of air, it is possible that low levels of $CaCO_3$ have precipitated alongside the HAp material and slightly influenced this Ca:P ratio.

The results in the table above show that all elements of interest fall either below detection limit, or below any "concerning" levels, and so it is possible that these could be used in biomedical applications, such as a feedstock for plasma spray coating of HAp on implants. This has been reported already for HAp materials reprecipitated from bovine bones[26], however the advantage of utilising fish bones instead is these are already small to begin with, and so grinding these down to powders for digestion requires fewer labour intensive steps than it does when using the larger animal-sourced bones.

2.4.6 General findings from chemical processing techniques

A summary of the appearances of the range of chemically treated bone samples is given in appendix 2. It was found that the best process for removing the organic material from the bone materials was through heating the bones in a solution of NaOH under reflux for two hours. This process produced a material which was a slight off-white cream colour, and had significantly reduced organics peaks in the FT-IR spectra. Additionally, this process had the advantage of breaking down the bone flakes to a fine powder, which negates the need to perform any further grinding steps to produce a powdered material, this was not achieved using any of the other chemical processing techniques.

When using raw bone materials in the reprecipitation experiments it was found that HCl was the superior digesting acid as use of HNO_3 led to a discoloured orange final material through the production of xanthoproteic residues. This however can be avoided through pre-treating the bone materials, either chemically using NaOH, or thermally using temperatures > 700 ^{o}C. Pre-treating the materials also increases the solubility of the bone materials in both mineral acids, which reduces the time needed for the materials to digest in the acids.

When these pre-treatments are used, the use of the two different acids produced no significant differences in the final products in terms of their appearances, FT-IR spectra and XRD diffractograms. It has been reported however that the use of HCl can lead to chloride ion substitution into the HAp lattice in place of OH^- ions, and hence an impure (substituted) product could be produced. This does not happen with HNO_3 as the nitrate ions are not known to become incorporated into the HAp

lattice. Therefore, the preferred method for reprecipitating HAp from natural bone materials is as follows:

- Thermally treat fish bone-derived powders to at least 700 ^{o}C for two hours
- Digest calcined product in HNO_3 with heating
- Reprecipitate using a solution of NaOH (ideally with protection from the atmosphere to avoid carbonate contamination in the product)

The final products were fine white powders, the characterisations of which (FT-IR and XRD) showed the materials to be poorly crystalline HAp, with possible carbonate contamination from the atmosphere when performing the reprecipitation This can be avoided through purging the reaction vessel using N_2 gas as intimated above in the preferred method.

Previous studies have indicated these types of reprecipitated materials can be coated onto metallic implants via plasma spraying procedures to produce an implant with improved compatibility in the body. It is possible that the powders produced in this study could also be used as an HAp feed-stock for plasma spray purposes, however investigating this was beyond the scope of this project.

References for Chapter Two

1. Lee, Y.-C.; Chiang, C.-C.; Huang, P.-Y.; Chung, C.-Y.; Huang, T. D.; Wang, C.-C.; Chen, C.-I.; Chang, R.-S.; Liao, C.-H.; Reisz, R. R., Evidence of preserved collagen in an Early Jurassic sauropodomorph dinosaur revealed by synchrotron FTIR microspectroscopy. *Nature Communications* **2017,** *8*, 14220.
2. Duer, M. J.; Friščić, T.; Proudfoot, D.; Reid, D. G.; Schoppet, M.; Shanahan, C. M.; Skepper, J. N.; Wise, E. R., Mineral Surface in Calcified Plaque Is Like That of Bone. *Further Evidence for Regulated Mineralization* **2008,** *28* (11), 2030-2034.
3. Kesava Reddy, G.; Enwemeka, C. S., A simplified method for the analysis of hydroxyproline in biological tissues. *Clinical Biochemistry* **1996,** *29* (3), 225-229.
4. Mucalo, M.; Foster, D., *A method for avoiding the xanthoproteic-associated discolouration in reprecipitated (nitric-acid-digested) hydroxyapatite prepared from mammalian bone tissue*. 2004; Vol. 77, p 509.
5. Cacciotti, I., Cationic and Anionic Substitutions in Hydroxyapatite. In *Handbook of Bioceramics and Biocomposites*, Antoniac, I. V., Ed. Springer International Publishing: Cham, 2016; pp 145-211.
6. University, S. https://web.stanford.edu/group/Urchin/mineral.html (accessed January 2018).
7. Antonakos, A.; Liarokapis, E.; Leventouri, T., Micro-Raman and FTIR studies of synthetic and natural apatites. *Biomaterials* **2007,** *28* (19), 3043-54.
8. Loftus, E.; Rogers, K.; Lee-Thorp, J., *A simple method to establish calcite: Aragonite ratios in archaeological mollusc shells*. 2015; Vol. 30, p 731-735.
9. He, P.; Chen, J.; Su, M.; Han, J.; Cheng, K., Analysis of chemical composition and structure characteristics of shells. *Huagong Xuebao (Chin. Ed.)* **2015,** *66* (s2), 450-454.
10. W. Papenguth, H.; J. Kirkpatrick, R.; Montez, B.; A. Sandberg, P., *13C MAS NMR spectroscopy of inorganic and biogenic carbonates*. 1989; Vol. 74.
11. Venkatesan, J.; Kim, S. K., Effect of Temperature on Isolation and Characterization of Hydroxyapatite from Tuna (Thunnus obesus) Bone. *Materials* **2010,** *3* (10), 4761.
12. Bunsiri, R.; Thamaphat, K.; Limsuwan, P., Synthesis and Characterization of Pure Natural Hydroxyapatite from Fish Bones Bio-Waste. *Advanced Materials Research* **2012,** *506*, 206-209.
13. Boutinguiza, M.; Pou, J.; Comesaña, R.; Lusquiños, F.; de Carlos, A.; León, B., Biological hydroxyapatite obtained from fish bones. *Materials Science and Engineering: C* **2012,** *32* (3), 478-486.
14. Hosseinzadeh, E.; Davarpanah, M.; Nemati, N.; Tavakoli, S. A., *Fabrication of a Hard Tissue Replacement Using Natural Hydroxyapatite Derived from Bovine Bones by Thermal Decomposition Method*. 2014; Vol. 5, p 23-31.
15. Rothwell, W. P.; Waugh, J. S.; Yesinowski, J. P., High-resolution variable-temperature phosphorus-31 NMR of solid calcium phosphates. *Journal of the American Chemical Society* **1980,** *102* (8), 2637-2643.
16. Miculescu, F.; Stan, G.; Ciocan, L.; Miculescu, M.; Berbecaru, A.; Antoniac, I., *Cortical bone as resource for producing biomimetic materials for clinical use*. 2012; Vol. 7, p 1667-1677.
17. Buasri, A.; Chaiyut, N.; Loryuenyong, V.; Worawanitchaphong, P.; Trongyong, S., Calcium Oxide Derived from Waste Shells of Mussel, Cockle, and

Scallop as the Heterogeneous Catalyst for Biodiesel Production. *The Scientific World Journal* **2013,** *2013*, 7.
18. Yoshioka, S.; Kitano, Y., Transformation of aragonite to calcite through heating. *GEOCHEMICAL JOURNAL* **1985,** *19* (4), 245-249.
19. Nebel, H.; Neumann, M.; Mayer, C.; Epple, M., On the Structure of Amorphous Calcium Carbonate—A Detailed Study by Solid-State NMR Spectroscopy. *Inorganic Chemistry* **2008,** *47* (17), 7874-7879.
20. Kezuka, Y.; Kawai, K.; Eguchi, K.; Tajika, M., Fabrication of Single-Crystalline Calcite Needle-Like Particles Using the Aragonite–Calcite Phase Transition. *Minerals* **2017,** *7* (8), 133.
21. Beltes, P.; Koulaouzidou, E.; Kotoula, V.; Kortsaris, A. H., In vitro evaluation of the cytotoxicity of calcium hydroxide‐based root canal sealers. *Dental Traumatology* **1995,** *11* (5), 245-249.
22. Aligent 240/280 Series AA User's Guide. Fifteenth Edition ed.; Aligent Tecnologies Australia Pty Ltd: Victoria, Australia, 2016.
23. Zhang, G.; Yue, X.; Fan, A.; Liu, G. In *Reutilization of Waste Chicken Bone as Nutrients Source*, 2010 4th International Conference on Bioinformatics and Biomedical Engineering, 18-20 June 2010; 2010; pp 1-4.
24. Foster, D. L. Studies on calcium phosphates derived from New Zealand animal bone. Thesis (M. Sc. Chemistry)--University of Waikato, 2001., 2001.
25. Al‐Qasas, N. S.; Rohani, S., Synthesis of Pure Hydroxyapatite and the Effect of Synthesis Conditions on its Yield, Crystallinity, Morphology and Mean Particle Size. *Separation Science and Technology* **2005,** *40* (15), 3187-3224.
26. Mucalo, M. R.; Foster, D. L.; Wielage, B.; Steinhaeuser, S.; Mucha, H.; Knighton, D.; Kirby, J., The Novel Use of Waste Animal Bone from New Zealand Agricultural Sources as a Feedstock for Forming Plasma Sprayed Hydroxyapatite Coatings on Biomedical Implant Materials. *Journal of Applied Biomaterials and Biomechanics* **2004,** *2* (2), 96-104.

Chapter Three: Potential Applications of the Fishbone-derived Materials.

Surveying of the literature identified several potential applications for these bone-derived materials. The immobilisation of enzymes is of interest as doing so offers several advantages over in solution enzymes for use in industry, such as improvement of thermal and pH stabilities, increasing in the availability of the enzyme to the substrate, and offer an easy method of recovery of the enzyme after use. A common disadvantage to current immobilisation technologies is that the cost of producing the solid support material can be high, and immobilisation methods can be complex. The use of bone materials with a coupling reagent has the potential to mitigate both of these disadvantages, as these materials are produced in significant quantities as a by-product and hence are low-cost and high volume.

Studies have also suggested that bone-derived materials have the potential to act as an adsorbent for a range of cation and anion species, such as nickel[1], cadmium[2], strontium[3], arsenic[4] and fluoride[5], all of which can be of concern in drinking water sources. Hence, these bone materials could offer a cost-effective method of remediating these ions from contaminated water solutions.

The above applications are just some examples of the numerous applications bone-derived materials can have, due to time constraints these were the applications investigated in this study.

3.1 Methodology

3.1.1 Enzyme immobilisation experiments

3.1.1.1 Synthesis of the coupling reagent

Tris(hydroxymethyl)phosphine (THP) was chosen as the coupling reagent. The synthesis of THP is as follows:

NaOH (5 mL, 1.26 $molL^{-1}$) was added dropwise, with stirring to an equimolar amount of $[P(CH_2OH)_4]^+Cl^-$ (1.5 g of an 80 % w/w aqueous solution) in water (15 mL). A test which can be performed quickly to determine the success of the procedure involved the addition of 1 mL of the product to 1 mL of nickel chloride reagent, nickel is known to complex strongly with two of the phosphine molecules, producing a strongly coloured orange product.

3.1.1.2 Attachment of THP to as received bone materials

As received bone-powder materials (0.1 g) were immersed in the synthesised THP solution for two hours, without stirring at room temperature (22 ^{o}C). These materials were then filtered under vacuum and were thoroughly washed with type 1 water. The materials were left to dry under suction for 10 minutes before being transferred to vacuum sealed desiccators for 24 hours (at 22 ^{o}C).

3.1.1.3 Immobilisation of enzymes to the bone materials

The enzyme chosen for this study was the MalL enzyme, due to its ease of assay, and availability from the Biology Department at the University of Waikato. This was produced and purified by Dr Erica Prentice, following the method outlined in previous studies from Erica's research group at the University of Waikato[6], general methods for the purification of the enzyme are given in appendix 1 at the end of this thesis.

THP-bone complex materials (0.05 g, weighed out to 4 d.p.) were immersed in the dilute enzyme solution (approximately 22 mgL^{-1}). These were left to sit for 60 minutes (without stirring, at room temperature: 22 ^{o}C), with aliquots (200 uL) taken from the supernatant after 60 minutes to assay the change in activity of the enzyme and hence the amount of enzyme which has been immobilised. The solid bone materials were also isolated for assay.

3.1.1.4 Assay of the enzyme solutions

The substrate used for the assay of the enzymes in this study was *p*-nitrophenyl-α-D-glucopyranoside, the cleavage of which forms glucose and *p*-nitrophenol. Substrate and assay buffer (40 mM sodium-phosphate, pH 6.5, 150 mM NaCl) were mixed to give appropriate substrate concentration in a final volume of 200 µL in a quartz cuvette (Starna Scientific Ltd, UK). Reactions were initiated with the addition of 200 µL of enzyme solution, the solutions were then quickly mixed with the reaction progression followed at 405 nm with a Heλios γ spectrophotometer (ThermoFisher, USA) taking 0.125 second readings using Vision32 software (version 1.25). Due to the results from these experiments, the assay results were not converted into enzyme activity units.

Qualitative analyses of the isolated enzyme-bone solid materials were done through exposure of the solid to 500 µL of the substrate solution. The presence of a yellow/orange colour (due to the generation of *p*-nitrophenol) was deemed indicative of enzymes bound to the solid materials.

3.1.2 Adsorption experiments

3.1.2.1 Stock solution generation

The sources of each of the metals used is given in Table 3-1 below.

Table 3-1: Source of metal compounds used in the adsorption studies

Chemical Name	Grade	Brand
$NiCl_2.6H_2O$	Analytical reagent	Univar
$CdBr_2.4H_2O$	Analytical reagent	British Drug House
$SrCl_2.6H_2O$	Analytical reagent	British Drug House
$(CH_3COO)_2Pb.3H_2O$	Analytical reagent	Univar
NaF	Analytical reagent	British Drug House
$Na_2HAsO_4.7H_2O$	Analytical reagent	Sigma

These compounds were used in the generation of the stock ion solutions displayed below. The general method for generating each stock solution was the same. The desired salts were weighed out accurately to 4 d.p. into 1 L volumetric flasks (grade A). These were then filled and mixed thoroughly to the 1 L mark.

The salts used, and their weights are given below in Table 3-2.

Table 3-2: Masses of salts used in the generation of adsorption experiment stock solutions.

Element	Salt	Mass (g)	Conc. of element (mg/L)
Ni	$NiCl_2.6H_2O$	0.4049	100
Cd	$CdBr_2.4H_2O$	0.3064	100
Ni & Cd	$NiCl_2.6H_2O$ & $CdBr_2.4H_2O$	0.2024 & 0.1532	50 & 50
Pb	$Pb(CH_3COOH)_2.3H_2O$	0.1831	100
Sr	$SrCl_2.6H_2O$	0.3043	100
As	$Na_2HAsO_4.7H_2O$	0.4164	100
F	NaF	0.2211	100
F	NaF	0.0221	10

It is possible that there may be errors in the true concentrations of these due to the material's hygroscopicity.

3.1.2.2 Experiments comparing a range of adsorbent materials

Prior to being used in the adsorption experiments, all adsorbents were subjected to a grinding step using a ring mill (for 1 minute).

Ground adsorbents were weighed out to 4 d.p. into plastic tubes. Stock salt solutions (10 mL) were pipetted into these tubes, and the capped tubes immediately mixed using a vortex shaker for 10 seconds. The tubes were then transferred to a shaker and were allowed to mix for a given length of time (2 hours). The samples were then centrifuged and passed through a syringe filter to separate the solid from the

supernatant. The supernatant samples were kept and analysed for their specific element content. All adsorption experiments (unless otherwise stated) were carried out at room temperature in the laboratory (22 ^{o}C)

3.1.2.3 Adsorption kinetic experiments (adsorption over time)

These were only carried out for the nickel and cadmium salts. These experiments were done in the same manner as the material comparison experiments, however the samples were allowed to mix for varying lengths of time to determine how long is required for an equilibrium to be established. Equilibria were identified when successive changes in the adsorbate concentration were small.

3.1.2.4 Adsorption Isotherm experiments

Adsorbents were accurately weighed out to a range of masses. Fixed concentrations of stock solutions (10 mL) were added to each of these weighed out adsorbents. These were then allowed to mix until equilibrium was reached (as determined by the kinetic experiments). To highlight the effect of differing lengths of contact times, a range of isotherm experiments were carried out using the cadmium ion/bone adsorbent systems at varying time lengths.

3.1.2.5 Variation of the starting pH

These experiments were only carried out for nickel and cadmium adsorption experiments. Aliquots of salt solutions had their pH altered using HNO_3 and NaOH to generate a range of solutions, with pH values between 2 and 8. The pH of each solution was measured to 2 d.p. using a pH meter. pH measurements were not recorded following immersion of the adsorbents with the salt solutions. A sample using the stock solution without any pH adjustment was used for a control, with its pH being measured.

3.1.2.6 Variation of the reaction temperature

This type experiment was only carried out for the nickel ion adsorption. The samples were treated using the same methods as the batch experiments, however continuous mixing was not possible as the heated samples were placed in incubating ovens (45 ^{o}C, 80 ^{o}C). Instead the tubes were laid on their sides (for 2 hours) so as to achieve maximum surface contact between the water sample and the adsorbent. A sample at room temperature (22 ^{o}C) was also used as a control

3.1.2.7 Generation of mock filter for fluoride removal

This experiment was only carried out for the fluoride ion-HAp system adsorption. HAp was added (~0.1 g) to a syringe connected to a 0.45-micron syringe filter. To

this syringe, an aqueous fluoride sample (100 mg/L F^-, 10 mL) was added and pushed through. The filtrate was collected and analysed for its fluoride content.
For control, the same stock solution (10 mL) was also passed through a syringe attached to a 0.45-micron filter, with no HAp powder present. The filtrate from this was also measured.

3.1.3 Particle sizing using a laser particle sizer

Bone powders treated to 500 ^oC which had been ground using a ring mill (for 1 minute) were analysed for their particle sizes using a Malvern Mastersizer 3000, with the following parameter set:
Set refractive index: 1.629
Aborption index: 0.01
Stirring speed: 3000 RPM
Analysed using the "general-purpose settings" on the instrument.

3.1.4 Measurement of nickel and cadmium concentration using AAS

Atomic absorbance spectroscopy (AAS) was used to analyse the nickel, cadmium, lead and calcium ion concentrations in solution during the adsorption experiments. These were measured on a GBC Avanta, 25th anniversary edition spectrometer.
Wavelengths: 341 nm (nickel) 228.8, nm (cadmium), 283.3 (lead), 422.7 nm (calcium).
Gas mixture: air/acetylene
Known standards of each element were generated by Annie Barker, University of Waikato, the concentrations of these are given in Table 3-3 below.

Table 3-3: Standard concentrations used for AAS analyses.

Standard	Concentration (mg/L)		
	Nickel	Cadmium	Calcium
Standard 1	0.5	0.5	1
Standard 2	1	1	2
Standard 3	2	1.5	5
Standard 4	4	2	8
Standard 5	8	-	10

In adsorption samples where the concentration of the samples was found to be above the range of these standards, dilutions were made using accurate variable pipettes, and type 1 water.

3.1.5 Measurement of metal ion concentrations using ICP-MS

Following adsorption experiments, the suspension was filtered off through a 0.45-micron syringe filter. A portion of this filtrate (1 mL) was then added to a solution of type 1 water and concentrated HNO_3 (8.8 mL H_2O, 0.2 mL conc. HNO_3) giving a final volume of 10 mL, a dilution of 1:10. Nitric acid was added for matrix consistency in the ICP-MS measurements.

The samples were introduced into the ICP-MS instrument for analysis by Steve Cameron, University of Waikato, along with the stock solutions used in the adsorptions. The ICP-MS instrument details are reported earlier (section 2.1.5.5).

3.1.6 Measurement of fluoride concentrations using ion chromatography

Fluoride containing samples were analysed using a Dionex ICS-2000 ion chromatography system. The eluent used was a known mixture of Dionex™ EGC III KOH with type 1 water. The mixture was generated by the instrument, with the concentration of 25 mmol. Chromatograms were recorded over a period of 13 minutes.

Standards were generated through dilution of a Dionex™ Combined Seven Anion standard with a fluoride concentration of 20 mg/L, the volumes of this stock solution and type 1 water used to make these dilutions are given in Table 3-4 below.

Table 3-4: Volumes of stock solution and type 1 water used to generate calibration curves for the fluoride experiments.

Standard	Dionex™ standard (mL)	Type 1 H_2O (mL)	F^- concentration (mg/L)
Standard 1	1	4	4
Standard 2	0.5	4.5	2
Standard 3	0.25	4.75	1
Standard 4	0.125	4.875	0.5

These standards were generated and analysed prior to each IC experiment.

3.1.7 Adsorption calculations

3.1.7.1 General calculations

To allow comparisons between samples, the results of the adsorption experiments were reported in values of q_t, (mg/g) milligrams of adsorbate adsorbed per gram of adsorbent (after a given length of time). These were calculated using the formula given in Equation 3-1 below.

Equation 3-1: Formula for the calculation of q_t

$$q_t = \left(\frac{C_0 - C_t}{m}\right) * V$$

Where C_0 is the initial concentration of adsorbate (mg/L), C_t is the concentration of adsorbate after the adsorption experiment concluded (mg/L), m is the mass of adsorbent used (g), and V is the volume of adsorbate solution used (L).

Another value reported was the removal percentage (R%), this gives information on the overall change in adsorbate concentration, however does not account for the amount of adsorbent used. The calculation of this is given in Equation 3-2

Equation 3-2: Calculation of removal percentage (R%)

$$R\% = \left(\frac{C_0 - C_t}{C_0}\right) * 100$$

The definitions of C_0 and C_t are consistent with Equation 3-1.

3.1.7.2 Determination of adsorption kinetics

Using data from experiments measuring adsorption as a function of contact time for the nickel-bone and cadmium-bone powder systems, reaction kinetics were determined. The first model applied was the pseudo first order (PFO) adsorption model, represented by the equation below.

Equation 3-3: Pseudo first order adsorption model

$$q_t = q_e(1 - e^{-k_1 t})$$

One of the linear forms of the PSO model is given in Equation 3-4 below:

Equation 3-4: Linearised PFO adsorption model

$$\ln(q_e - q_t) = lnq_e - k_1 t$$

In which k_1 is the first order adsorption rate constant, q_e is the adsorption capacity of the adsorbent at the equilibrium point (mg/g), q_t is the adsorption capacity at a given time (mg/g), and *t* is time (minutes). If the PFO adsorption model is followed, then a plot of $\ln(q_e\text{-}q_t)$ against should give a linear trend, with an intercept of lnq_e and a slope of k_1, which allows for the calculation of q_e and k_1.

The second model applied to the data was the pseudo second order (PSO) adsorption model, represented by Equation 3-5 below.

Equation 3-5: Pseudo second order adsorption model equation

$$q_t = \frac{k_2 q_e^2 t}{1 + k_2 q_e t}$$

One of the linearised forms of this model, the one used in this study, is given by Equation 3-6

Equation 3-6: Linearised form of PSO adsorption model

$$\frac{t}{q_t} = \frac{1}{k_2 q_e^2} + \frac{1}{q_e} t$$

Where k_2 is the rate constant of second order adsorptions, the definitions of q_e, q_t and *t* are the same as in Equation 3-4. If this model is followed, plotting t/q_t against *t* should result in a linear trend. The straight-line equation of which will have a slope of $1/q_e$, and an intercept of $1/k_2 q_e^2$, allowing for calculations of q_e and k_2 to be made. Regression analyses were done on each of the models for the data sets to determine the most applicable model.

3.1.7.3 Isotherm generation

Adsorption isotherms were generated through plotting calculated values of q_r for each of the samples, against their respective C_0 values.

These data sets were fitted to two different isotherm types, the Langmuir and Freundlich isotherms. The Langmuir isotherm equation is given below in Equation 3-7[7]

Equation 3-7: Langmuir isotherm equation

$$q_e = \frac{q_{max} b C_e}{1 + bC_e}$$

Where q_e is the amount of adsorbate adsorbed per unit weight of adsorbent, at the equilibrium point (mg/g), C_e is the concentration of adsorbate in the solution at equilibrium, q_m is the maximum adsorption capacity (mg/g), and *b* is a constant related to the free energy of adsorption (L/mg).

This can be linearised into 5 different forms[7]. The linearised Langmuir equation used in these studies is given in Equation 3-8 below.

Equation 3-8: Linearised Langmuir Isotherm

$$\frac{1}{q_e} = \frac{1}{bq_m} * \frac{1}{C_e} + \frac{1}{q_m}$$

This linear equation is in the form of y = mx + c, and generating a plot of $1/C_e$ vs $1/q_e$ produces a line with an intercept of $1/q_m$, and a slope of $1/bq_m$, which allows for an easy calculation of values for maximum adsorption capacity (q_m) and the free energy of adsorption constant (*b*).

The Freundlich model was also used in the adsorption experiments, this model can be represented by Equation 3-9 below[7].

Equation 3-9: Freundlich Isotherm Equation

$$q_e = K_F C_e^{1/n}$$

In which, K_F represents a constant which indicates the relative adsorption capacity of the solid adsorbent ($mg^{1-(1/n)}L^{1/n}g^{-1}$), n is a constant which represents the intensity of adsorption. The linear form of the Freundlich equation is given in Equation 3-10 below.

Equation 3-10: Linearised Freundlich Isotherm Equation

$$lnq_e = lnK_F + \frac{1}{n} lnC_e$$

Therefore, if the Freundlich model is followed, a plot of ln q_e vs ln C_e should yield a straight line, from which values of K_F and *n* can be calculated (intercept = lnK_F, slope = 1/n).

These linear models were both applied to the data, with regression analyses determining which model was the best fit for the system.

3.2 Results and Discussion

Previous studies have indicated an ability for bovine bone materials to be used as a solid support for the immobilisation of enzymes, through combination with a phosphine coupling reagent tris-hydroxymethyl phosphine (THP). The immobilisation of enzymes is of interest as doing so enhances reusability of enzymes[8], as well as allowing an easy means of isolating the enzymes following the reaction, leading to a final product with higher purity. The advantage of attaching these to bone materials is that natural bone derived materials are insoluble in a range of matrices, and are resistant to pH values above 4. In this study, fishbone-derived powders were combined with THP to investigate the possibility of using these as a solid support for enzymes.

3.2.1 Enzyme Immobilisation

The enzyme immobilisation investigations were broken two main parts, the synthesis and attachment of the coupling reagent, and the attachment of enzymes to the bones followed by the activity assay of the immobilised enzymes.

3.2.1.1 Synthesis and attachment of the coupling reagent.

The coupling reagent, tris(hydroxymethyl)phosphine, structure in Figure 3-1 was successfully synthesised.

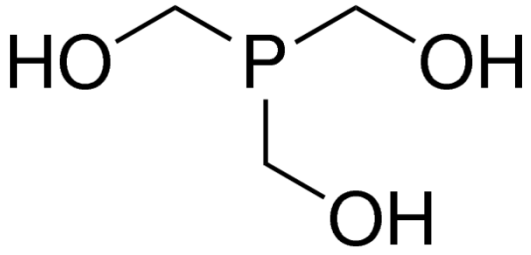

Figure 3-1: Chemical structure of tris(hydroxymethyl)phosphine.

The synthesis of THP was confirmed by carrying out a colour change test with a solution of nickel chloride. A colour change of green (from the nickel chloride solution) to a strongly coloured orange square planar nickel-THP species confirmed of the presence of THP, as shown in Figure 3-2 below.

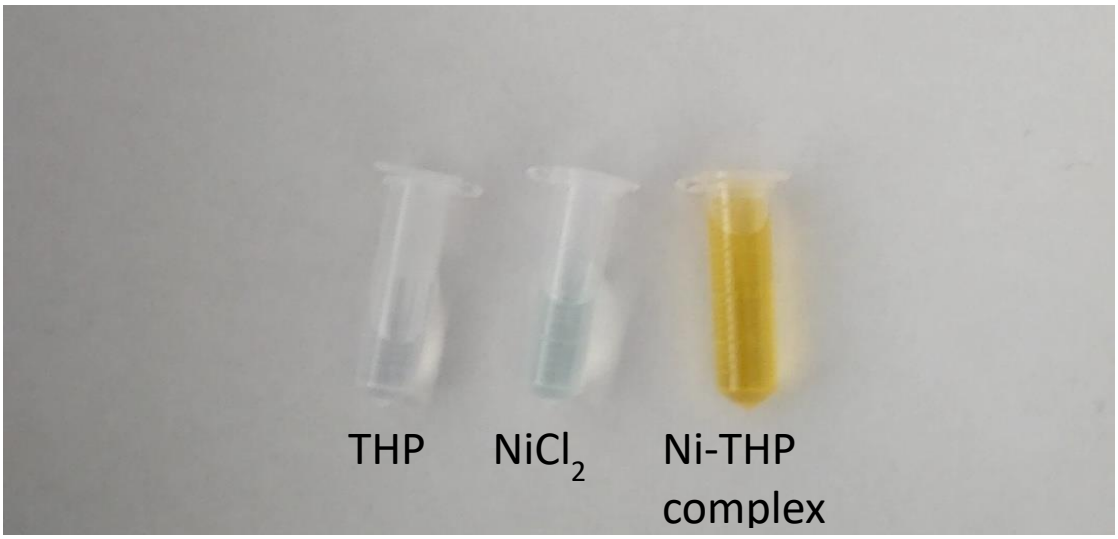

Figure 3-2: Samples showing the reaction of THP with $NiCl_2$ to confirm the presence of THP.

Equation 3-11 below is responsible for the reaction between $NiCl_2$ and THP.

Equation 3-11: Reaction between nickel chloride and THP

$NiCl_{2\,(aq)} + 2THP_{\,(aq)} \rightarrow NiCl_2(THP)_{2\,(aq)}$

Following immersion with the coupling reagent THP, the hoki bone materials had a lighter colour, and appeared to be more 'clumped' together than untreated bones. Additionally, they had a much more pungent odour. The gurnard sample while appearing unchanged, also carried a similar odour. Only raw bones were used in these immersion studies, as it was understood that the method of THP binding to the bone would be through Mannich-type condensation reactions with N-H groups[9],

this occurs spontaneously at room temperature As these groups are found in the collagen in natural bone, the desired intent was that these would be the active sites to which the THP would bind, and form amino methyl phosphine linkages (P-CH_2-N-).

Quantification of the amount of THP which had attached to the bone was attempted using two different methods. The first of these was through the use of spectrophotometric methods with nickel chloride. The principle behind this being that the colourless phosphine molecule complexes with the nickel in nickel chloride solution to form a square-planar orange nickel-phosphine complex. This reaction does not occur when the THP precursor salt $P(CH_2OH)_4Cl$ is added to nickel chloride. This served as a good initial qualitative test to confirm synthesis of the phosphine had taken place.

A more quantitative test was attempted which utilised UV/Vis spectrophotometry to measure to the UV/Vis spectra of the nickel chloride solution, the THP solution and the nickel-THP solution with the intention of finding an absorption maximum which could be measured to test for Beers' Law type relationship. These are given in Figure 3-3 below. These spectra were recorded using a Cary100 UV-Visible spectrophotometer.

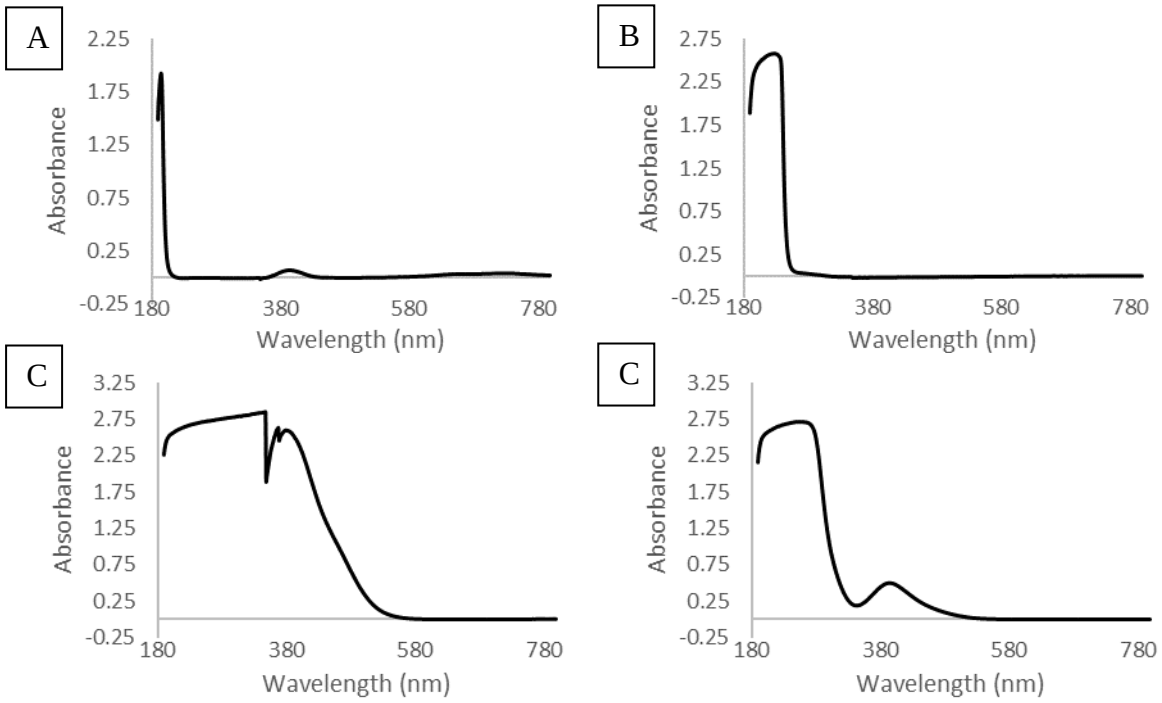

Figure 3-3: UV/Vis absorption spectrum of A) Nickel Chloride (1 mg/L). B) THP. C) Ni-THP complex using the reagents shown in A and B. D) Ni-THP complex diluted from C.

As shown in Figure 3-3, the solution of $NiCl_{2.6}H_2O$ has two main absorption peaks in the UV/Vis spectrum, namely one peak with a maximum of 396 nm, and a broad set of peaks in the 600-750 nm region. This is consistent with what has been found in the literature[10]. As expected, the colourless solution of THP in water did not give any detectable absorption in the visible spectrum. When the two solutions are mixed an intense orange colour is observed, as shown in Figure 3-2 above with the resulting solution being much more intensely coloured than the pale green $NiCl_2$-$.6H_2O$ solution used to generate it. This is believed to be the result of a charge transfer band, which is likely associated with the presence of an intense broad peak at approximately 260 nm. The solution also has a less intense absorption maximum at 396 nm which is also found in the green nickel solution. This is understood to be the result of d-d transitions between orbital energy levels located on the nickel atom itself (i.e. via crystal field splitting in the d^8 octahedral complex). Hence for this study it would not be possible to use this peak to study the reaction of $NiCl_2$ to produce the $NiCl_2$-THP complex,

The charge transfer peak also cannot be used to quantify this, due to the uncertainty in the concentration of the initial $P(CH_2OH)_4Cl$ salt solution (~80% w/w) meaning that accurately generating a range of Ni-THP standards would be difficult. It is possible that the broad set of peaks in the $NiCl_2.6H_2O$ UV spectrum (between 600 and 700 nm) could be used to monitor the concentration as these are absent in the Ni-THP complex UV spectrum and are indicative of a Ni(II) species, however it was decided that trying to measure these through UV/Vis spectroscopy was not overly practical.

AAS was used to analyse the digested samples for their nickel content, and this was related back to an amount of THP attached to the bone, based on the assumption that all of the nickel detected was a result of nickel attached to the THP. These experiments, however, were also problematic. This was because experiments which varied the amount of THP added to the bone showed no correlation in their nickel readings with their respective calculated amounts of THP/g of bone material. Furthermore, increasing the concentration of the $NiCl_2$ solution during the analysis while fixing the amount of THP solution used, lead to an increased concentration of Ni measured, and hence an increase in the value of the calculated amount of THP/g bone solution, despite numerous washing steps to remove residual nickel. So it is likely that the assumption that any nickel present is bound to the THP is an

invalid assumption. It has been shown in previous studies[11], and even later in this study (*section 3.2.2*), that nickel has a natural affinity for bone materials through substitution into the HAp lattice in place of calcium. This natural affinity could be the source of the issues here. It was concluded that for this system, it is not possible to determine the amount of THP attaching to the bone materials due to "nickel association" with the HAp not being specific enough to attribute it all to THP complex formation. Previous similar work proposes that after a reaction time of 2 hours, approximately 17 mg of the phosphine attaches per gram of the bone material[12], however this study relies on the above assumption, which we have found to be invalid due to the affinity of HAp for nickel.

3.2.1.2 Attachment of the enzyme to the THP-bone complex, and activity assays of these materials

After the 2 hours immersed in the enzyme solution, the washed and dried bones were unchanged in terms of their appearance. The enzyme solutions used were kept after the immersion and were put through an activity assay using the well-studied hydrolysis of p-nitrophenol to determine if the concentration of enzymes in these solutions had decreased. Table 3-5 summarises the samples used in these immobilisation studies.

Table 3-5: Sample ID's and descriptions for enzymatic assays.

Sample	Description
21A,B	Ground raw hoki bones, immersed in THP for 2 hours, dried, then immersed in enzyme for 2 hours
22A	Ground raw hoki bones, immersed in THP for 2 hours, dried, then immersed in enzyme for 2 hours
24A,B	Ground raw hoki bones, immersed in enzyme for 2 hours, no THP exposure, control sample
26A,B	Ground raw gurnard bones, immersed in THP for 2 hours, dried, then immersed in enzyme for 2 hours
27A,B	Ground raw gurnard bones, immersed in THP for 2 hours, dried, then immersed in enzyme for 2 hours
29A,B	Ground raw gurnard bones, immersed in enzyme for 2 hours, no THP exposure, control sample

The first of these assay experiments is presented in Figure 3-4 below.

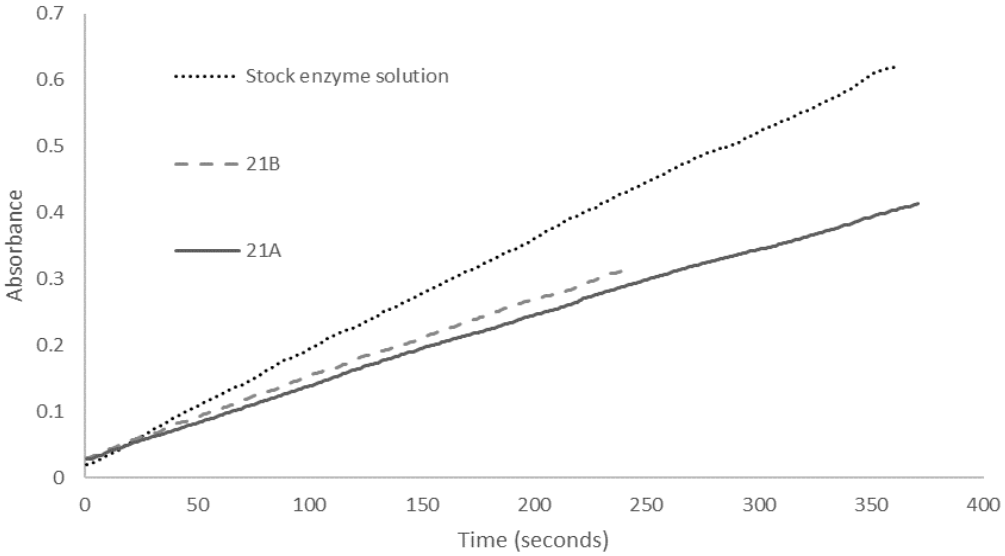

Figure 3-4: MalL enzyme assay for samples 21A and 21B

These results suggested the possibility of enzymes being immobilised, as the activity of the solutions which had been exposed to the THP-bone complexes were lower in activity than the original stock solution. This was then repeated for sample 22A (Figure 3-5 below).

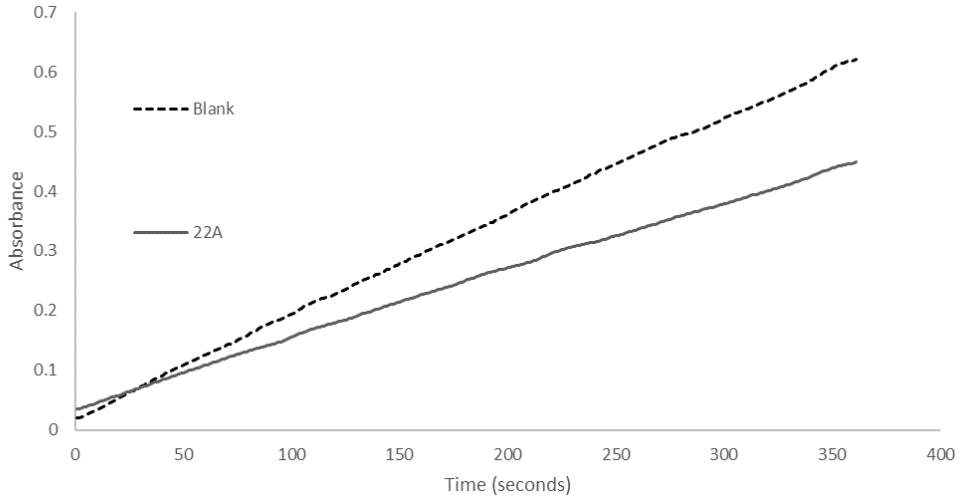

Figure 3-5: Enzyme assay for sample 22A

Although only one sample was used in this particular assay, the trend was still the same, the THP-bone treated solution had a lower activity than the stock solution, giving further apparent support for the enzyme immobilisation.

For control, a ground bone sample which had never been in contact with the THP reagent was immersed in the enzyme solution. It was expected, that the activity of this solution would remain approximately the same as the stock solution. Figure 3-6 below shows the results of this experiment.

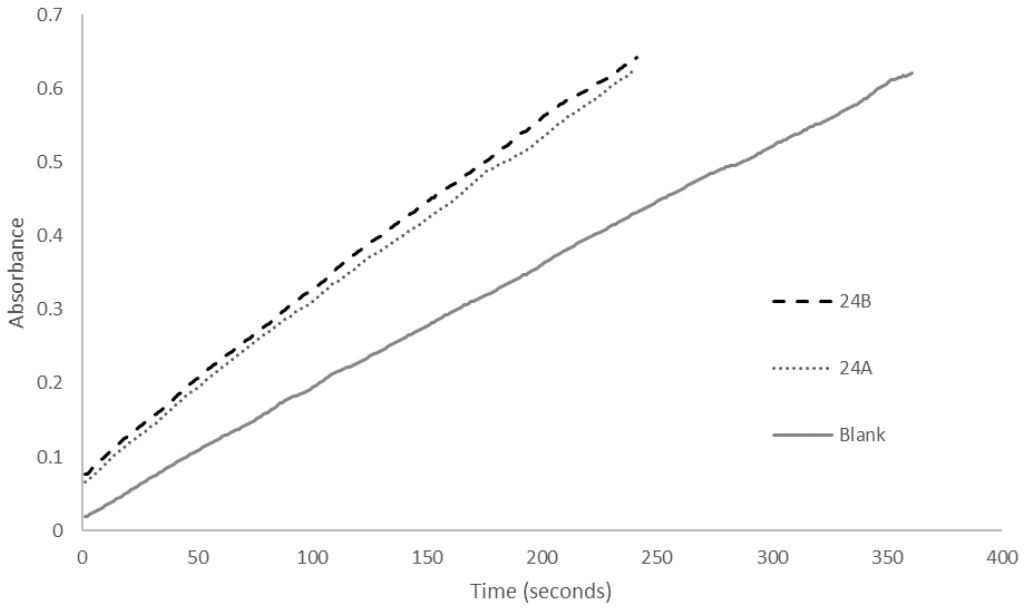

Figure 3-6: Enzyme assay for control samples 24A and 24B

The activity of these solutions did not stay the same, but it also did not decrease. Interestingly, the activity increased, suggesting something had promoted enzyme activity in the materials. The experiments were then repeated with the raw gurnard bones.

Figure 3-7 below shows the results from the first of these.

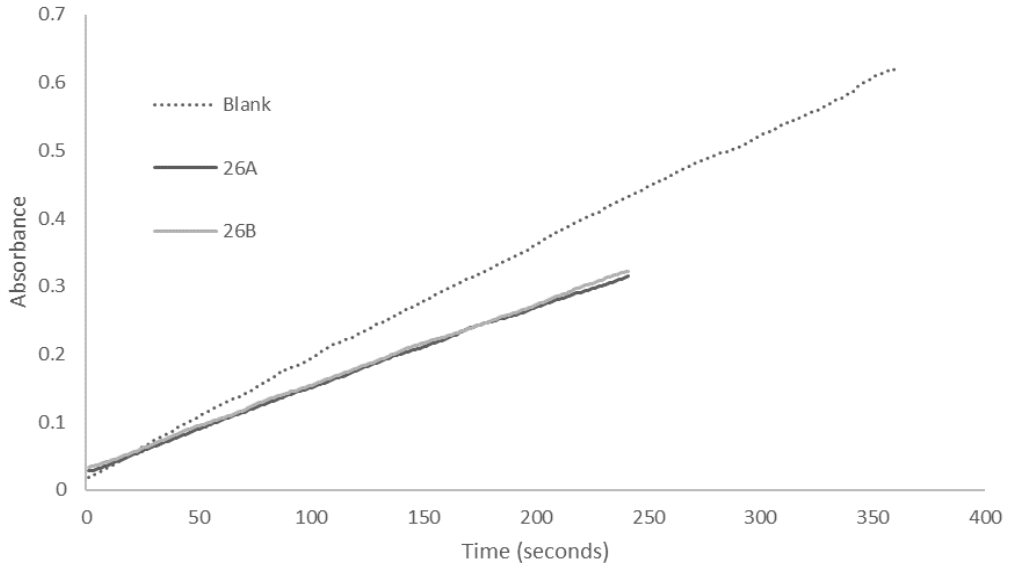

Figure 3-7: Enzyme assay for samples 26A and 26B

In these the activity of the enzyme solutions exposed to the THP-bone complex had also decreased. This was repeated, for samples 27A and B, in agreement with the ground hoki samples. A control gurnard sample (blank) was also ran, and in this instance also, the bones used had never come in contact with any THP. These results are given in Figure 3-8.

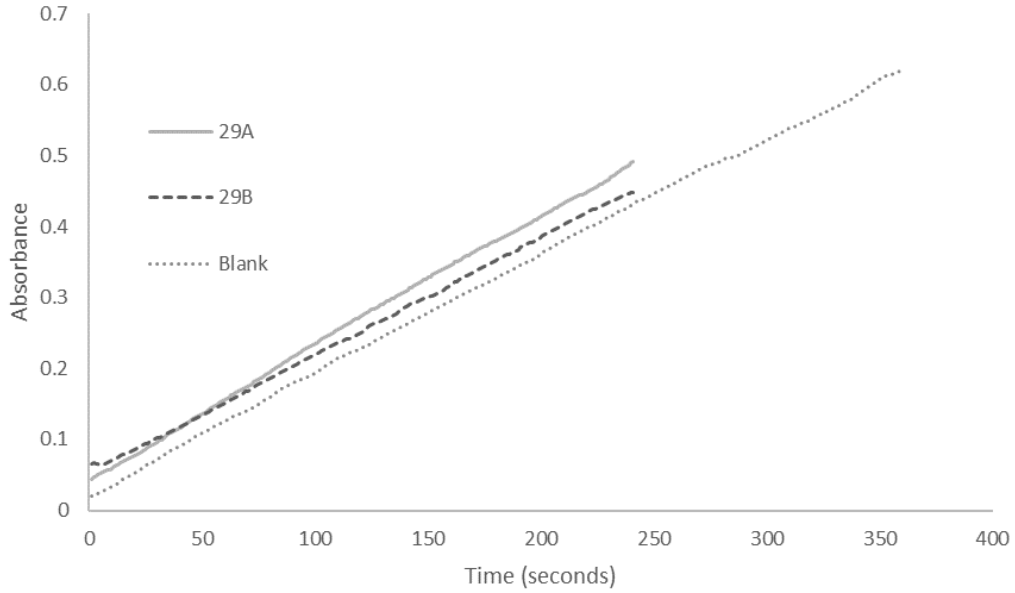

Figure 3-8: Enzyme assay for control gurnard samples 29A and 29B

Although the difference in this experiment was smaller than with the raw hoki bones, there was still an increase in enzyme activity compared to the stock solutions. It was initially thought that there could be a pH influence on the solutions, which could cause a change in activity of the malL enzyme, as well as influence the hydrolysis of p-nitrophenol as this is a pH sensitive indicator. The raw bones were then placed in water samples to measure the pH change. While the bones did make the water more alkaline, the change was small (only to ~pH 8). While a pH of 8 could cause a colour change in the substrate (above 7.5 the solution begins to turn yellow[13]) this small pH change would be corrected for by the buffer solution used.

It is possible that something in the raw bone materials is leaching into the enzyme solutions and causing an increase in the activity. However, as these raw materials are crude, it would not be possible to draw any conclusions on what this might be. The solid materials which were immersed in the enzyme solutions were also kept for a qualitative analysis. These materials were dried, and immersed in the substrate solution, which were then left overnight. The results are summarised in Table 3-6.

Table 3-6: Qualitative analysis on activity of enzyme-bone samples.

Sample	Colour change
21	No change
22	No change
24	Light yellow developed
26	No change
27	No change
29	Light yellow developed

No obvious change in colour was seen in any the bone-THP complex samples. Hence, if there are enzymes being immobilised as the assay results suggest, once immobilised they have a significantly reduced activity and are unable to be used. A decrease in enzyme activity was expected with immobilisation, especially when the mechanism of immobilisation is chemical in nature[14]. Additionally, although the chemical reaction of the THP ligand with collagen, and the enzyme is understood, it is not possible to control where, and in what orientation these reactions take place in. As there are three reactive groups in the THP molecule, and many reactive amino sites in the collagen-bone materials, it is entirely possible that in some cases, all three ligands may already be bound to collagen in the bone, and hence these sites would not be available for binding by the enzymes.

This however would not account for the decrease in activity of the enzyme solutions seen in the activity assays earlier. THP on the surface of the bone materials could be binding enzymes in a way which restricts access to, or even chemically changes the active site, which could prevent catalysis of the reaction. Another possibility, is that enzymes may also be bound to two separate THP linkages, which would further restrict orientation of the enzyme. These problems are commonly found as a consequence of the simplicity of methodology to produce covalently linked immobilised enzymes[14].

These could be mitigated, if there was a way in which the THP could be bound in a specific way to the bone surface which allows for the binding of enzymes in a uniform orientation, with their active sites exposed to the substrates. This could potentially be something future work investigates.

In contrast, the control samples 24 and 29, although thoroughly washed after exposure to the enzyme, caused a light-yellow colour to develop in the substrate solution. Hydroxyapatite has been previously shown to be a potential solid substrate on its own, through physical adsorption to the HAp surfaces[15]. It is possible that this physical adsorption is occurring, and presence of THP on the bone may interfere with this.

To further investigate these interesting results, raw bone materials, and bones treated to 800 ^{o}C, which had never been in contact with THP or the enzyme solution, were also immersed in the substrate solution. These were carried out in duplicate. The thermally treated materials did not cause any colour change in the substrate, however the raw materials, despite never contacting an enzyme solution, did cause

a slight colour change in the solution. This suggests that something in the raw materials is catalysing the reaction. The colour change was less drastic than what was observed in sample 24 and 29, however it was intense enough to cause a visible change in the colour of the solution. Given the crude nature of the materials in this experiment also, there is a range of species which may leach into the solution. Determining what it is about these raw materials that catalyses the reaction would not be a simple task and was outside the scope of this study.

Previous work using materials sourced from bovine bones presented promising results in using the THP reagent to bind enzymes to collagenous bone materials[12]. These however used trypsin as the enzyme with BAEE as the substrate molecule instead. It is thought, that the enzyme substrate system used in this study may have contributed to the interesting results. Due to lack of availability, alternative enzymes were not trialled in these experiments, however these could be the subject of future work.

3.2.2 Removal of nickel ions from water samples

Previous studies have shown that HAp, and HAp derived materials have an affinity to adsorb a range of metal ions, such as ions of nickel[1, 16], cadmium[17-18], lead[17] and strontium[3]. Hence bone-derived materials in this study were applied in similar experiments to assess the viability of this as an application for these materials.

The first candidate ion tested was the divalent nickel ion. The initial experiments aimed to assess a range of materials, both raw and processed, for their abilities to reduce the concentration of nickel ions in solution. It was decided to use an immersion period of two hours for these experiments.

3.2.2.1 Comparison of adsorbent materials

The as received materials were trialled first, with the results of this given below in Table 3-7.

Table 3-7: Results from nickel removal experiments onto as received materials.

Sample	Mass (g)	C_t (mg/L)	q_t (mg/g)	R %
Pure HAp	0.2258	47.61	2.015	48.9
Pure HAp	0.1922	50.92	2.195	45.3
Pure HAp	0.2246	48.25	1.997	48.2
Hoki raw	0.2016	18.22	3.714	80.4
Hoki raw	0.2273	16.42	3.374	82.4
Hoki raw	0.2065	17.26	3.673	81.5
Gurnard raw	0.2008	57.37	1.779	38.4
Gurnard raw	0.2073	59.07	1.642	36.6

Mussel	0.2012	56.67	1.811	39.1
Mussel	0.2281	54.05	1.712	41.9
Mussel	0.2106	53.18	1.896	42.9
Initial [Ni]	-	**93.1**	-	-

These results show that the most efficient raw material (out of those trialled) was the as received hoki bone powders. These performed much better than the as received gurnard bone powders. It is possible that these differences arise from the organics and oily content of the bone-powders. As shown in chapter 2.2, the as received hoki and flounder bones were low in organic components relative to the gurnard and snapper bones. It is possible that the increased organic content on the surface of these materials (as shown in the SEM images in chapter 2.2.1.4) is creating a phase barrier between the powders and the water samples, hence partially inhibiting the ability of nickel to move from solution onto the bone samples. Hence wettability of the samples could be a factor.

The mussel shells were not as effective in reducing the concentration of nickel in solution as the bone powders were. It is thought that the dominant mechanism for the bone's ability to remove nickel is through substitution of Ni for Ca in the HAp lattice. This same substitution is not possible with the mussel shells as these were shown to be primarily composed of $CaCO_3$. There was however a slight decrease in Ni^{2+} concentration, it is possible that this is due to precipitation of nickel as $Ni(OH)_2$, a precipitate which would be removed from the solution with the filtration used, hence the measured concentration of nickel in solution would be lower.

Materials which had been thermally treated were also trialled in these experiments. With the expectation that increasing the treatment temperature, and purifying the HAp phase, would lead to an increased ability to adsorb nickel. The results of this experiment are summarised in Table 3-8 below.

Table 3-8: Results from nickel removal experiments onto as received materials.

Sample	Mass (g)	C_t (mg/L)	q_t (mg/g)	R %
Gurnard 300 °C	0.2009	22.84	3.497	75.5
Gurnard 300 °C	0.211	27.75	3.097	70.2
Gurnard 500 °C	0.2189	0.91	**4.212**	**99**
Gurnard 500 °C	0.2023	1.2	**4.543**	**98.7**
Gurnard 600 °C	0.2152	20.6	3.369	77.9
Gurnard 600 °C	0.2015	21.48	3.554	76.9
Gurnard 1000 °C	0.2006	81.5	0.578	12.5

Gurnard 1000 °C	0.2033	81.37	0.577	12.6
Initial [Ni]	-	**93.1**	-	-

This experiment identified that the gurnard bones thermally treated to 500 °C were the most effective material for nickel removal, according to the calculated values of q_t. This result is interesting as the bones cooked at 300 °C and 600 °C were not as efficient. Bone-derived materials heated to 300 °C were found to still contain organic materials, and so it is possible that these are interfering with adsorptions just as the observed in the raw gurnard sample. When heated at 500 °C the organic content was shown to be significantly reduced and hence this interference is not present in these materials. As surface area plays an important role in adsorptions, it was thought that this may be influencing these differences observed. Particle size analyses via laser diffraction (mastersizer) measurements were then carried out on the thermally treated materials used in the adsorptions. These revealed no significant differences in the distribution of particle sizes, with all of the samples (post ring-mill grinding) having approximately 90% of the particle size distribution below 200 µm.

It is also possible however that the crystallite size changes with increasing temperature. It has already been shown (in chapter 2.3.1.5) that as the temperature increases, the crystallinity of the material also increases. This can also be associated with an increase in the crystallite size, Monshi et al, 2012[19] showed through the use of pXRD and the Scherrer equation that the crystallite size of bovine bone materials increased with increasing the treatment temperature from 600 °C through to 1100 °C. Their reported crystallite sizes for bones treated at 600 °C and 900 °C were 22.8 nm and 37.3 nm respectively[19]. While they do not report data for bone materials treated to 500 °C, it is likely that the crystallite size of these materials would be smaller or similar to the materials treated at 600 °C. This increase in crystallite size is associated with a decrease in the surface area: volume ratio of a solid material, therefore as the treatment temperature increases, the available surface area per unit of mass of the adsorbent decreases, which can then be linked with a decrease in adsorption abilities.

Heating the materials up to 1000 °C produced a material which was ineffective for reducing the nickel content. Earlier characterisations (chapter 2.3.1) showed that the HAp lattice may be partially decomposing at this temperature to form TCP.

Thermally treated shell-derived powders were also trialled. After immersion, it was apparent that the precipitation of $Ni(OH)_2$ onto the surface of the materials was occurring, as a fine green layer of solid was observed to deposit after exposure to the nickel solution. This was observed to a greater extent on the shell derived solids that had been heated at higher temperatures (700 ^oC and above). Above these temperatures, as shown in chapter 2.3.2, a phase change from $CaCO_3$ to CaO through the reaction: $CaCO_{3\,(s)} \rightarrow CaO_{\,(s)} + CO_{2\,(g)}$. As CaO is known to induce alkalinity in water samples via formation of $Ca(OH)_2$, it is likely that these solid materials when immersed in the nickel solutions induce the precipitation of nickel as $Ni(OH)_2$ onto the surface of the shell derived materials that have been heated.

To confirm this, the shell materials were immersed in DI water to measure the change in pH of the water after an immersion length of 30 minutes. These results are given in Table 3-9 below.

Table 3-9: pH measurements of DI water sample after immersion of shell derived materials.

Sample	pH after 30 mins
Untreated cockle	10.029
500 °C cockle	10.203
600 °C cockle	10.463
800 °C cockle	12.607
1000 °C cockle	12.65

As expected, an increase in temperature led to an increase in the pH change of the water sample. This provides support for the increasing presence of CaO as the treatment temperature increases. CaO hydrolyses to $Ca(OH)_2$ via the following equation: $CaO + H_2O \rightarrow Ca(OH)_2$, which then causes the observed increase in pH. It is possible that nickel is also adsorbing to the surfaces of these shell-derived materials, however the dominating mechanism is likely through the precipitation of $Ni(OH)_2$. This $Ni(OH)_2$ can be removed through centrifugation and filtration, however the overall influence on the pH of the water sample is a significant disadvantage, so it is unlikely that these materials could practically be used in metals removal applications. Because of these results, the shell derived materials were not included in any further adsorption experiments.

It is understood that the carbonate presence in the bone materials would undergo a similar decomposition, with CaO being produced in these powders. To reduce the possibility of this influencing the adsorptions, the thermally treated bone-derived

materials were washed with water to reduce the presence of any CaO prior to immersion in the nickel solution during the adsorption experiments.

To support the results in Table 3-8 above, additional comparison experiments were carried out, using snapper bones (Table 3-10), hoki bones and a mixture of all species bones (Table 3-11), to determine if this trend observed earlier was dependent on the species from which the bones were sourced.

Table 3-10: Averaged results from Ni removal by snapper bone-derived powders (~0.2 g).

Sample	q_t (mg/g)	R%
Snapper 500 °C	3.988	98.8
Snapper 800 °C	2.325	55.6
Snapper 300 °C	0.559	13.4
Snapper 1000 °C	1.287	32.1

As shown above, the bone materials heated to 500 °C were confirmed as being the most efficient for removing nickel from the water samples, demonstrating that the adsorption efficiency is not dependent on species type. Further support for this is given in Table 3-11 below.

The sample 'bone mix 500 °C' presented in this table was generated by the addition of 0.1 g of each species bone powder to a crucible and treating these at 500 °C. Following this, the material was ground to a powder using a ring mill, consistent with the processing of all other samples. It should be noted, the differences between the q_t values displayed Table 3-11 and the values presented in Table 3-10 are due to the differences in the quantity of adsorbents used in the separate experiments.

Table 3-11: Nickel removal comparison of hoki bones to the mixed species bone sample.

Sample	m(bone)	C_t (mg/L)	q_t (mg/g)	R%
Hoki 500 °C	0.1023	21.835	6.210	74.4
Hoki 500 °C	0.1009	22.455	6.234	73.7
Bone mix 500 °C	0.1022	23.69	6.034	72.2
Bone mix 500 °C	0.1015	22.95	6.149	73.1

The 'bone mix 500 °C' sample performed equally well to the hoki bones treated to 500 °C. Therefore, separating the bones into different species is unlikely to be a necessary step for this application.

An experiment comparing the fish species bones to a bone sample of bovine origin, both of which had been heated to 500 °C was also carried out. The results are given below in Table 3-12.

Table 3-12: Nickel removal experiment comparing fish and bovine bone materials.

Sample	m(sample)	C_t (mg/L)	q_t (mg/g)	R%
Bovine 500 °C	0.2007	5.383	3.985	93.7
Bovine 500 °C	0.2053	5.124	3.908	94.0
Hoki 500 °C	0.2072	2.89	3.999	96.6
Hoki 500 °C	0.2047	2.92	4.046	96.6

The bovine bones were also equal in performance to the hoki bone derived materials. Hence the source of the bone-derived powders does not significantly influence the material's ability to adsorb nickel. As mentioned earlier however, the advantage to fish bones over bovine bones is their ease of processing to produce a powder, due to the small sizes of fish bones.

3.2.2.2 Investigating the mechanism of adsorption

It was suspected that one of the main mechanisms for this removal process would be through ion exchange, via the substitution of Ni ions for Ca ions in the HAp lattice. If this were the case, there should be a corresponding increase in Ca^{2+} concentration in solution with a decrease in Ni^{2+} ions. Ca^{2+} can also be measured using AAS, and an experiment was run where the water samples had both their nickel and calcium concentrations measured. The results of this are given in Figure 3-9 below. For control, a sample of the 500 °C treated powder was also immersed in a DI water sample, while the concentration of Ca was not recorded over time, the concentration was recorded after an immersion length of 2 hours, and was found to be 0.282 mg/L.

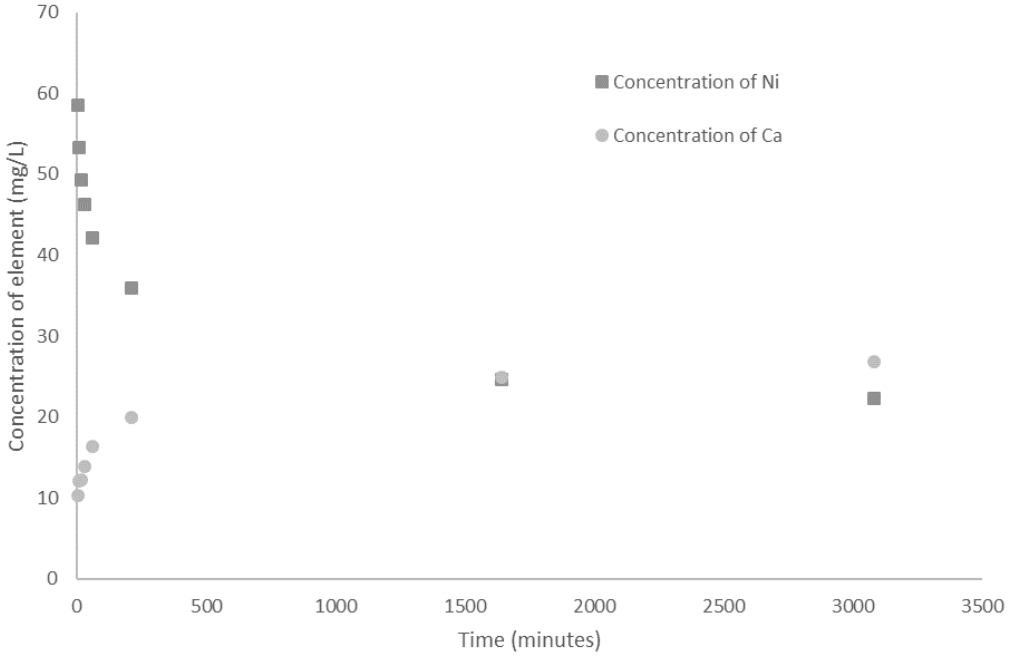

Figure 3-9: Concentration of nickel and calcium over time of bone material immersion.

These results show that there is a clear increase in the concentration of calcium in solution over time, as the concentration of nickel decreases. After a contact time of two hours, the Ca concentration was found to be 19.89 mg/L, which is a significant increase compared to the control sample (0.282 mg/L Ca). This provides support for the ion exchange mechanism suggested above.

From these results, ratios for the change in concentration nickel to the change in calcium in each sample were calculated, these are given in Table 3-13 below. This was done to determine if the mechanism was acting alone, or if there may be other factors aiding in the adsorption of nickel ions to the substrate.

Table 3-13: Ratios for the change in concentration of nickel and calcium.

t(min)	d[Ni]/d[Ca] ratio
5	1.8
10	1.83
15	2.03
30	1.93
60	1.82
210	1.71
1640	1.68

If the mechanism was acting alone, with one nickel ion swapping for one calcium ion, the values of these ratios should be approximately 1. Values above this, indicate that there is more nickel being removed from solution, than there is calcium being removed from the HAp lattice. It is possible that this substitution is the dominating mechanism, however it is certainly not acting alone. The overall reduction in Ni^{2+} observed is likely to be the outcome of a combination of adsorption and precipitation processes, such as the physical adsorption onto the surface of the materials as a precipitate. As the materials used are a brown colour, it is also possible that there is some carbon black content in the material influencing adsorption, as carbon black has been shown to have nickel adsorbing properties[20].

3.2.2.3 Determination of adsorption kinetics

The concentration of nickel over time of adsorption (Figure 3-9 presented earlier) onto bone-derived powders treated to 500 ^{o}C were used in the determination of the adsorption kinetics. The raw data of this is given below Table 3-14.

Table 3-14: Raw data of nickel concentrations over time of adsorption.

Time (mins)	C_t (mg/L)	q_t (mg/g)
Initial concentration	**85.28**	**-**
5	58.56	5.8725

10	53.27	7.0352
15	49.29	7.9099
30	46.31	8.5648
60	42.17	9.4747
210	**35.91**	**10.8505***

**this value is assumed to be the q_e experimental value.*

Calculation of the $\ln(q_e-q_t)$ values was done using a q_e value of 10.8505 mg/g. These calculated values are given in Table 3-15 below.

Table 3-15: PFO adsorption calculations.

Time (mins)	$\ln(q_e-q_t)$
5	1.6050
10	1.3390
15	1.0786
30	0.8267
60	0.3191

These values were then plotted against each other with a linear trend line fitted to the data, in Figure 2-1.

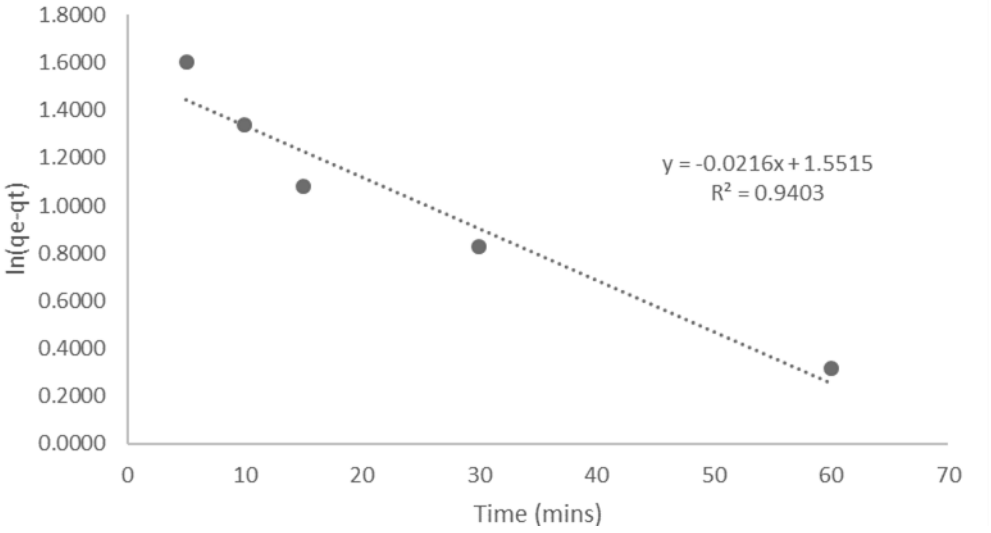

Figure 3-10: Linear PFO model for adsorption of Ni onto bone-powders treated at 500 °C.

Values of q_e and k_1 were calculated using the slope and intercept of the above trend line (Figure 3-10):

q_e (calc):

$\ln q_e$ = intercept

$\ln q_e$ = 1.5515

$q_e = e^{1.5515}$

$q_{e\,(calc)}$ = 4.7185 mg/g

k_1:

k_1 = slope

k_1 = -0.0216

R^2:

R^2 = 0.9403 (from Figure 3-10)

The PSO model was also fitted to the data, through calculating values of t/q_t (Table 3-16) and plotted against time (minutes) in
Figure 3-11 below.

Table 3-16: PSO adsorption calculations.

Time (mins)	T/q_t
5	0.8514
10	1.4214
15	1.8964
30	3.5027
60	6.3326

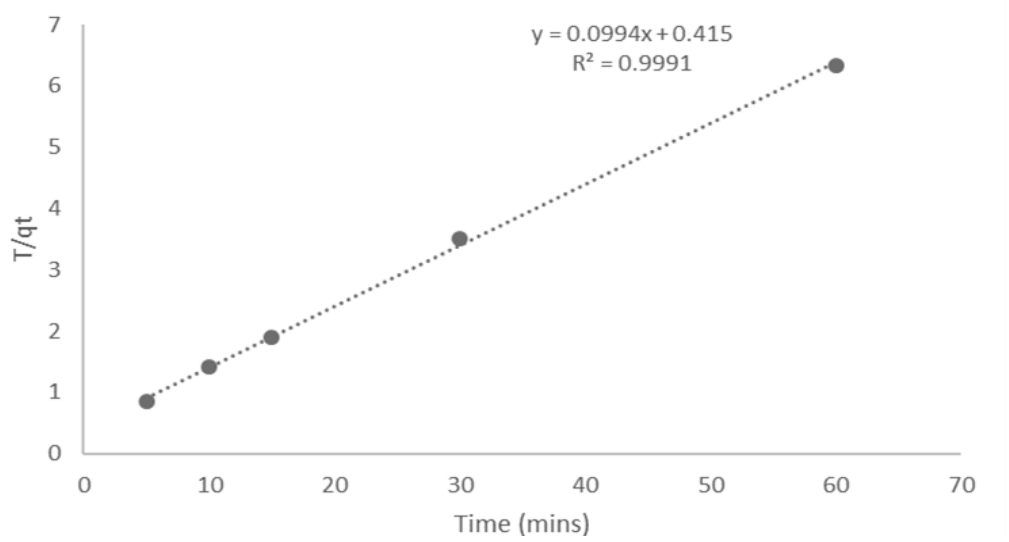

Figure 3-11: Linear PSO model for adsorption of Ni onto bone-powders treated at 500 °C.

The slope and intercept values of the above trend line were then used to calculate k_2 and q_e as follows:

$q_{e\ (calc)}$:

$1/q_e$ = slope

$1/q_e$ = 0.0994

$q_{e\ (calc)}$ = 10.0604 mg/g

k_2:

$1/k_2q_e^2$ = intercept

$1/k_2$ x 10.0604^2 = 0.415

$k_2 = (1/0.415)/(10.0604^2)$

k_2 = 0.0238

R^2:

0.9991 (from

Figure 3-11)

Comparison of the R^2 for the two kinetic model's relationships shows that the PSO model is the best fit for the nickel-bone powder system. Furthermore, the experimentally obtained value for q_e was 10.8505 mg/g. The PFO model gave a calculated q_e value of 4.7185 mg/g, while the PSO model gave a value of 10.0604 mg/g. The value obtained by the PSO model is much closer to the experimentally obtained value.

The PSO relationship indicates that the rate-limiting step in the adsorption process is a chemisorption interaction between the adsorbate and the adsorbent[21-23]. This is consistent with similar systems found in literature[24]. It is also consistent with the substitution mechanism of Ni^{2+} for Ca^{2+} in the HAp lattice, as this is a chemical substitution reaction. These results also indicate that a contact time of 210 minutes is sufficient for the system to reach an equilibrium state. All further nickel-bone adsorption experiments were mixed for 4 hours, to ensure an equilibrium concentration was reached.

3.2.2.4 Adsorption isotherm experiments

To understand the type of adsorption occurring, isotherm experiments were carried out. These varied the amount of adsorbent, while fixing the concentration and volume of the adsorbate solution. Alternatively, these can be studied through varying the concentration of adsorbate and fixing the amount of adsorbent. Varying the mass of adsorbent was an easier way of doing this as it avoids the need to generate a number of different metal ion concentration solutions. A plot of the final equilibrium adsorbate concentration (C_e, after 4 hours) against the calculated adsorptive capacity (q_e) is given in Figure 3-12 below.

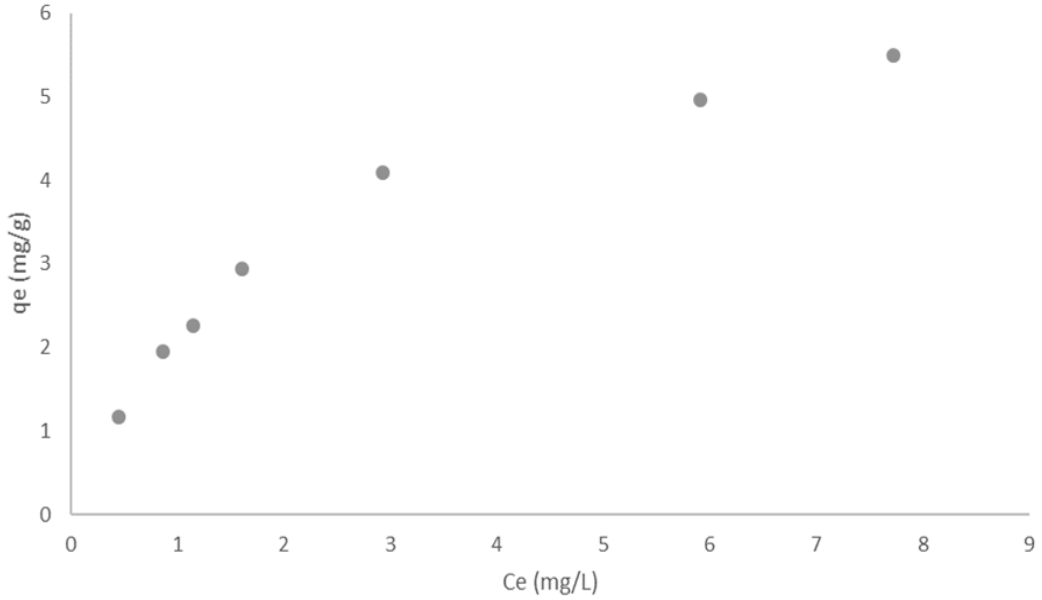

Figure 3-12: Adsorption isotherm of varying amounts of hoki bones heated at 500 ºC exposed to fixed volume (10 mL) of a containing of 100 mgL^{-1} nickel.

A linearised form of the above isotherm is given below in Figure 3-13, generated using the methods outlined in section 3.1.7.2.

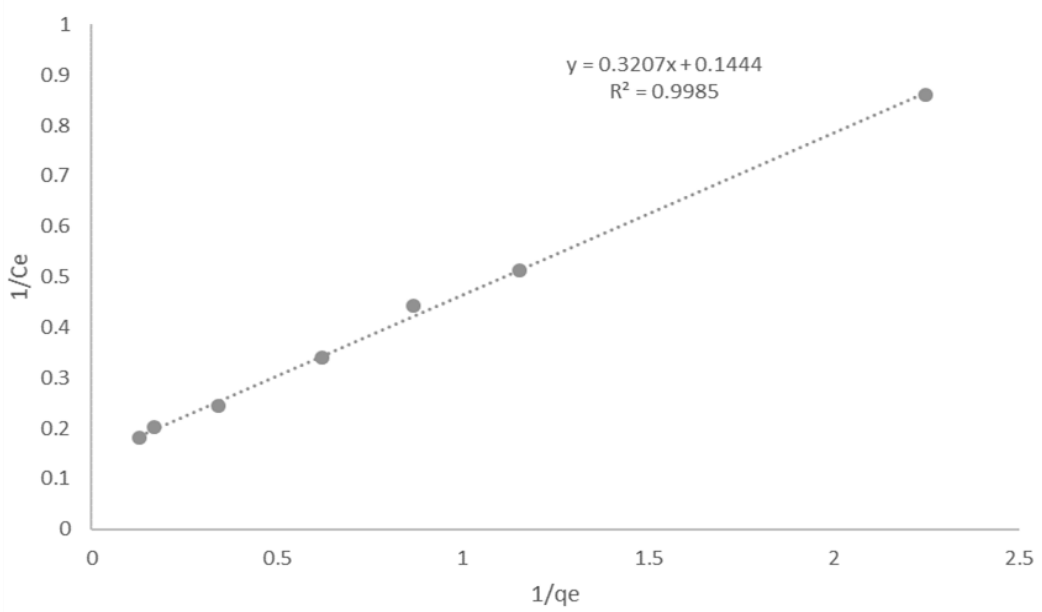

Figure 3-13: Linearised Langmuir isotherm for nickel adsorption onto hoki bones treated at 500 ºC.

Using the linear form of the isotherm equation, and the equation of the line in Figure 3-13 in the form y = mx + c, values of q_m and *b* can be calculated:

Intercept = $1/q_m$

$q_m = 1/0.1444$

$1/0.1444 = 6.925$

q_m = 6.925 (mg/g) milligrams of nickel per gram of adsorbent material, after a contact time of four hours.

Slope = $1/bq_m$

b = $(1/slope)/q_m$

b = (1/0.3207)/6.925

b = 0.4503 (L/mg)

The Freundlich isotherm model was also fitted to this data set and is given in Figure 3-14 below.

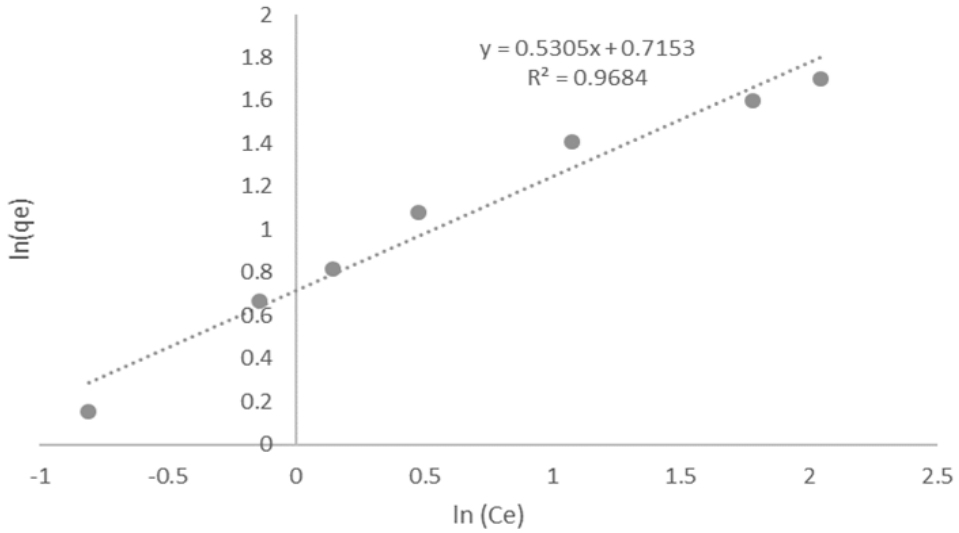

Figure 3-14: Linearised Freundlich Isotherm for nickel-bone powder system.

Freundlich isotherm parameters were calculated from the trend-line given in Figure 3-14:

Intercept = lnK_F

$K_F = e^{0.7153}$ = 2.0448

Slope = 1/n

n = 1/0.5305 = 1.8850

It is clear from these two linearised data sets, that the Langmuir isotherm is the best fit for this system. This is consistent with literature data for similar nickel-hydroxyapatite systems[1, 25], suggesting the system follows more closely to the monolayer adsorption model as described by the Langmuir isotherm.

3.2.2.5 Effect of temperature on adsorption

The effect of three different temperatures on the adsorption of nickel onto the bones was studied with the results summarised in Table 3-17 below.

Table 3-17: Effect of reaction temperature on adsorption.

Temperature (°C)	C_t (mg/L)	C_o (mg/L)
20	31.15	100.06
45	22.83	100.06
70	7.65	100.06

The influence of temperature is generally dependent on the adsorption system, i.e. the type of adsorption, and the nature of the adsorbent and adsorbate. In general for physical adsorptions, an increase in temperature leads to a decrease in the strength of the attractive forces between the surface of the adsorbent and the adsorbate, and hence a decrease in adsorption[26].

When the opposite trend is observed, it can suggest a chemical adsorption is dominating the mechanism. Such chemical adsorptions require an activation energy for the reaction to occur, and so increasing the temperature increases the likelihood that this activation energy will be achieved when an adsorbate ion comes into contact with the adsorbent surface.

In the present study, across the range of 20 – 70 °C, an increase in temperature lead to an increase in adsorption. This is consistent with literature[1] values on similar nickel hydroxyapatite systems. These results provide further support for the chemical adsorption mechanism being the dominating process. Generally, in chemical adsorptions however, there is an optimum temperature, and further increasing temperature past this point leads to a decrease in adsorption. This trend was not observed in the temperature range studied, it is possible that increasing the temperature further may have identified an optimum treatment temperature, however higher temperatures would be difficult to achieve practically in this study. It is understood that tracking the adsorptions over time at these different temperatures would enable calculations of activation energy through determination of rate constants at different temperatures[27-28]. These experiments however were not carried out in this study due to time constraints but could be investigated in future studies.

3.2.2.6 Effect of pH on adsorption

The influence of pH on the adsorption of nickel was also studied, using pH values between 2 and 7. Values above 7 were not used, as it was assumed that increasing pH past 7 would lead to an increase in the precipitation of nickel as $Ni(OH)_2$, and this would interfere with the results. The results of the study are given in

Figure 3-15 below. It should be noted, that the pH values of these samples were measured and adjusted prior to exposure to the bone-derived materials.

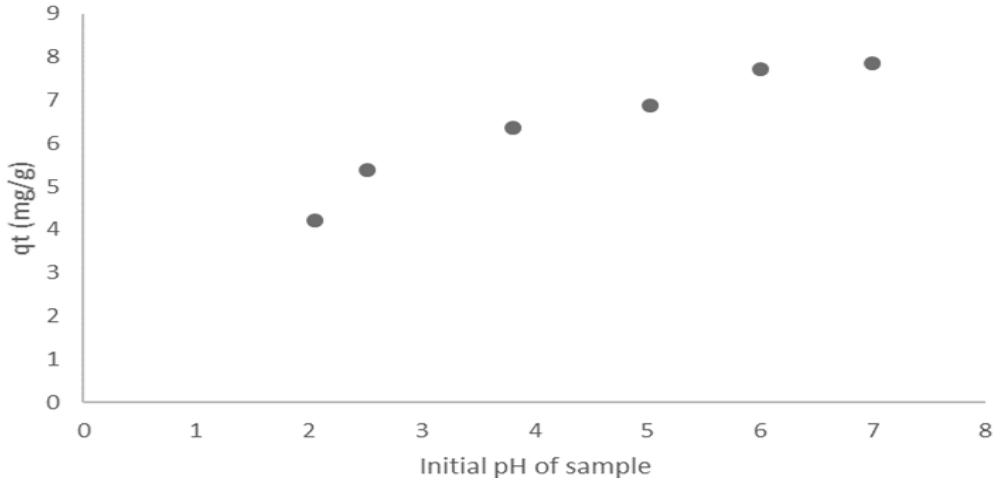

Figure 3-15: q_t values for adsorption of nickel onto hoki bones treated at 500 °C as a function of pH.

Increasing the pH over the range of 2-7 lead to an increase in adsorptive capacity of the material. This result was expected, and is consistent with the literature[18], at lower pH values (< pH 4), breakdown of the HAp lattice should occur, which would decrease the availability of active sites for the substitution reaction to occur. Varying the pH of a solution in which a solid is immersed is known to influence the potential difference between the bulk medium, and the layer of fluids attached to the surface of the solid, this difference in potential is known as the zeta potential[29]. The zeta potential can be influenced by a number of factors, including pH.

When hydroxyapatite is immersed in water, the following reactions are possible[30].

Equation 3-12: $Ca^{2+} + OH^- \rightleftharpoons CaOH^+$

Equation 3-13: $CaOH^+ + OH^- \rightleftharpoons Ca(OH)_{2\,(aq)}$

Equation 3-14: $Ca(OH)_{2\,(aq)} \rightleftharpoons Ca(OH)_{2\,(s)}$

Equation 3-15: $H_3PO_4 \rightleftharpoons H^+ + H_2PO_4^-$

Equation 3-16: $H_2PO_4^- \rightleftharpoons H^+ + HPO_4^{2-}$

Equation 3-17: $HPO_4^{2-} \rightleftharpoons H^+ + PO_4^{3-}$

Equation 3-18: $Ca^{2+} + HPO_4^{2-} \rightleftharpoons CaHPO_{4\,(aq)}$

Equation 3-19: $CaHPO_{4\,(aq)} \rightleftharpoons CaHPO_{4\,(aq)}$

Equation 3-20: $Ca^{2+} + H_2PO_4^- \rightleftharpoons H_2PO_4^- \rightleftharpoons CaH_2PO_4^{+}{}_{(aq)}$

The positions of the equilibria in these equations are significantly influenced by the pH of the solution. For example, in Equation 3-12 - Equation 3-17, an increase in pH will drive the reactions to the right-hand side. The net result of which will be an increase in the activity of negatively charged species surrounding the solid, and a

decrease in the zeta potential. In these experiments, this negatively charged layer on the surface will result in an increase in the number of positive metal ions from solution being attracted to the surface of the material, and hence an increase in adsorption would observed. A decrease in pH will have the opposite effect, leading to a surface which will be positively charged, and have a repelling effect on the metal ions. This is likely the reasoning behind the trends observed in the pH experiments.

3.2.3 Removal of cadmium ions from water samples

It has been reported, that cations with a smaller ionic radii than Ca^{2+} (0.099 nm), such as Ni^{2+} (0.072 nm) have a lower affinity for substitution in place of Ca^{2+} in HAp than cations with more similar, or larger ionic radii (compared to Ca^{2+}), such as Cd^{2+} (0.097 nm) and Pb^{2+} (0.118 nm)[31]. Hence it was suspected, that if the mechanism of removal was through direct substitution of the calcium ion, that cadmium would have a greater affinity for the HAp than nickel.

3.2.3.1 Comparison of adsorbent materials

An adsorption experiment was hence run measuring the ability to remove cadmium ions as a function of processing technique with the assumption being that the Langmuir model applies. The results of these are given in Table 3-18 below.

Table 3-18: Cadmium removal experiments for hoki bone materials.

Sample	q_t (mg/g)	R%
Raw hoki	4.966	99.3
Hoki 300 °C	4.933	98.7
Hoki 500 °C	5.000	100.0
Hoki 600 °C	4.990	99.8
Hoki 800 °C	4.979	99.6

These results are consistent with the nickel removal results, the bones treated to 500 ^{o}C were the most effective for cadmium removal. However, all of these materials used were also judged to be effective, with removal percentages of 98 % and above observed.

The bones treated to 500 ^{o}C were then subjected to a removal over time experiment, with the cadmium concentration of the solution being measured at a range of time points. The exact same experiment was done with the nickel solution as well, to compare the affinities of each ion to the materials. A plot summarising these results is given below in Figure 3-16

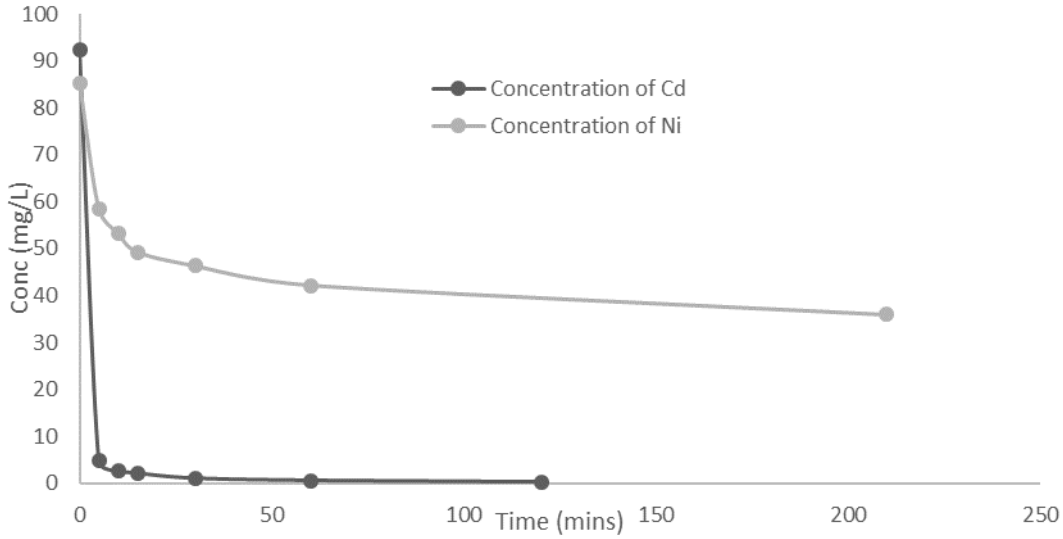

Figure 3-16: Concentration of metals over time of immersion with bones treated at 500 ºC.

It is clear from this that the affinity of this material for cadmium is far greater than the affinity for nickel. In the first 5 minutes, the concentration of the cadmium solution is reduced to less than 5 mg/L, while the nickel solution remains around 50 mg/L. This provides further support for the substitution mechanism.

It is possible, that this ion substitution is leading to the formation of a new phase. pXRD patterns were recorded for bones heated at 500 ºC, after being immersed in a 100 ppm Cd^{2+} solution for two hours.

The resulting diffractogram, compared with the bones heated at 500 ºC prior to immersion, is given in Figure 3-17 below.

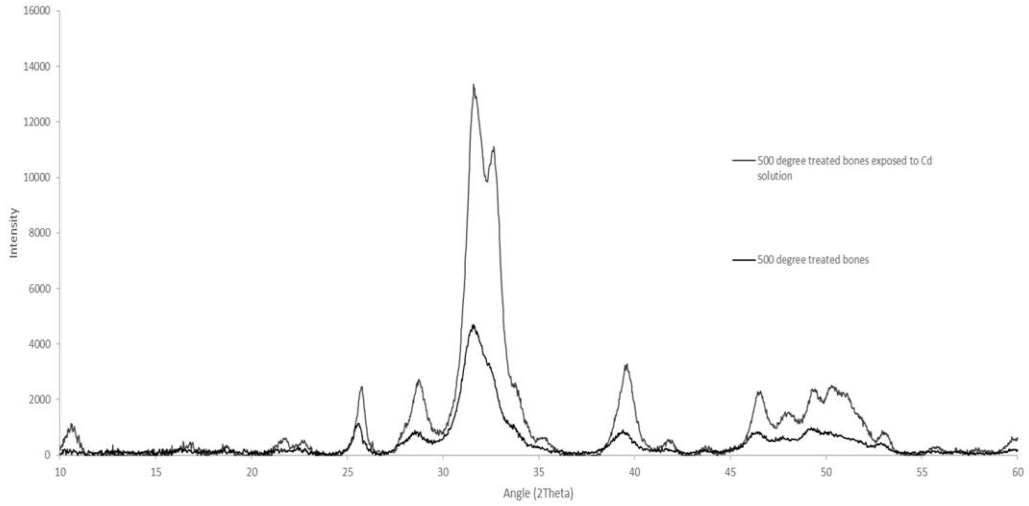

Figure 3-17: Diffractograms of bones heated at 500 ºC both exposed to a Cd solution of 100 ppm Cd^{2+}, (grey) and not exposed to Cd (black).

There two patterns appear to match closely, the bone powders exposed to Cd however have a more resolved and intense pattern. At a Cd^{2+} concentration of 100

ppm, it is possible that there is the generation of small amounts of a new phase, however this is new phase is not present in sufficient amounts that it can be detected through XRD. Previous studies report that differences in the pattern of pure HAp with Cd substituted HAp are small, and are generally due to differences in the unit cell and hence crystalline size[32]. It is possible that the employment of the Scherrer equation in this study would have identified these small differences between the diffractograms, however this was beyond the scope of this study.

3.2.3.2 Determination of adsorption kinetics

As with the nickel studies, adsorption kinetic models were applied to cadmium adsorptions. These were carried out for a range of adsorbent masses, and plots of Cd concentration over time were generated for each sample. An example of these plots is given in Figure 3-18 below (adsorbent mass of 0.2675 g). The data in these plots were then fitted to the PFO and PSO adsorption kinetic models, with the summary of these given in Table 3-19 below.

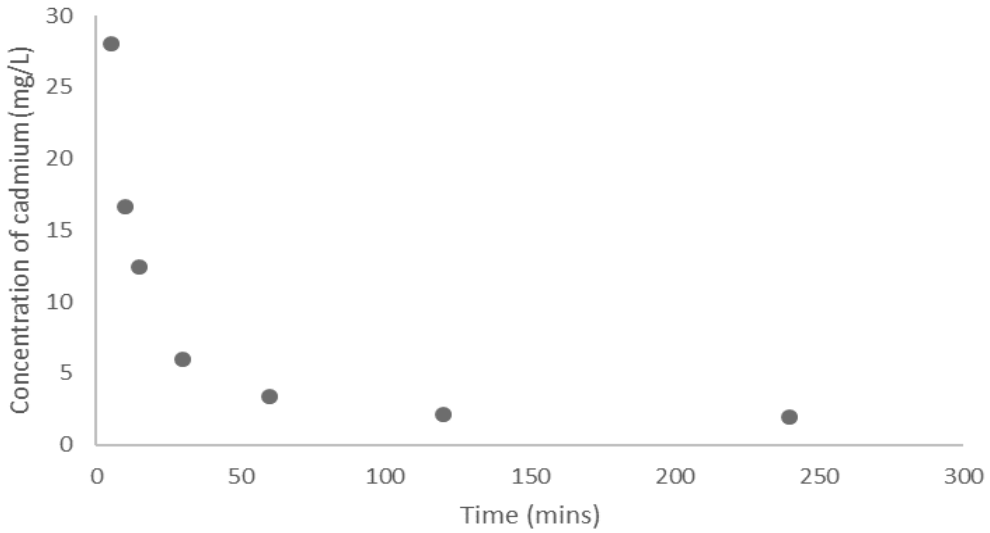

Figure 3-18: Cadmium concentration over adsorption contact time with 0.2675 g of bone powder treated to 500 ºC.

Table 3-19: PFO and PSO adsorption models applied to cadmium-bone adsorption systems.

Pseudo first order adsorption model						
Mass of adsorbent (g)	**0.1045**	**0.1263**	**0.1514**	**0.1856**	**0.2675**	**0.3028**
R^2	0.9132	0.9558	0.9961	0.9212	0.9704	0.9896
k_1	-0.0212	-0.0228	-0.0399	-0.0335	-0.0399	-0.0692
$q_{e\ (calc)}$ (mg/g)	22.5560	16.3757	14.8887	7.2384	3.4563	3.5335
$q_{e\ (exp)}$ (mg/g)	34.3378	29.8646	26.0221	21.5641	15.2209	13.5134
Pseudo second order adsorption model						
Mass of adsorbent (g)	**0.1045**	**0.1263**	**0.1514**	**0.1856**	**0.2675**	**0.3028**
R^2	0.9978	0.9973	0.9996	0.9995	1	1

k_2	0.0017	0.0034	0.0055	0.0109	0.0308	0.0492
$q_{e\ (calc)}$ (mg/g)	36.6300	30.8642	27.1739	22.1729	15.4560	13.7174
$q_{e\ (exp)}$ (mg/g)	34.3378	29.8646	26.0221	21.5641	15.2209	13.5134

The PSO adsorption model provided the best fit for these experiments, consistent with the nickel-bone powder system. It is therefore likely that these metal adsorption systems are operating through a PSO adsorption model, and that the rate limiting step involves a chemical interaction between the Cd^{2+} ion and the adsorbent material with rate determined by the number of available sites and the concertation of adsorbent. The experiments showed that a contact length of four hours was sufficient to obtain experimental values of q_e, therefore for further Cd adsorption experiments, immersion lengths of four hours were used to ensure the system had enough time to reach equilibrium[21-23].

3.2.3.3 Adsorption isotherm experiments

Isotherm experiments were then carried out for the system with cadmium. To understand when an equilibrium is reached in these systems, a range of isotherms were generated for several contact times. The linearised Langmuir isotherms generated from these experiments are presented in Figure 3-19.

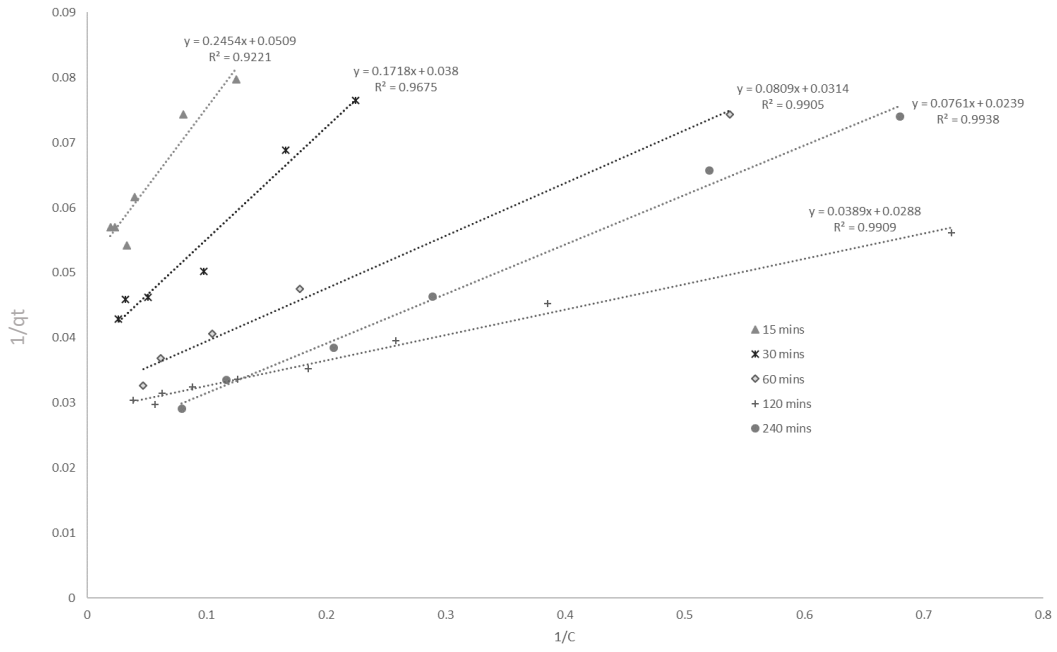

Figure 3-19: Linearised Cd^{2+} adsorption isotherms for different contact times (onto bone derived materials heated at 500 ^oC).

These results were then used to calculate values of q_m and *b* for each length of contact time, given in Table 3-20 below. The data was also fitted to the Freundlich model for comparison, with values of *K*L and 1/n also displayed in Table 3-20.

Table 3-20: Calculated isotherm values for linear Langmuir and Freundlich isotherms.

	Freundlich			Langmuir		
Time (mins)	K_F	n	R^2	q_m (mg/g)	B (Lmg^{-1})	R^2
15	8.247	4.864	0.8789	19.646	0.2074	0.9221
30	9.512	3.893	0.8843	26.316	0.2212	0.9675
60	10.701	2.882	0.9659	31.847	0.3881	0.9905
120	12.169	2.920	0.9884	34.722	0.7404	0.9938
240	11.850	2.276	0.9751	41.841	0.3141	0.9909

As with the nickel adsorptions, the R^2 values produced through the linear Langmuir isotherm were higher than the values produced by the linear Freundlich isotherm. This is consistent with previous studies[33]. Hence for these systems, it is likely that each reactive site on the surface of the material has an equal affinity to each metal ion in solution and can only physically adsorb one ion per active site. This can also be applied to the substitution mechanism. While a monolayer may not result from the substitution, each calcium ion can only substitute for one cadmium ion, so it will appear to follow a similar trend to a monolayer adsorption.

With increasing contact time, the calculated value of q_m also increased. While these did not reach a plateau, it appears that these are beginning to level out, with a value of 41.841 mg/g after mixing for four hours, which was shown by the kinetic experiments to be sufficiently long enough for the system to reach equilibrium.

3.2.3.4 Investigating the mechanism of adsorption

It was thought that a possible reason behind why the bones treated to 500 ^oC were the most effective, could be due to a residual carbon black content. Carbon black materials are known to be good adsorbents, and due to the brown nature of the materials it was thought that some carbon black could be present, despite the lack of a ^{13}C signal in the NMR spectra. To determine if this was the case, some of the alkali treated raw materials were heated to 500 ^oC. These were found to have a lower carbon content than the raw materials, and so thermally treating these should produce a material with a correspondingly lower carbon black content due to the 'cleaning' effect of the NaOH. The results of the first of these experiments are given below in Table 3-21.

Table 3-21: Adsorption capacity values for chemically and thermally processed materials fishbone materials.

Adsorbent type	q_t (mg/g)	R%
Hoki cooked at 500	4.617	99.0
Hoki refluxed in NaOH then cooked at 500	4.415	99.6
Gurnard refluxed in NaOH then cooked at 500	4.364	95.9

Snapper Refluxed in NaOH then cooked at 500	4.233	93.5
Hoki refluxed in NaOH	4.517	100.0
Flounder refluxed in NaOH	4.568	99.6

Treating these materials with NaOH prior to thermal treatment did not appear to significantly affect the adsorption capacities of the materials. So it is unlikely that a residual carbon black content is significantly influencing these adsorptions.

A similar experiment was done with a number of processed materials, however in this instance, the calcium content of the water samples was also measured and the results summarised in Table 3-22 below. Control samples were also run, which involved immersing each of the samples in a 10 mL sample of DI water, and measuring the concentration of [Ca] in these after two hours (the same length of time allowed for the adsorption experiment) to ensure the calculated ratio values accounted for the natural leaching of Ca into solution from the calcium phosphate materials.

Table 3-22: Comparison of processed bone materials for cadmium removal.

Sample	Control [Ca] (mmol/L)	d[Cd]:d[Ca] ratio	q_t (mg/g)	R%
Hoki refluxed in NaOH.	**0.0030**	1.503	47.069	99.0
Gurnard refluxed in NaOH	**0.0010**	1.369	47.310	99.3
Hoki refluxed in NaOH, then heated to 500 °C	**0.0018**	1.277	39.249	82.2
Hoki cooked at 500 °C	**0.0071**	1.117	37.217	77.6
Fluka Pure HAp	**0.2134**	1.036	32.211	67.4

The q_t values for these materials are higher than for previous experiments as a smaller mass of adsorbent was used, while still using the same 100 mg/L solution of cadmium. It was noticed that when using 0.2 grams of the materials with 10 mL of a 100 mg/L cadmium solution, the removal percentages were all in the range of 95-100 %, despite varying the type of adsorbent. It should be noted that 0.05 g of each material was instead exposed to 10 mL of the 100 mg/L Cd^{2+} solution, which has led to the high q_t values.

The d[Cd]:d[Ca] ratio was calculated through calculating the change in concentration of each ion (in moles). Calculation of the change in [Ca^{2+}] accounted for the natural leaching of Ca^{2+} into solution of water for each sample. A ratio of 1 would suggest a direct 1:1 substitution of cadmium for calcium in the HAp lattice. Fluka pure hydroxyapatite had a value close to 1, of 1.036, so it is likely that this substitution is the driving force in this adsorption, with adsorption of a precipitate to the surface having a smaller contribution. The bones treated to 500 °C returned a

value of 1.117, suggesting that the substitution is the predominant mechanism, however there are other factors which have a small influence, as with the nickel system, this could be through interaction with small amounts of carbon black in the material, as well as adsorption of a Cd precipitate on the surface of the materials. It is also possible, that despite washings, small amounts of CaO could be inducing a slight pH change, and Cd could be precipitating as $Cd(OH)_2$ both in solution and on the surface of the materials.

The materials refluxed in NaOH had much higher ratios, it is possible that despite numerous washings, residual alkali is present in these materials and is causing the precipitation of $Cd(OH)_2$, which would occur alongside the substitution of Cd^{2+} for Ca^{2+}. The samples refluxed in NaOH prior to being heated to 500 ^oC showed no significant advantage over the materials just treated to 500 ^oC, so this extra processing step is not considered to be necessary for this application.

3.2.3.5 Effect of pH on adsorption of cadmium

The influence of pH on cadmium adsorption to the materials heated to 500 ^oC was assumed to be similar to the nickel adsorption (Figure 3-15), for this reason only a few pH values were used for these adsorptions, to determine if the same general trend was followed. The results are given in Figure 3-20 below.

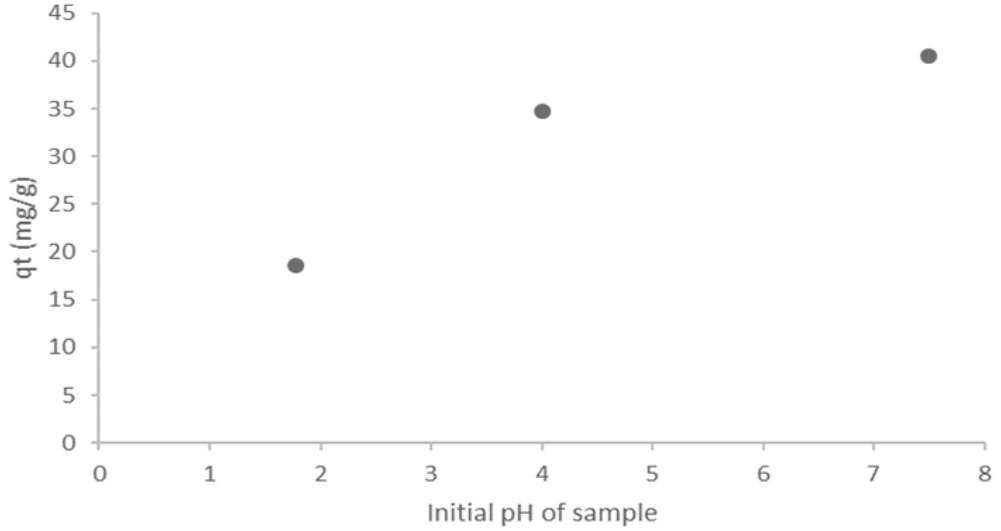

Figure 3-20: q_t values for the adsorption of cadmium onto hoki bones thermally treated to 500 ^oC as a function of pH.

These results suggest that the same trend is followed in the cadmium system. pH values above 8 were not trialled as these would lead to an increase in the precipitation of Cd as $Cd(OH)_2$.

3.2.3.6 Application of materials to a "binary" metal ion solution (Cd^{2+} and Ni^{2+})

To investigate whether the materials heated at 500 ºC could be used to adsorb more than one divalent metal ion simultaneously, a standard containing both nickel and cadmium was generated, and exposed to varying amounts of these bone materials. The results of this experiment are summarised in Table 3-23 below.

Table 3-23: Results from adsorption of a "binary" Ni^{2+}-Cd^{2+} solution onto bone powders heated at 500 ºC

m(adsorbent) (g)	Ct (Ni, mg/L)	Ct (Cd, mg/L)	R% Ni	R% Cd
0.0516	18.9195	0.6123	63.7	98.8
0.1008	5.1671	0.1453	90.1	99.7
0.1505	1.6787	0.0577	96.8	99.9
0.2095	0.5824	0.0574	98.9	99.9
Initial Concentration	**52.1621**	**63.7158**	**-**	**-**

Increasing the amount of adsorbent in the experiment corresponds with decreasing C_t values, suggesting that the reduction in concentration of the metal ions is due to the presence of the bone materials. The results showed that despite having a higher initial concentration, Cd^{2+} ions were reduced to a greater extent than the Ni^{2+} ions. This agrees with earlier results suggesting that Cd^{2+} ions have a greater affinity to these bone-derived materials than Ni^{2+} does, which is likely due to the similar ionic radii of Cd^{2+} and Ca^{2+}. These results are promising for potential application of these materials to adsorb a range of metal ions from a contaminated water sample simultaneously.

3.2.4 Removal of strontium and arsenate ions from water samples

The concentration measurements of strontium and arsenate ions in solution were not as simple to obtain as with the cadmium and nickel ions. These were unable to be measured using AAS, due to the unavailability of the appropriate gas mixture required to analyse these metals. Instead, these were analysed using ICP-MS. Due to the extra costs associated with using ICP-MS, experiments comparing the different adsorbent materials were the only ones completed and thorough investigations into the adsorption isotherms and kinetics were not carried out.

3.2.4.1 Comparison of adsorbent materials on adsorbing strontium

Table 3-24 below summarises the results from the adsorption of divalent strontium cations onto a range of hoki bone-derived adsorbent materials.

Table 3-24: Comparison of adsorbents for the adsorption of Sr^{2+} from solution.

Sample	C_t (mg/L)	q_t (mg/g)	R %
Sr^{2+} Standard	111.7705	-	-
As received hoki bone powder	29.0725	7.9979	74.0
300 °C bone powder	35.8051	7.5587	68.0
500 °C bone powder	11.8274	9.3667	89.4
600 °C bone powder	39.7972	6.9272	64.4
800 °C bone powder	57.8532	5.0674	48.2
Reprecipitated HAp	43.9290	6.6122	60.7
HAp pure (Fluka)	70.4481	3.9848	37.0

Consistent with previous results for nickel and cadmium adsorptions, the bone materials heated at 500 °C were the most efficient adsorbent for the removal of Sr^{2+} ions from solution. This is likely to be for the same reasons suggested in section 3.2.2.1.

3.2.4.2 Comparison of adsorbent materials on adsorbing arsenate

It is understood that the mechanism behind arsenate removal may be different to the mechanism for the earlier trialled metals, as arsenate is known to substitute for phosphate into the HAp lattice[4, 34], instead of for Ca^{2+} as found with the divalent metal ions earlier. The summarised results from the adsorption of arsenate onto a range of bone-derived materials are given in Table 3-25.

Table 3-25: Comparison of adsorbents for the adsorption of As(V) (arsenate ions) from solution.

Sample	Ct (mg/L)	qt (mg/g)	R%
Arsenate Standard	87.9281		
As received hoki bone powder	77.6971	1.0150	11.6
300 °C bone powder	66.5658	2.1256	24.3
500 °C bone powder	77.8986	0.9970	11.4
600 °C bone powder	83.8664	0.3891	4.6
800 °C bone powder	86.3589	0.1563	1.8
Reprecipitated HAp	35.3134	4.9824	59.8
HAp pure (Fluka)	80.1681	0.7239	8.8

These results suggest that reprecipitated hydroxyapatite was the most efficient material for the removal of As(V) from solution. In contrast to the divalent metal ion adsorption systems, the affinity of AsO_4^{3-} to the bone powder heated at 500 °C was low, supporting the fact that this system follows a different mechanism of adsorption. It is possible that conducting these experiments at higher pH may have led to an improved uptake. The presence of the arsenate ion is favoured at higher pH values, and at lower pH values other As(V) species (such as $H_2AsO_4^-$) tend to dominate[35]. Unfortunately, due to time constraints this system could not be

investigated further, however these initial results suggest the materials do have the potential to act as a cheap adsorbent material for the arsenate ion.

3.2.5 Removal of fluoride ions from water samples

Previous studies have identified the potential for hydroxyapatite materials to adsorb fluoride ions from solution, through the substitution of these for the OH^- in the HAp lattice[5]. While it is well understood and accepted that the presence of fluoride in drinking water in the concentration range of 0.5 – 1.0 mg/L is beneficial to human health, in particular dental health, there are areas in which the natural fluoride concentration exceeds the U.S EPA recommended safe level (4 mg/L)[36]. In these areas, this application of HAp as a fluoride removal agent could be of interest as it may offer a cheap method of lowering the fluoride content to an optimum level, to gain the health benefits from fluoride without the added risk of skeletal fluorosis associated with higher concentrations of fluoride (>10 mg/L).

Adsorption experiments were carried out in a similar manner to the metal ion removal experiments described earlier, however the fluoride content in the samples was not able to be measured through AAS, and instead ion chromatography was used to calculate fluoride concentrations and measure the adsorptions.

3.2.5.1 Calibration curve generation

Figure 3-21 below displays a chromatogram obtained from the DIONEX multi anion standard, the instrument output does not display units on the graph, but these are, minutes (x axis) and intensity (y axis), these units are consistent for all chromatographs presented in this study.

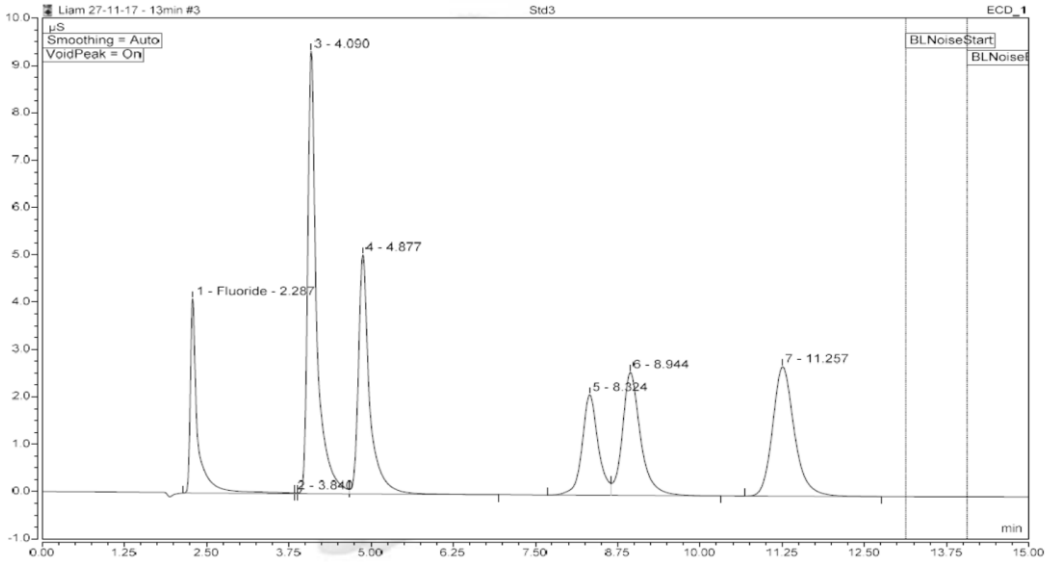

Figure 3-21: Chromatogram of DIONEX multi anion standard.

Based on previous experiments using the ICS-2000, it was understood that fluoride would elute first from the DIONEX standard, and the retention time would be approximately 2.29 minutes. In these experiments, fluoride was found to have a retention time between 2.280 and 2.320 minutes, and so peaks in this region were assigned to represent the fluoride content.

For each chromatographic experiment, a new fluoride concentration calibration curve was generated. For most experiments, this was successful, with R^2 values >0.9990. Experiments which did not achieve an R^2 of at least 0.9990 were repeated until a satisfactory relationship was found. An example of the calibration curves generated is given in Figure 3-22 below.

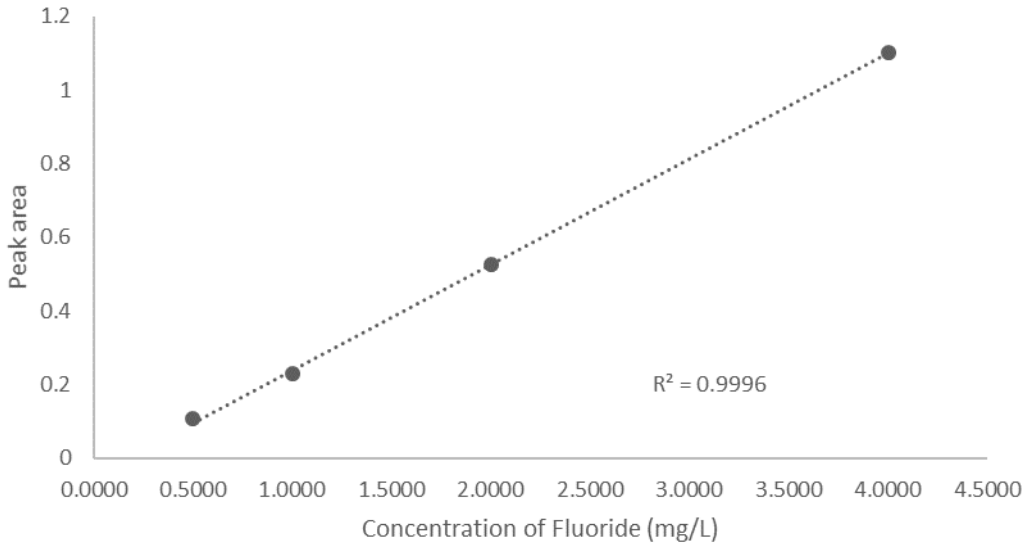

Figure 3-22: Sample calibration curve obtained for the IC experiments.

For a control, a sample of type 1 water was included in every sequence as this was used to make up each of the standards, as well as the samples themselves. A sample chromatogram of type 1 water is given below in Figure 3-23.

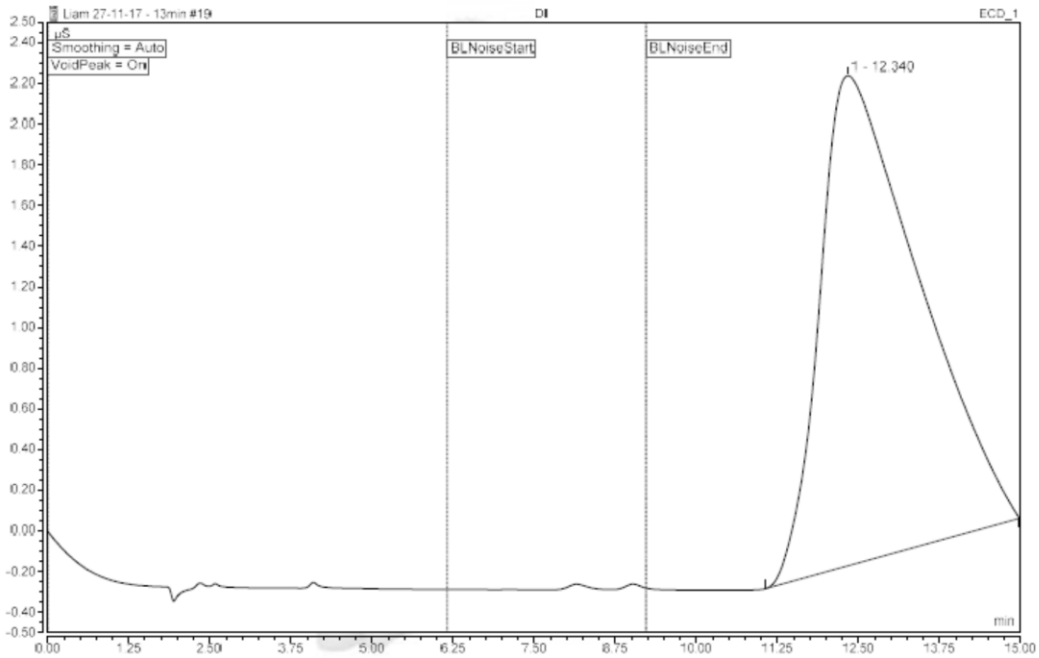

Figure 3-23: Sample chromatogram of type 1 water.

The appearance of this chromatogram was consistent across all of the IC experiments, and showed that the type 1 water had an undetectable fluoride level, hence giving confidence in the results by ensuring the fluoride content measured is from that of the sodium fluoride used to make the stocks, and any changes in the concentration of F^- should be as a result of adsorption processes.

3.2.5.2 Fluoride removal experiments

As with the metal ions removal section, the initial tasks for fluoride removal were to assess the removal abilities as a function of processing technique. The following material types were trialled:

- Commercial $CaCO_3$
- Ground shell species (mussel, scallop, oyster, cockle)
- Raw ground hoki bones
- Thermally treated fish bones (500, 600, 800, 1000 ^oC)
- Chemically treated fish bones (NaOH washed, digested & reprecipitated)
- Commercial (Fluka brand) HAp.

A range of experiments to determine the most efficient samples for F^- removal were carried out. Due to the inability to grind down the as received flounder, snapper and gurnard raw samples to a homogenous powder, these were not trialled in these experiments. A typical chromatogram obtained from the water samples after exposure to, and isolation from the solid materials is given below, in Figure 3-24.

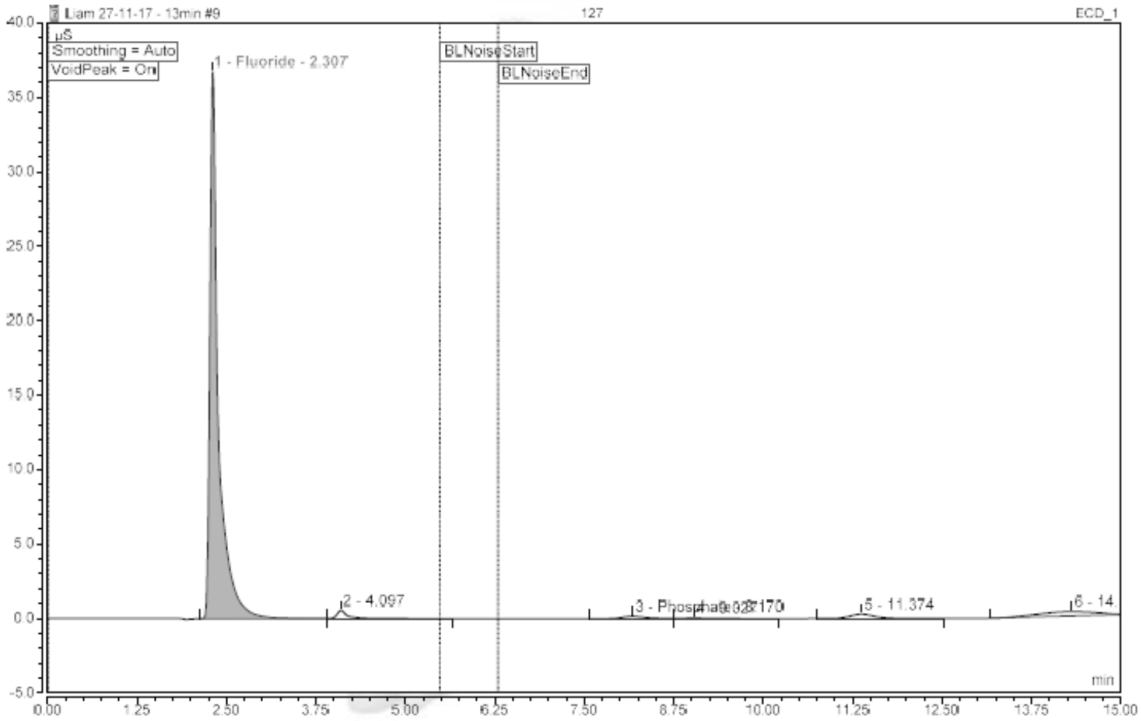

Figure 3-24: Sample ion chromatogram for an aqueous fluoride sample.

Table 3-26 presents the results from the adsorption of a 100 mg/L fluoride solution onto a range of materials (~0.1 g) while Table 3-27 contains the averaged results from this experiment.

Table 3-26: Results from fluoride adsorption onto a range of materials

Sample	m(solid) (g)	C_t (F^-) (mg/L)	q_t (mg/g)	R%
Stock 100ppm		**97.137**		
Tap Water		**0.967**		
HAp (Fluka)	0.1077	9.318	8.154	90.4
HAp (Fluka)	0.1034	7.028	8.715	92.8
NaOH washed	0.1024	50.495	4.555	48.0
NaOH washed	0.1026	50.859	4.511	47.6
Reprecipitated	0.1091	45.619	4.722	53.0
Reprecipitated	0.1032	57.567	3.834	40.7
500 °C	0.1025	57.690	3.849	40.6
500 °C	0.1061	57.449	3.741	40.9
600 °C	0.1044	68.013	2.790	30.0
600 °C	0.1033	69.142	2.710	28.8
Mussel	0.1018	70.798	2.587	27.1
Mussel	0.1020	70.859	2.576	27.1
800 °C	0.1059	66.099	2.931	32.0
800 °C	0.1013	85.210	1.177	12.3
1000 °C	0.1028	73.959	2.255	23.9
1000 °C	0.1013	94.760	0.235	2.4

Table 3-27: Averaged results from Table 3-26 above.

Sample	q_t (mg/g)	R%
HAp (Fluka)	8.434	91.6
NaOH washed bone	4.533	47.8
Reprecipitated	4.278	46.9
Hoki 500 °C	3.795	40.7
Hoki 600 °C	2.75	29.4
Mussel	2.582	27.1
Hoki 800 °C	2.054	22.1
Hoki 1000 °C	1.245	13.2

Pure HAp was found to be the most efficient fluoride adsorbent in terms of the calculated values of q_t for each material. This was expected, as mentioned earlier it is understood that the mechanism by which fluoride would bind to HAp materials is through substitution into the lattice for the hydroxide ions, to form fluorapatite ($Ca_{10}(PO_4)_6F_2$). The pure form of HAp should contain more available OH groups for substitution than a sample of carbonated HAp, which would lead to an increase in the amount of substitution which could take place.

It was thought that the removal of carbonaceous content from the bone-derived powders through an increase in the treatment temperature would increase the adsorbent's affinity for fluoride, as this should lead to an increasingly pure HAp product. However, this was not observed, instead as the treatment temperature of the bones increased their ability to remove fluoride decreased. It was shown earlier (section 2.3.1) that increasing the treatment temperature of the bones not only leads to an increased removal of carbon materials, but also the generation of other calcium phosphate phases, such as TCP. It is possible that the generation of TCP, hence the loss of OH^- from the material, reduces the ability to remove F^- from the water samples. The as received hoki bone-powders refluxed in NaOH were the next best material for this application, followed by bone powders which had been thermally treated at 800 °C prior reprecipitation using HNO_3 and NaOH.

Another similar material comparison experiment was carried out using hoki bone-derived materials to see if this trend was repeated. The averaged results are given in Table 3-28 below.

Table 3-28: Averaged results from comparison of materials for fluoride removal.

Sample	Average q_t (mg/g)	Average R%
HAp Pure	8.279	88.0
Reprecipitated	7.826	79.4
NaOH washed	4.023	42.0

500 °C	2.265	23.1
800 °C	0.980	10.2
1000 °C	0.165	1.8

The same general trends were observed in this experiment, pure HAp was the most efficient, and the increased treatment temperature decreased F^- removal ability. This experiment however identified that reprecipitated materials from bone-derived powders could be effective. It was shown in section 2.4.5, that the main reprecipitation product is poorly crystalline hydroxyapatite which is free from collagen and other organic impurities. There is also a significantly reduced level of carbonate in these materials, which could have led to an increased amount of OH in the material available for substitution.

It was clear from the results above that the best material for removing fluoride from aqueous water samples was the pure HAp, and that the chemically treated materials were the next best. It was then thought that digesting and reprecipitating a bone-derived material which had previously been refluxed in NaOH, would produce a superior material for fluoride adsorption. These materials were washed thoroughly and trialled in another material comparison experiment and results of this experiment are summarised below in Table 3-29.

Table 3-29: Averaged results from fluoride adsorption onto different chemically treated materials.

Sample	Average q_t (mg/g)	Average R%
NaOH washed, then reprecipitated	8.456	91.5
HAp pure	8.058	88.3
800 °C, then reprecipitated	4.447	50.4

These results showed that the coupling of the two chemical methods was successful in producing a material with an affinity for fluoride similar to that of the pure HAp. In comparison, the thermally treated to 800 degrees and reprecipitated using HNO_3 and NaOH sample had a much lower affinity.

3.2.5.3 Adsorption isotherm of fluoride onto pure HAp

Pure HAp was used in this isotherm generation as it had a consistently high affinity for fluoride throughout the material comparison experiments, and was most likely to provide useful isotherm results. The results from this isotherm experiment are given in Table 3-30 below. The samples were allowed to mix for 6 hours in these experiments.

Table 3-30: Summary of results from the adsorption isotherm experiment of fluoride ions onto pure HAp (Fluka brand).

m(solid)	C_t (F-) (mg/L)	q_t (mg/g)
0.0508	71.395	5.631
0.1063	46.903	4.995
0.1519	34.283	4.326
0.2021	22.499	3.835
0.3047	10.604	2.934
0.4018	6.886	2.317
0.5038	4.691	1.892
0.6079	3.892	1.581

These values are reported as C_t and q_t, instead of the usual isotherm parameters of C_e and q_e. This is because kinetic experiments were not carried out for this fluoride-HAp system (due to time constraints and the large amount of time required for IC analyses), and so it is not known if samples were allowed to mix long enough for equilibrium to be reached. A plot of q_t against C_t was generated from the values in Table 3-30, and is given in
Figure 3-25 below.

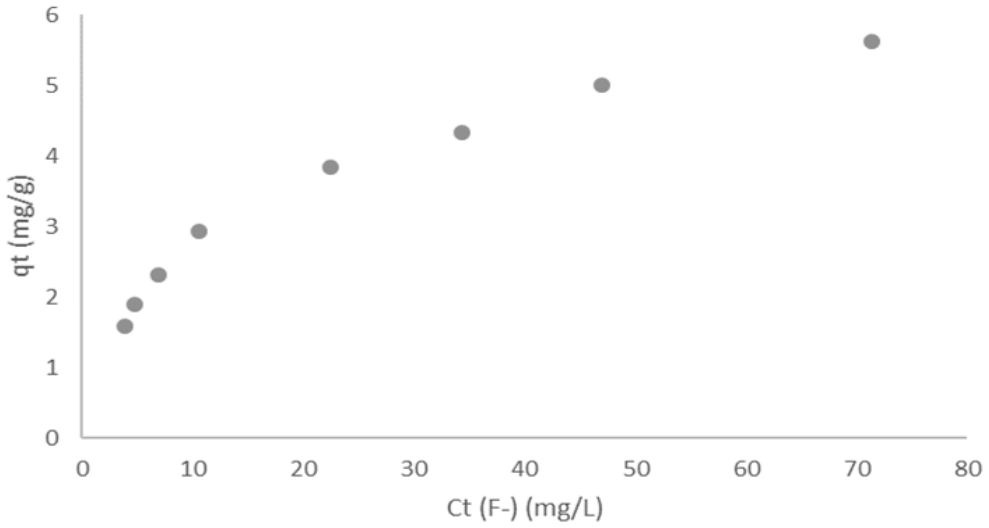

Figure 3-25: Adsorption isotherm of fluoride onto pure Fluka HAp.

Linearised Langmuir and Freundlich models were applied to this data, these are given in Figure 3-26 and Figure 3-27 respectively

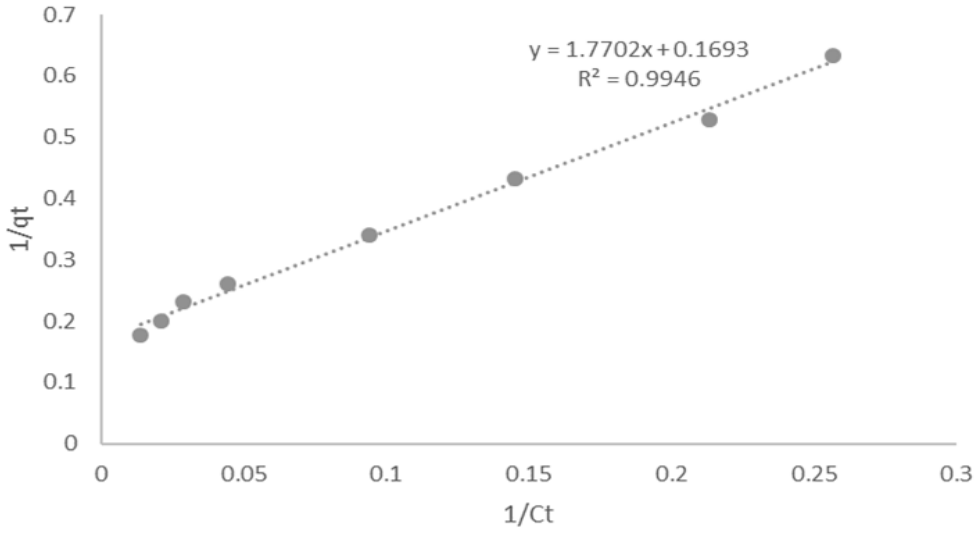

Figure 3-26: $1/C_t$ vs $1/q_t$ linearised Langmuir plot.

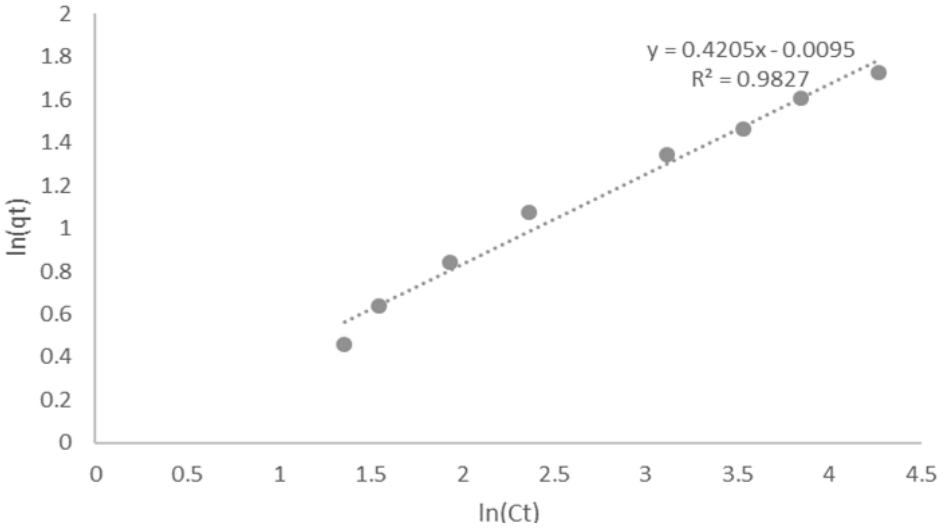

Figure 3-27: $\ln(C_t)$ vs $\ln(q_t)$ linearised Freundlich plot

These linear plots were then used to calculated Langmuir and Freundlich parameters, given in Table 3-31 below.

Table 3-31: Calculated parameters from the linearised isotherm parameters

Linearised Langmuir Parameters			**Linearised Freundlich parameters**		
q_m (mg/g)	***b* (L/mg)**	**R^2**	**K_F**	**n**	**R_2**
5.9067	0.0956	0.9946	0.9905	2.378	0.9827

As with the heavy metal-bone powder systems, this system is best described by the Langmuir adsorption isotherm. However, a q_m value of 5.9067 mg/g is smaller than some of the observed q_t values presented earlier for fluoride onto pure HAp (Table 3-29), despite identical reaction times being used. It is noticed that in Figure 3-25 where the original isotherm data is presented, a plateau is not reached, and so it is

possible that further data points (using weights of HAp below 0.05 g) may have identified a plateau.

As mentioned earlier, these samples were allowed to mix for 6 hours, however it is not known if this would be sufficiently long for equilibrium to be reached, hence this q_m value is unreliable as an official value. q_m values of 3.12[37] mg/g and 1.400[38] are reported in the literature for similar fluoride ion adsorptions with hydroxyapatite as the adsorbent, and so based on these the value obtained in the present study could be a reasonable approximation. Regardless of the accuracy of the calculated q_m value, these experiments outlined that the system behaves in a Langmuir-like manner and offer an approximation on the value of q_m for the HAp-fluoride system.

3.2.5.4 Generation of a mock F^- filter using HAp

While periods of at least 1 day may be required to reach equilibrium, it may not be economical or practical in a real-world application to leave the materials in a water sample for such an extended period. Instead it is possible that sufficient F^- removal could be achieved through 1-2 hours of reaction time, or even as column-like filtration system. To investigate the possibility of this, a mock filter was generated using HAp, and a syringe-syringe filter setup. The fluoride containing water sample was passed through this syringe setup, the filtrate from which was analysed for its fluoride content. The results of this are given in Table 3-32 below.

Table 3-32: Averaged results from mock-filter study

Sample	C_0 (mg/L)	C_t (mg/L)	Average R%
HAp filter	100.2	60.1	40.1

These results show that from simply passing a solution through filter system containing HAp material, a process which takes less than 10 seconds, can drop the concentration of fluoride significantly. While this has not decreased the fluoride concentration to the recommended level, it serves as a proof of concept that these types of materials could be incorporated into a cheap filtration system for treating drinking water with unsafe levels of fluoride. It is possible that the use of a larger mass of HAp in the filters could lead to further decreases in the fluoride content of a solution, so this could be investigated in future work.

3.2.6 General findings from potential application studies

3.2.6.1 Enzyme immobilisation studies

Tris-hydroxymethyl phosphine was successfully synthesised and is assumed to have attached to the raw bone materials, however it was not possible to determine the amount of THP which had attached to the materials. It is possible that this could be analysed through measuring the phosphorus content of a sample, however the amount of phosphorus naturally in the bone samples would need to be measured extensively first to understand how much P is present as a result of the binding reagent.

Attempts to immobilise the malL enzyme onto the bone-THP materials produced promising, interesting and unexpected results. While the results suggest some of the enzyme is able to be immobilised by the materials, the control experiments (bones with no THP added) produced results in which the activity of the enzyme solution had increased after immersion. This was completely unexpected and remains unaccounted for. It is possible that some component of the raw materials is leaching into the enzyme solution and causing an increase in the activity, however it is not known what this component might be. Overall this study identified that there is a potential for enzymes to be immobilised onto these raw bone materials when combined with THP, and so future studies could investigate this further, potentially with the use of a range of enzyme-substrate systems, and a greater number of samples.

3.2.6.2 Heavy metal adsorption studies

In general, for the nickel, cadmium and strontium systems, the most effective bone-derived materials (from those trialled) was found to be the bones heated at 500 ^{o}C. It is possible that this observation is linked to the respective crystallite size of each material, which has been shown (in other studies) to increase with an increase in the treatment temperature. Because of this, this material was further studied for its adsorption kinetics and isotherms with the nickel and cadmium metal systems.

The adsorption kinetic experiments for the nickel-bone and cadmium-bone derived powder system found that pseudo second order adsorption kinetics were obeyed in all experiments. This suggested that the rate limiting step in these adsorption processes is due to a chemical interaction (likely due to the substitution reaction of the metal ion for Ca^{2+} in the HAp lattice). These experiments also found that a contact time length of four hours was sufficient for the systems to reach equilibrium, and so this time length was employed in all of the isotherm experiments.

The isotherm experiments showed that the Langmuir model was the best fit for both heavy metal systems (compared to the Freundlich model) through the strong relationships observed when the data was linearised. This led to a calculated q_m value of 6.925 mg/g and 41.841 mg/g for the nickel and cadmium systems respectively. To put these values into perspective, Table 3-33 and
Table 3-34 below, which have been adapted other studies[1, 18], compare a range of similar adsorbent materials from the literature for their Ni^{2+} and Cd^{2+} adsorption capacities respectively.

Table 3-33: Literature adsorptive capacity values for Ni^{2+} onto a range of sorbent materials

Adsorbent material	Particle size	q_m (mg/g)
PAC (powdered activated carbon)[39]	150 µm	31.08
Calcium-alginate[40]	NA	10.5
Baker's Yeast[41]	NA	11.4
Nano-HAp[1]	20-30 nm	46.17
Peanut hull carbon[42]	575 µm	53.65
Activated carbon from coir pith[43]	200-500 µm	62.5
Bone-powders heated at 500 °C (this study)	200-300 µm	6.925

Table 3-34: Literature adsorptive capacity values for Cd^{2+} onto a range of sorbent materials

Material	Particle Size	q_m (mg/g)
Apatite II™ derived from fish bones[44]	NA	92
Activated carbon (Filtrasorb)[45]	< 75 µm	307.5
Nano-HAp (by microwave heating H_3PO_4, $Ca(NO_3)_2.4H_2O$)[46]	68 nm	88.5
n-HAp from Anpuruinano material Co. (Nanjing, China)[47]	20-200 nm	64.07
Nano crystallite HAp[2]	20-30 nm	142.86
Hoki treated to 500 °C (this study)	200-300 µm	41.841

The q_m values for nickel and cadmium adsorptions from this study appear to be low relative to these literature values. However, when preparation of the materials is considered, the materials presented in this study offer an advantage. Some of the literature materials reported above require several steps to produce, in particular the nano-HAp precipitate samples with particle sizes in the nm range. In contrast, the materials in this study can be prepared simply through thermal treatment (albeit at a relatively high temperature of 500 °C) and a fast (1 min) grinding step. It is understood that the particle size of an adsorbent material has a significant influence on the adsorption properties of that material. The particle size of the material used in this study was found to be 200 nm (section 3.2.2.1) and were found to be approximately 200 µm. For comparison, the nano-crystallite HAp material reported in

Table 3-34 above was found to have particle sizes in the range of 20-30 nm^2. If it were possible to further grind these materials to a smaller particle size, it is likely that the adsorptive capacities of the materials would increase. For real world applications however, smaller particle sizes of these materials may not be required. The concentrations of Ni^{2+} and Cd^{2+} used in these experiments (100 mg/L) exceed the maximum safe levels of these elements in drinking water, and so typical contamination incidents may not have concentrations as high as 100 mg/L. The US EPA states[48] that the maximum nickel level in drinking water should be 0.1 mg/L, while the WHO states[49] that the maximum allowable cadmium level in drinking water is 0.003 mg/L. If metal concentrations closer to the maximum safe levels were used, it is possible that the above literature materials with higher q_m values would be surplus to requirement, and the cheap materials from this study with lower q_m values could be equally as effective. If this were the case, the best material would not be the one with the highest q_m value, but the material which is the most economical to produce, and which can achieve the adsorption in the shortest length of time, and ideally be implemented as a column-like filter.

The bones heated at 500 ^oC produced promising results when applied as an adsorbent for a multi-cation system (with Ni^{2+} and Cd^{2+}) with preferential adsorbing of Cd^{2+} occurring. Previous studies have also suggested similar bone derived materials can be used in the adsorption of a binary metal system consisting of Zn^{2+} and Cu^{2+} ions[24]. Hence it is possible that this could be extended to systems containing several ions and, potentially to systems containing both cations and anions. Investigating these aspects further would be necessary as 'real world' water contamination incidents are likely to be complex matrices with a range of cations and anions present.

The results also identified that strontium in the form of Sr^{2+}, and the arsenate ion (AsO_4^{3-}) have promising potential to be adsorbed onto these bone derived materials, providing support for future investigations into these metal-bone powder adsorption systems, and demonstrating that these bone-derived materials can be used for a range of adsorptions.

3.2.6.3 Fluoride adsorption studies

Given the right processing, these raw bone materials can be adapted to be used in the treatment of water samples with unsafe fluoride levels. In contrast to the adsorption of heavy metals, the most effective adsorbent materials were those

produced through chemical reprecipitation processes, as opposed to thermal treatments. The isotherm studies of fluoride onto hydroxyapatite suggested that these materials would follow a Langmuir type adsorption, and although it is not known if an equilibrium concentration was reached (due to lack of kinetic data) an approximate q_m value was obtained of 5.9067 mg/g.

A range of technologies currently exist to treat drinking waters which are high in fluoride content. Some of these are coagulation/precipitation (i.e. through the addition of lime to promote precipitation of CaF_2), membrane processes (i.e. reverse osmosis) and electrochemical methods[50]. Each of these techniques have associated advantages and disadvantages. For example, the coagulation/precipitation method requires the addition of a large amount of solid (i.e. lime) to achieve significant adsorptions. This also then leads to the issue of filtering such a large quantity of solid from the water sample, as well as disposal of the sample[51]. Reverse osmosis is an extremely effective, yet expensive technique, and so poorer regions with high fluoride content in their drinking water are unlikely to be able to afford this technique.

In contrast, adsorption onto materials like the ones presented in this study can offer a cheap method for fluoride removal, without the need to add large quantities of solids to the water samples. There are however still disadvantages, such as disposal of the adsorbent materials after exposure to the water samples. But this issue can be mitigated, in a similar study using chicken bone char[52], it was possible to reuse the bone char after exposure to the fluoride samples through addition to a concrete mix. The potential to reuse/regenerate these HAp materials after exposure to fluoride was not investigated in this study, as the main intentions were to determine what the potential applications for these materials might be, to provide support and direction for future more thorough research.

References for Chapter Three

1. Mobasherpour, I.; Salahi, E.; Pazouki, M., Removal of nickel (II) from aqueous solutions by using nano-crystalline calcium hydroxyapatite. *Journal of Saudi Chemical Society* **2011,** *15* (2), 105-112.
2. Mobasherpour, I.; Salahi, E.; Pazouki, M., Removal of divalent cadmium cations by means of synthetic nano crystallite hydroxyapatite. *Desalination* **2011,** *266* (1), 142-148.
3. Nishiyama, Y.; Hanafusa, T.; Yamashita, J.; Yamamoto, Y.; Ono, T., Adsorption and removal of strontium in aqueous solution by synthetic hydroxyapatite. *Journal of Radioanalytical and Nuclear Chemistry* **2016,** *307* (2), 1279-1285.
4. Mahsa, M.; Esmaeil, B.; Keivan, S., Removal of Arsenic from Drinking Water by Hydroxyapatite Nano Particles. *Current World Environment 26* (28), 331-338.
5. Lin, J.; Raghavan, S.; Fuerstenau, D. W., The adsorption of fluoride ions by hydroxyapatite from aqueous solution. *Colloids and Surfaces* **1981,** *3* (4), 357-370.
6. Hobbs, J. K.; Jiao, W.; Easter, A. D.; Parker, E. J.; Schipper, L. A.; Arcus, V. L., Change in heat capacity for enzyme catalysis determines temperature dependence of enzyme catalyzed rates. *ACS chemical biology* **2013,** *8* (11), 2388-93.
7. Hamdaoui, O.; Naffrechoux, E., Modeling of adsorption isotherms of phenol and chlorophenols onto granular activated carbon: Part I. Two-parameter models and equations allowing determination of thermodynamic parameters. *Journal of Hazardous Materials* **2007,** *147* (1), 381-394.
8. Homaei, A. A.; Sariri, R.; Vianello, F.; Stevanato, R., Enzyme immobilization: an update. *Journal of Chemical Biology* **2013,** *6* (4), 185-205.
9. Cochrane, F. C.; Petach, H. H.; Henderson, W., Application of tris(hydroxymethyl)phosphine as a coupling agent for alcohol dehydrogenase immobilization. *Enzyme and Microbial Technology* **1996,** *18* (5), 373-378.
10. Zhang, N.; Brugger, J.; Etschmann, B.; Ngothai, Y.; Zeng, D., *Thermodynamic Modeling of Poorly Complexing Metals in Concentrated Electrolyte Solutions: An X-Ray Absorption and UV-Vis Spectroscopic Study of Ni(II) in the NiCl2-MgCl2-H2O System*. 2015; Vol. 10, p e0119805.
11. Al-Asheh, S.; Banat, F.; Mohai, F., Sorption of copper and nickel by spent animal bones. *Chemosphere* **1999,** *39* (12), 2087-2096.
12. Johnson, G. S.; Mucalo, M. R.; Lorier, M. A.; Gieland, U.; Mucha, H., The processing and characterization of animal-derived bone to yield materials with biomedical applications. Part II: milled bone powders, reprecipitated hydroxyapatite and the potential uses of these materials. *Journal of materials science. Materials in medicine* **2000,** *11* (11), 725-41.
13. Merck 4-Nitrophenol. http://www.merckmillipore.com/NZ/en/product/4-Nitrophenol,MDA_CHEM-106798?ReferrerURL=https%3A%2F%2Fen.wikipedia.org%2F#anchor_Specifications (accessed January 2018).
14. Dwevedi, A., Basics of Enzyme Immobilization. In *Enzyme Immobilization: Advances in Industry, Agriculture, Medicine, and the Environment*, Dwevedi, A., Ed. Springer International Publishing: Cham, 2016; pp 21-44.

15. Salman, S.; Soundararajan, S.; Safina, G.; Satoh, I.; Danielsson, B., Hydroxyapatite as a novel reversible in situ adsorption matrix for enzyme thermistor-based FIA. *Talanta* **2008,** *77* (2), 490-493.
16. Thanh, D. N.; Novák, P.; Vejpravova, J.; Vu, H. N.; Lederer, J.; Munshi, T., Removal of copper and nickel from water using nanocomposite of magnetic hydroxyapatite nanorods. *Journal of Magnetism and Magnetic Materials* **2017**.
17. Park, S.; Gomez-Flores, A.; Chung, Y. S.; Kim, H., Removal of Cadmium and Lead from Aqueous Solution by Hydroxyapatite/Chitosan Hybrid Fibrous Sorbent: Kinetics and Equilibrium Studies. *Journal of Chemistry* **2015,** *2015*, 12.
18. Zhu, X.-h.; Li, J.; Luo, J.-h.; Jin, Y.; Zheng, D., Removal of cadmium (II) from aqueous solution by a new adsorbent of fluor-hydroxyapatite composites. *Journal of the Taiwan Institute of Chemical Engineers* **2017,** *70*, 200-208.
19. Monshi, A.; Foroughi, M. R.; Monshi, M. R., Modified Scherrer Equation to Estimate More Accurately Nano-Crystallite Size Using XRD. *World Journal of Nano Science and Engineering* **2012,** *Vol.02No.03*, 7.
20. Ankica, R.; Jadranka, M., Adsorption ability of the carbon black for nickel ions uptake from aqueous solution. *Hemijska industrija* **2013,** *67* (1), 51.
21. Ho, Y. S.; McKay, G., The kinetics of sorption of divalent metal ions onto sphagnum moss peat. *Water Research* **2000,** *34* (3), 735-742.
22. Robati, D., Pseudo-second-order kinetic equations for modeling adsorption systems for removal of lead ions using multi-walled carbon nanotube. *Journal of Nanostructure in Chemistry* **2013,** *3* (1), 55.
23. Joshi, P.; Manocha, S., Kinetic and thermodynamic studies of the adsorption of copper ions on hydroxyapatite nanoparticles. *Materials Today: Proceedings* **2017,** *4* (9), 10455-10459.
24. Ramesh, S. T.; Rameshbabu, N.; Gandhimathi, R.; Nidheesh, P. V.; Srikanth Kumar, M., Kinetics and equilibrium studies for the removal of heavy metals in both single and binary systems using hydroxyapatite. *Applied Water Science* **2012,** *2* (3), 187-197.
25. Moreno, J. C.; Gómez, R.; Giraldo, L., Removal of Mn, Fe, Ni and Cu Ions from Wastewater Using Cow Bone Charcoal. *Materials* **2010,** *3* (1), 452-466.
26. Horsfall Jnr, M.; Spiff, A., *Effect of Temperature on the Sorption of Pb2+ and Cd2+ from Aqueous Solution by Caladium bicolor (Wild Cocoyam) Biomass*. 2005; Vol. 8.
27. Ghahremani, D.; Mobasherpour, I.; Salahi, E.; Ebrahimi, M.; Manafi, S.; Keramatpour, L., Potential of nano crystalline calcium hydroxyapatite for Tin(II) removal from aqueous solutions: Equilibria and kinetic processes. *Arabian Journal of Chemistry* **2017,** *10*, S461-S471.
28. Mobasherpour, I.; Salahi, E.; Ebrahimi, M., Thermodynamics and kinetics of adsorption of Cu(II) from aqueous solutions onto multi-walled carbon nanotubes. *Journal of Saudi Chemical Society* **2014,** *18* (6), 792-801.
29. Harmata, A. J.; Guelcher, S. A., 3 - Effects of surface modification on polymeric biocomposites for orthopedic applications A2 - Liu, Huinan. In *Nanocomposites for Musculoskeletal Tissue Regeneration*, Woodhead Publishing: Oxford, 2016; pp 67-91.
30. Symposium on Adsorption, o.; Surface Chemistry of, H., *Adsorption on and surface chemistry of hydroxyapatite*. New York : Plenum Press: New York, 1984.
31. LeGeros, R. Z.; Legeros, J. P., Phosphate Minerals in Human Tissues. In *Phosphate Minerals*, Nriagu, J. O.; Moore, P. B., Eds. Springer Berlin Heidelberg: Berlin, Heidelberg, 1984; pp 351-385.

32. Fawcett, D.; Poinern, E.; Brundavanam, S.; Tripathy, S.; Suar, M., *Kinetic and Adsorption Behaviour of Aqueous Cadmium Using a 30 nm Hydroxyapatite Based Powder Synthesized Via a Combined Ultrasound and Microwave Based Technique*. 2016; Vol. 6, p 11-22.
33. Barka, N.; Khalid, O.; Qourzal, S.; Assabbane, A.; Abdennouri, M.; El Makhfouk, M.; Nounah, A.; Ait-Ichou, Y., *Kinetics and equilibrium of cadmium removal from aqueous solutions by sorption onto synthesized hydroxyapatite*. 2012; Vol. 43, p 8-16.
34. Young Lee, P. S., Yuanzhi Tang, Wei Li, Brian L. Phillips, John Parise, Richard Reeder, Arsenate substitution in hydroxylapatite: Structural characterization of the Ca5(PxAs1–xO4)3OH solid solution. *American Mineralogist* **2009,** *94* (5-6), 666-675.
35. Wei, Z.; Liang, K.; Wu, Y.; Zou, Y.; Zuo, J.; Arriagada, D. C.; Pan, Z.; Hu, G., The effect of pH on the adsorption of arsenic(III) and arsenic(V) at the TiO2 anatase [101] surface. *Journal of colloid and interface science* **2016,** *462*, 252-9.
36. Fawell, J.; Bailey, K.; Chilton, J.; Dahi, E.; Fewtrell, L.; Magara, Y., *Fluoride in Drinking-water*. IWA Publishing: 2006.
37. Mourabet, M.; El Rhilassi, A.; El Boujaady, H.; Bennani-Ziatni, M.; El Hamri, R.; Taitai, A., Removal of fluoride from aqueous solution by adsorption on hydroxyapatite (HAp) using response surface methodology. *Journal of Saudi Chemical Society* **2015,** *19* (6), 603-615.
38. Mondal, P.; George, S., Removal of Fluoride from Drinking Water Using Novel Adsorbent Magnesia-Hydroxyapatite. *Water, Air, & Soil Pollution* **2015,** *226* (8), 241.
39. Rao, M.; Parwate, A. V.; Bhole, A. G., Removal of Cr6+ and Ni2+ from aqueous solution using bagasse and fly ash. *Waste Management* **2002,** *22* (7), 821-830.
40. Huang, C.; Chung, Y. C.; Liou, M. R., *J. Hazard. Mater.* **1996,** *45*, 265.
41. Patmavathy, V.; Vasudevan, P.; Dhingra, S., Adsorption of nickel (II) ions on Baker's yeast. *Process Biochem* **2003,** *38* (10), 1389-1395.
42. Periasamy, K.; Namasivayam, C., Removal of nickel(II) from aqueous solution and nickel plating industry wastewater using an agricultural waste: Peanut hulls. *Waste Management* **1995,** *15* (1), 63-68.
43. Kadirvelu, K.; Thamaraiselvi, K.; Namasivayam, C., Adsorption of nickel(II) from aqueous solution onto activated carbon prepared from coirpith. *Separation and Purification Technology* **2001,** *24* (3), 497-505.
44. Oliva, J.; De Pablo, J.; Cortina, J.-L.; Cama, J.; Ayora, C., Removal of cadmium, copper, nickel, cobalt and mercury from water by Apatite II™: Column experiments. *Journal of Hazardous Materials* **2011,** *194*, 312-323.
45. Kapoor, A.; Viraraghavan, T.; Cullimore, D. R., Removal of heavy metals using the fungus Aspergillus niger. *Bioresource Technology* **1999,** *70* (1), 95-104.
46. Elkady, M. F.; Mahmoud, M. M.; Abd-El-Rahman, H. M., Kinetic approach for cadmium sorption using microwave synthesized nano-hydroxyapatite. *Journal of Non-Crystalline Solids* **2011,** *357* (3), 1118-1129.
47. Zhang, Z.; Li, M.; Chen, W.; Zhu, S.; Liu, N.; Zhu, L., Immobilization of lead and cadmium from aqueous solution and contaminated sediment using nano-hydroxyapatite. *Environmental Pollution* **2010,** *158* (2), 514-519.
48. National Primary Drinking Water Regulations - Nickel. US Environment Protection Agency: 1995.
49. Cadmium in Drinking-water. World Health Organisation: 2011.

50. Arfin, T.; Waghmare, S., *Fluoride removal from water by various techniques: Review*. 2015; Vol. 2, p 560-571.
51. Piddennavar, R., *Review on Defluoridation Techniques of Water*. 2013; Vol. 2, p 86-94.
52. Ismail, Z. Z.; AbdelKareem, H. N., Sustainable approach for recycling waste lamb and chicken bones for fluoride removal from water followed by reusing fluoride-bearing waste in concrete. *Waste Management* **2015,** *45*, 66-75.

Chapter Four: Conclusions and Future Work

4.1 Conclusions and review of objectives

The significant quantity of waste by-products from the fishing industry in New Zealand presents an attractive opportunity to utilise some of these low-cost materials with the ideal intent of adding value, which could be beneficial both environmentally and economically for New Zealand. The purpose of this study, was to extensively characterise the bone-derived powders of four fish species, as well as the mineral exteriors from four shellfish species, and to investigate potential applications of these materials. The following objectives were looked at:

- Extensive characterisation of bone and shell derived materials.
- Process the materials through physical and chemical methods to remove the organic component (collagen proteins and lipids), with extensive characterisation of the products and determine optimum methods.
- Investigate the potential for the as received bone materials to act as a solid support surface for the immobilisation of enzymes with the use of a coupling reagent.
- Investigate the potential for the bone and shell-derived materials to remove heavy metal species from aqueous media, such as Ni^{2+}, Cd^{2+}, Sr^{2+} and AsO_4^{3-}
- Investigate the potential for the bone and shell-derived materials to remove fluoride from aqueous media to potentially be used as a water filter in areas with concerning natural fluoride levels.

Characterisation studies using FT-IR, SS-NMR, pXRD, SEM and ICP-MS gave valuable information on the nature and chemical composition of the as received bone and shell-derived materials. These studies found the bone-derived powders to be composed mainly of carbonated hydroxyapatite, with interdigitated collagen throughout the bone matrix. Generally, there were few differences between the results of different species, except for the snapper and gurnard samples both retaining a relatively high oil content. This however could be due to processing techniques before receiving the bone materials and not due to the nature of the species themselves. The shell-derived materials were found to be composed mainly of calcium carbonate, however the mussel and cockle shells showed FT-IR spectra

and pXRD diffraction patterns characteristic of the aragonite polymorph, while the scallop and oyster shells were characteristic of the calcite polymorph.

Thermal treatment of the bone materials found that organic material was effectively completely burnt off by 600 ^{o}C, supported by TGA and FT-IR analyses. The carbonate in the material begins to decompose at approximately 700 ^{o}C and above, which is associated with the production of CaO on the surface of the materials which can be washed away with water. Results from the materials heated to 1000 ^{o}C suggest that the HAp phase begins to decompose, possibly to form TCP through the loss of OH in the material. Therefore, in terms of HAp production, the optimum thermal treatment temperature appears to be 800 ^{o}C.

Thermal treatment of the shell materials showed that the aragonite polymorph in the cockle and mussel shells converts to the calcite polymorph at temperatures between 300 and 500 ^{o}C. Decomposition of the $CaCO_3$ phase to CaO and CO_2 begins to occur at 700 ^{o}C, with complete conversion occurring at 800 ^{o}C and above. Moisture in the atmosphere can then hydrolyse CaO to form $Ca(OH)_2$, which accounts for the traces of $Ca(OH)_2$ found in these materials.

The most effective chemical treatment found in terms of removing the organic content from the bone powders was to heat these under reflux with an NaOH solution. This treatment almost completely removed the organic material, as well as breaking down the bone structure to a fine powder, removing the need to grind down these materials post-treatment, this was not found in any of the other chemical treatments trialled.

Reprecipitation experiments demonstrated the use of HNO_3 on unprocessed bone materials leads to a discoloured reprecipitated powder and highlights the necessity for these to have their organic content removed to produce an aesthetically white product. The optimum method for reprecipitating HAp powder from these bone materials involved the treatment of these to 800 ^{o}C for two hours, digestion in HNO_3 followed by reprecipitation in NaOH, ideally with protection from the atmosphere to avoid carbonate contamination. It is possible that these reprecipitated HAp powders could be used in coating of implant materials, as has been done in previous studies.

Attempts to immobilise the malL enzyme onto bone-THP materials yielded promising yet unexpected results. The results suggest some enzyme can be bound

to the bone-THP material, however once attached they may become inactive. The unexpected results originated from the control experiments, in which enzyme activity was found to increase in the presence of as received bone materials which had not been exposed to the binding reagent THP. This observation remains mostly unaccounted for.

Bone materials heated at 500 ^{o}C showed consistent promising results for the adsorption of divalent metal ions, such as Ni^{2+}, Cd^{2+} and Sr^{2+}, most likely through the exchange of these ions for Ca^{2+} in the HAp lattice. Adsorption kinetic experiments revealed the systems obey pseudo second order kinetics, which allowed for the identification of an equilibrium point during the adsorptions. This was found to be four hours hence this was the time period used in the adsorption isotherm experiments. Isotherm experiments identified that the systems follow a Langmuir-type isotherm with adsorption capacities of 6.925 and 41.841 mg/g for the Ni^{2+} and Cd^{2+} ions respectively with bone powders heated at 500 ^{o}C. Comparison to literature found these values to be relatively low, however these offer the advantage of being easy to produce and are available in high volumes.

It is thought that the superior adsorption abilities of the materials heated at 500 ^{o}C originates from the crystallite size, which other studies have found to increase as a function of treatment temperature. This leads to an overall decrease in the surface area: volume ratio and potentially accounts for the decrease in adsorption capabilities as the treatment temperature increases. Results from these studies also suggest the material could be used in the adsorption of multi-cation systems.

Other processed bone materials also showed promising results for the removal of the arsenate and fluoride anion. This suggests that that these materials could potentially be used in a filter system for the removal of a variety of species from drinking water.

4.2 Future Work

The results from this study discovered a range of aspects which could be investigated further in future research. As a result of the broad nature of this study and the limited time allocation some of these objectives could not be extensively investigated, hence there some knowledge gaps identified which could be the basis of future work.

- Further investigation into the enzyme immobilisation experiments. It may be beneficial to carry out similar studies with a different enzyme to determine if the unexpected results were specific to the use of the malL enzyme.
- Investigation into the heavy metal removal abilities of the materials using concentrations more similar to what may be found in typical drinking water situations. Exposure of the adsorbents to alternative metal ions considered to be contaminants could also be looked at.
- Studying of the effects the adsorbent materials have on water after exposure. It is possible that these materials may cause the water to be unsafe for consumption after exposure and would instead be better utilised as a treatment for waste water prior to being released to natural bodies of water.
- Determination on the reusability of the materials after being used in adsorptions, as well as potential ways to discard the adsorbents once used.

Exploring these areas could lead to the development of a value-added product from these fishbone-derived materials, which are currently regarded as waste by-products.

Appendix 1: General methodology for the purification of the malL enzyme

MalL protein expression:

Protein expression:

A 10 mL starter culture inoculated from frozen glycerol stocks of the relevant strain was grown overnight at 37 °C with shaking in LB containing 100 $\mu g.ml^{-1}$ ampicillin (AMP) in a 50 ml falcon tube. An expression culture (1 L LB in a 2 L baffled flask) containing 100 $\mu g.ml^{-1}$ AMP was inoculated with the starter culture and grown at 37 °C till mid log phase (OD_{600} between 0.5-0.7). Protein expression was induced in the mid log phase by the introduction of 1 mM IPTG. Protein expression was carried out at 18 °C with shaking for 20 hours, at which stage cells were harvested by centrifugation at 4500 g for 20 minutes at 4 °C. Cell pellets were frozen at -80 °C until immediately prior to protein purification steps.

General protein purification methodology:

Cell lysis:

Defrosted cell pellets were resuspended in ~20 ml of lysis buffer. Cells were lysed in 50 ml Falcon tubes on ice by sonication in six bursts of 15 seconds, with 30 second periods of cooling between each sonication. Cell debris was removed from the supernatant by centrifugation at 20,000 g for 20 minutes at 4 °C to separate the cellular supernatant from the insoluble debris.

Immobilised Metal Affinity Chromatography Purification:

An initial protein purification step was performed via Immobilised Metal Affinity Chromatography (IMAC) purification based on the hexa-histidine tag. Columns with immobilised nickel ions (5 ml HiTrap HP/FF; GE Healthcare, UK) were prepared by stripping with two column volumes of 100 mM EDTA (pH 8.0) to remove Ni^{2+} from the column. Columns were recharged with one column volume of 100 mM $NiCl_2$. Washing steps with two column volumes of MQ H_2O followed each of these steps. Prepared columns were equilibriated in lysis buffer.

Cellular supernatant was filtered successively through 1.2 μm, 0.45 μm, and 0.2 μm Minisart syringe filters (Sartorius AG, Germany) prior to loading onto the equilibriated IMAC column.

Protein elution from the column was performed with an ÄKTA Basic, Prime, or Purifier system (GE Healthcare, Sweden). Weakly bound non-target proteins were eluted from the column with a solution comprising of 4 % elution buffer: 96 % lysis buffer at a flow rate of 1 $ml.min^{-1}$. Washing was continued until the absorbance at 280 nm had plateaued. Target protein was eluted from the column over a gradient elution from 0-100 % elution buffer over 50 ml at a flow rate of 1 $ml.min^{-1}$, and collected in 2 ml aliquots.

Fractions with target protein were identified via the 280 nm absorbance trace, and/or SDS-PAGE.

Size exclusion chromatography:

Protein containing fractions from the IMAC purification were pooled and concentrated to ≤ 20 $mg.ml^{-1}$ for SEC. Protein was filtered through a 0.2 µm filter and 0.5 ml loaded onto a Superdex 200 10/300 GL column (GE Healthcare Life Science, UK) equilibriated with size exclusion buffer. Protein was separated and eluted with size exclusion buffer at a flow rate of 0.5 $ml.min^{-1}$, and collected in 0.5 ml aliquots.

Fractions with target protein were identified via the 280 nm absorbance trace, and/or SDS-PAGE.

Protein was concentrated to the required concentration for further analysis.

Buffer compositions:

Buffer compositions for the specific purification of malL are given below in Table 1.

Table 1: List of buffer compositions for IMAC and SEC purification of MalL variants.

Buffer	**Composition**
IMAC lysis buffer	10 mM KCl, 1 mM $MgCl_2$, 1 mM $CaCl_2$, 25 mM imidazole, pH 7.0 [1]
IMAC elution buffer	10 mM KCl, 1 mM $MgCl_2$, 1 mM $CaCl_2$, 1 M imidazole, pH 7.0
SEC buffer	20 mM HEPES, pH 7.0

Appendix 2: Summary of thermally treated shell materials

Table 2: Summarised observations from the thermal treatment of shells derived from different shellfish species.

Sample	Treatment temperature (°C)	Appearance
Cockle	As received	Off white/cream powder
Cockle	300	Cream fine powder
Cockle	500	Light grey fine powder
Cockle	600	Grey fine powder
Cockle	700	White fine powder
Cockle	800	White agglomerated powder
Cockle	1000	White agglomerated powder
Scallop	As received	Cream fine powder
Scallop	300	Cream fine powder
Scallop	500	Light grey fine powder
Scallop	600	Grey fine powder
Scallop	700	White fine powder
Scallop	800	White fine powder
Scallop	1000	White fine powder
Mussel	As received	Off white/cream grained powder
Mussel	300	Cream fine powder
Mussel	500	Light grey fine powder
Mussel	600	Dark grey fine powder
Mussel	700	White fine powder
Mussel	800	White fine powder
Mussel	1000	White fine powder
Oyster	As received	Off white/cream grained powder
Oyster	300	Cream fine powder
Oyster	500	Light grey fine powder
Oyster	600	Dark grey fine powder
Oyster	700	White fine powder
Oyster	800	White fine powder
Oyster	1000	White fine powder

Appendix 3: Summary of chemical treatment on bone-derived materials and reprecipitation products

Table 3: Summarised observations from chemical treatments on the bone materials

Sample	Treatment	Appearance of final product
Hoki	H_2O reflux x3	Orange flakes
Hoki	NaOH reflux x1	Off white flakes
Hoki	NaOH reflux x2	Off white powder
Hoki	Ethyl acetate reflux	Dark cream flakes
Hoki	Bleach soaking	Cream flakes
Hoki	NaOH reflux, then acetic acid	Off white powder
Snapper	H_2O reflux x3	Orange flakes
Snapper	NaOH reflux x1	Orange flakes
Snapper	NaOH reflux x2	Light orange/off white powder
Snapper	NaOH reflux x3	Off white powder
Snapper	Ethyl acetate reflux	Dark cream flakes
Snapper	Bleach soaking	Cream flakes
Gurnard	H_2O reflux x3	Orange flakes
Gurnard	NaOH reflux x1	Orange flakes
Gurnard	NaOH reflux x2	Off white powder
Gurnard	Ethyl acetate reflux	Dark cream flakes
Gurnard	Bleach soaking	Cream flakes
Flounder	H_2O reflux x3	Orange flakes
Flounder	NaOH reflux x1	Off white flakes
Flounder	NaOH reflux x2	Off white powder
Flounder	Ethyl acetate reflux	Dark cream flakes
Flounder	Bleach soaking	Cream flakes

Table 4: Summarised observations from reprecipitation methods with bone materials

Sample	Pre-treatment	Digestant	Powder appearance
Hoki	-	HNO_3	Light yellow/green
Hoki	-	HCl	Cream/off white
Hoki	NaOH reflux x2	HNO_3	Cream
Hoki	NaOH reflux x2	HCl	Cream
Hoki	800 ^oC 2 hours	HNO_3	White
Hoki	800 ^oC 2 hours	HCl	White
Hoki	1000 ^oC 2 hours	HNO_3	White
Hoki	1000 ^oC 2 hours	HCl	White
Snapper	-	HNO_3	Yellow/orange
Snapper	-	HCl	Cream/off white
Snapper	NaOH reflux x2	HNO_3	Cream
Snapper	NaOH reflux x2	HCl	Cream
Snapper	800 ^oC 2 hours	HNO_3	White
Snapper	800 ^oC 2 hours	HCl	White
Snapper	1000 ^oC 2 hours	HNO_3	White
Snapper	1000 ^oC 2 hours	HCl	White